

Bipartite causal inference with interference, time series data, and a random network

Zhaoyan Song Georgia Papadogeorgou

Department of Statistics, University of Florida

Abstract

In bipartite causal inference with interference, interventional units might receive treatment or control, and they might affect the outcome of outcome units through their connections on a bipartite network. We study bipartite causal inference with interference based on observational data across time and a changing bipartite network. Under an exposure mapping framework, we define the immediate and carryover causal effects for each outcome unit, representing contrasts of potential outcomes under different values of the immediately preceding and past exposures, respectively, averaged over time. We establish unconfoundedness of the exposure received by outcome units based on unconfoundedness assumptions on the interventional units' treatment assignment and the random network, hence respecting the bipartite structure of the problem. Our results hold for binary, continuous, and multivariate exposure mappings. In the special case of binary exposure and carryover mappings, we propose algorithms for the immediate and carryover causal effects that combine matching and covariate balancing. We show that the bias of the resulting estimators is bounded. In our motivating study, we find some evidence that smoke from wildfires has an immediate impact on reducing transportation by bicycle in San Francisco.

1 Introduction

Causal inference methodology most often focuses on the scenario where units are assigned to treatment or control, and an outcome is measured on the same set of units. However, in some cases, the units that receive the treatment are distinct from the units that experience the outcome. We refer to the former as interventional units, and the latter as outcome units. The outcome units do not receive the treatment themselves. Instead, their exposure to the treatment is through their connections to potentially treated interventional units. The causal dependencies between interventional and outcome

units can be described in a bipartite network, and, as a result, this setting has been termed bipartite interference [Zigler and Papadogeorgou, 2021].

In this manuscript, we focus on bipartite causal inference with interference from observational data measured over time. The treatment level of an interventional unit and the bipartite network can change over time according to unknown mechanisms that depend on past covariates of the interventional units, the outcome units, and the network. The outcomes of outcome units can be influenced by the immediately preceding and past exposures to the treatments of the interventional units through the bipartite network.

Existing work in bipartite causal inference with interference is cross-sectional and mostly considers a fixed and known bipartite network. Zigler and Papadogeorgou [2021] introduced causal estimands for bipartite causal inference, and developed weighting estimators under clustered interference. The concept of an exposure mapping introduced in unipartite causal inference [e.g., Aronow and Samii, 2017, Forastiere et al., 2021] has been extended to the bipartite setting, stating that potential outcomes depend on the interventional units' treatment through known functions of the treatment and the bipartite network. In Zigler et al. [2025], interventions on power plants (interventional units) can affect health outcomes across zip codes (outcome units) and the bipartite network describes complex atmospheric and geographic dependencies among units. In experimental settings and under a linear model for the potential outcomes, Harshaw et al. [2023] designed estimators and inferential techniques for the effect of assigning all or none of the interventional units to treatment. Pouget-Abadie et al. [2019] developed experimentation techniques for bipartite interference that improve the efficiency of estimators with applications in marketplace experiments where discounts on Amazon listings (interventional units) can influence the behavior of customers (outcome units). Brennan et al. [2022] focused on avoiding inferential bias due to interference. Doudchenko et al. [2020] proposed using propensity scores to account for confounding due to the network structure. In experimental settings, previous work has also studied bipartite causal inference from a design-based perspective [Chattopadhyay et al., 2023, Papadogeorgou et al., 2025, Lu et al., 2025]. All these studies have fixed causal networks, except Wikle and Zigler [2023], which considers a probabilistic bipartite network in a cross-sectional design.

For time series data, most of the causal inference literature focuses on the case without interference [see Abadie and Cattaneo, 2018, Imbens, 2024, for surveys on the topic]. Recently, panel data methodology has been extended to the case with unit-to-unit interference. In Cao and Dowd [2019], Grossi et al. [2020], Di Stefano and Mellace [2020]; and Menchetti and Bojinov [2020], some units receive the treatment at some point in time and remain treated thereafter, and in Clark and Handcock [2021] and Agarwal et al. [2023] the units' treatment assignment changes over time. These methods

have yet to be extended to the bipartite setting, and assume the existence of multiple units measured over time.

Recent work on causal inference with data over time allows past treatments to affect future outcomes, called carryover effects. Relevant to our work is the literature on switchback experiments, where a single unit is followed over time, and its treatment changes according to an experimental design. [Bojinov and Shephard \[2019\]](#) proposed an IPW estimator for general temporal estimands. [Bojinov et al. \[2023\]](#) developed minimax decision rules for optimizing the treatment assignment in switchback experiments, and [Hu and Wager \[2022\]](#) used Markov models to allow for long-term carryover effects. In switchback designs the treatment assignment mechanism is known, which simplifies estimation. In contrast, in observational bipartite settings, the exposure assignment mechanism is unknown and potentially hard to model as it depends on unknown treatment and network dynamics.

Our motivating context is the evaluation of the effect of smoke from wildfires on population mobility using bicycles (Section 2). Forested geographical areas correspond to the interventional units on which a wildfire might take place and populated geographical areas are the outcome units on which biking activity is measured. Wildfires in forested areas can lead to smoke exposure in populated areas according to weather and atmospheric processes which, in turn, can affect cycling activity.

From a statistical perspective, our contributions are the following: (a) Under an exposure mapping framework, we define two causal estimands for an outcome unit, the *immediate* effect and the *carryover* effect which represent the effect of the most recent and past exposures, respectively (Section 3). These estimands are defined as contrasts of potential outcomes for a given outcome unit averaged across time. (b) We introduce unconfoundedness assumptions for the treatment and network processes conditional on variables of the interventional units, outcome units and the network. We establish the unconfoundedness for the outcome unit’s most recent and carryover exposures, which implies that we can estimate the outcome-unit-specific effects while conditioning *only* on temporally-varying information (Section 3). These results hold for binary, continuous, and multivariate exposures. (c) Focusing on binary exposure mappings for the most recent and past exposures, we propose estimators for the immediate and carryover effects that combine ideas from matching and covariate balancing. We show that the bias of the estimators is bounded, and can be made arbitrarily small based on the choice of algorithmic parameters (Section 4). (d) In an extensive simulation study, we showcase that our approach performs well for estimating the outcome-unit effects (Section 5). (e) Using this approach, we find that smoke exposure from wildfires leads to an immediate reduction in the number of bike rental hours in the city of San Francisco, but does not significantly alter bike usage in nearby regions, and it does not have carryover effects (Section 6). We conclude with a discussion (Section 7).

2 Wildfire smoke and transportation by bicycle

In recent years, climate change has led to more frequent and prolonged wildfires across North America. These events pose serious threats to human life, property, and ecological systems [Chen et al., 2021]. Wildfire smoke, a source of fine particulate matter, can be transported over long distances and poses a major public health concern. Exposure to smoke from wildfires has been associated with increased rates of respiratory infections and all-cause mortality [Reid et al., 2016]. Beyond direct health impacts, wildfire smoke influences human behavior in other ways as well. Doubleday et al. [2021] found a significant decline in daily bike usage during and after wildfire smoke events, and Rosenthal et al. [2020] found a significant reduction in individuals’ step counts with deteriorating air quality due to wildfires. Their findings suggest that wildfire smoke can disrupt urban transportation and physical activity with broader implications for physical and mental health.

We contribute to this literature by studying how North American wildfires affect biking activity in the San Francisco Bay Area. We use $\mathcal{N} = \{n_1, n_2, \dots, n_N\}$ to denote the interventional units corresponding to forested geographical areas. Data are measured over time periods $t \in \mathcal{T} = \{1, 2, \dots, T\}$ corresponding to daily information from January 2021 to September 2023 with $T = 1,003$. We use $A_{ti} \in \mathcal{A}$ to denote the treatment level of interventional unit n_i at time t , representing wildfire activity in that area. Then, $\mathbf{A}_t = (A_{t1}, A_{t2}, \dots, A_{tN})^\top$ is the treatment vector at time t across all interventional units, with $\mathbf{A}_t \in \mathcal{A}^N$. Figure 1a illustrates wildfire occurrence and intensity on August 31, 2021. The interventional units do not experience the outcome.

We study the effect of smoke from wildfires on biking activity in three populated geographical areas in northern California: San Francisco, San Jose and the East Bay. The outcome of interest is the total daily bicycle riding time in each area recorded by Lyft’s Bay Wheels bikeshare program, which has tracked bikeshare usage since 2017 across more than 450 stations. Figure 1b shows the locations of the stations in the three areas. Because bikeshare usage reflects daily patterns of outdoor activity, it can serve as a proxy for how populations respond to wildfire smoke. In our data, only 206 out of approximately 6 million rentals started and ended in different areas, implying minimal spatial spillover effects from one region to the other. This allows us to analyze each of the three outcome geographical areas separately. Therefore, we focus on a single outcome unit m throughout. We use Y_t to represent the total number of bike riding hours on day t . During our study period, the number of hours of bikeshare rentals was on average 1,359 in San Francisco, 105 in East Bay, and 612 in San Jose.

Smoke originating from a wildfire can travel long distances depending on weather and atmospheric conditions, with transport patterns that change over time. The vector $\mathbf{G}_t = (G_{t1}, \dots, G_{tN})^\top \in \mathcal{G}$

denotes the bipartite connectivity of all interventional units in \mathcal{N} with the outcome unit m . Specifically, G_{ti} represents the extent to which smoke from a wildfire in area n_i is transported to the populated area of interest at time t .

The treatment assignment of the interventional units, the outcome of the outcome unit, and the bipartite connectivity vector can all depend on covariates. We use $\mathbf{X}_{0i}^{\text{int}}$, $\mathbf{X}_0^{\text{out}}$, and $\mathbf{X}_{0i}^{\text{net}}$ to denote time-invariant covariates for the interventional unit n_i , the outcome unit m and their network relationship, of length p_0^{int} , p_0^{out} , and p_0^{net} , respectively. We use the same notation with subscript t for time-varying information, although the number of time-invariant and time-varying covariates might differ. Specifically, at time t , we use $\mathbf{X}_{ti}^{\text{int}} = (X_{ti1}^{\text{int}}, X_{ti2}^{\text{int}}, \dots, X_{tip^{\text{int}}}^{\text{int}})^{\top}$ to denote the p^{int} -vector of time-varying covariates associated with interventional unit n_i , $\mathbf{X}_t^{\text{out}}$ to denote the p^{out} -vector of time-varying covariates for the outcome unit m , and $\mathbf{X}_{ti}^{\text{net}} = (X_{ti1}^{\text{net}}, X_{ti2}^{\text{net}}, \dots, X_{tip^{\text{net}}}^{\text{net}})^{\top}$ to denote the p^{net} -vector of time-varying covariates characterizing the network relationship between units n_i and m . We use $\mathbf{X}_t^{\text{int}} = (\mathbf{X}_{t1}^{\text{int}\top}, \mathbf{X}_{t2}^{\text{int}\top}, \dots, \mathbf{X}_{tN}^{\text{int}\top})^{\top}$ to denote the Np^{int} time-varying covariate vector across all the interventional units. We similarly define $\mathbf{X}_t^{\text{net}}$ as the Np^{net} covariate vector for the time-varying network covariates. Finally $\mathbf{X}_0 = (\mathbf{X}_0^{\text{int}\top}, \mathbf{X}_0^{\text{net}\top}, \mathbf{X}_0^{\text{out}\top})^{\top}$ denotes all time-invariant covariates, while $\mathbf{X}_t = (\mathbf{X}_t^{\text{int}\top}, \mathbf{X}_t^{\text{net}\top}, \mathbf{X}_t^{\text{out}\top})^{\top}$ denotes all $(p^{\text{int}} + p^{\text{net}})N + p^{\text{out}}$ time-varying covariates measured at time t . We use an overline notation to denote a variable's history. For example, for a variable V_t measured over time, we use $\bar{V}_t = (V_t, V_{t-1}, \dots, V_1)^{\top}$, with realization \bar{v}_t . For an integer S , we use $\bar{V}_{t,S}$ to denote the value of V over the $S + 1$ time periods $t, t - 1, \dots, t - S$, as $\bar{V}_{t,S} = (V_t, V_{t-1}, \dots, V_{t-S})^{\top}$. A glossary is included in Supplement A.

Time-invariant covariates may include vegetation type for the interventional units, demographic information for the outcome unit, and the geographic distance of the two for the network information. As we discuss in Section 3.4, time-invariant information need not be collected within our framework. Furthermore, in Section 6 we discuss that, in our study, our approach does not require knowledge of N , nor does it rely on directly observing \mathbf{A}_t or the covariates $\mathbf{X}_t^{\text{int}}$. We acquire time-varying covariates for the outcome units, $\mathbf{X}_t^{\text{out}}$, representing weather information such as temperature, dew point, humidity, wind speed, and wind direction. Additional information on the data is available in Supplement I.

3 Bipartite interference with time series observational data and a random network

In this section, we formalize our causal inference framework for observational time series data with bipartite interference. We introduce exposure mappings for bipartite interference in Section 3.1 and

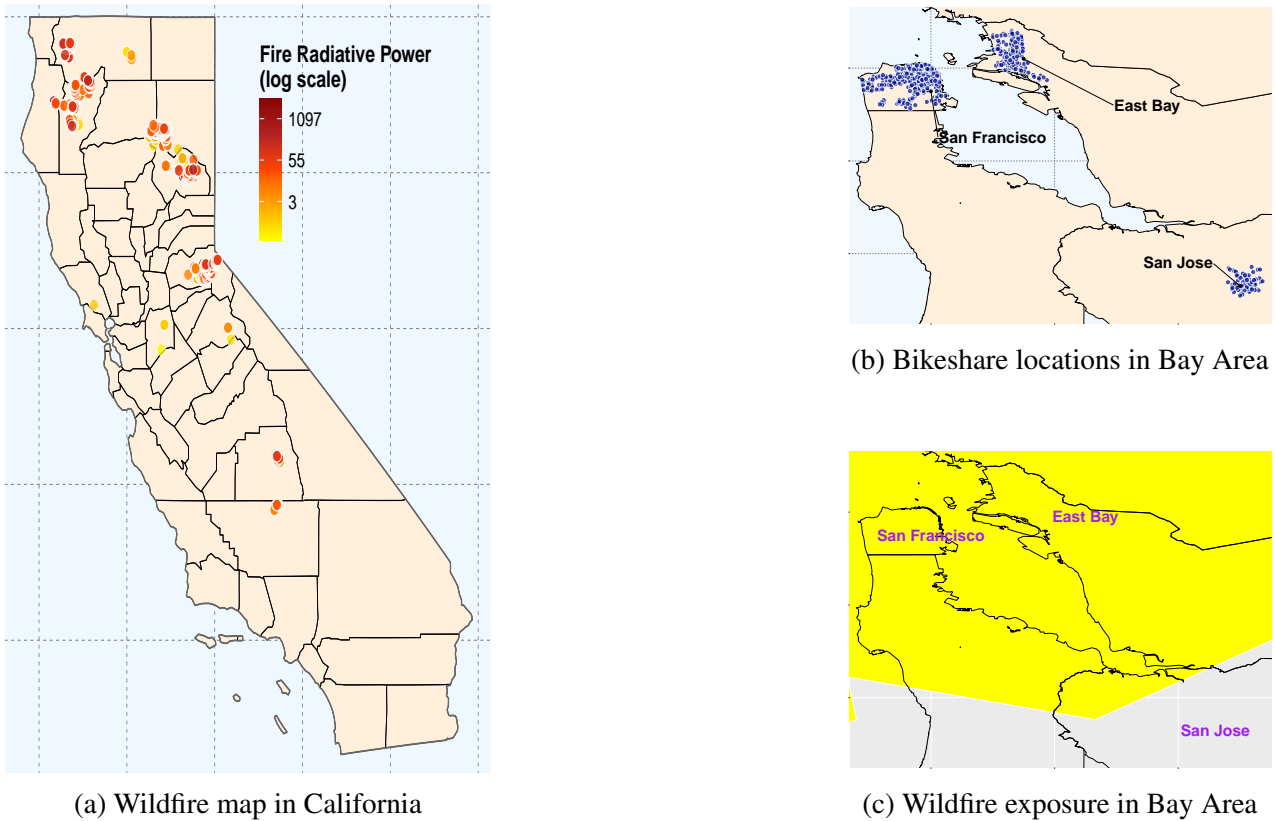


Figure 1: (a) Fire detection point data in California on August 31, 2021. Color scheme shows the fire radiative power which is rates of energy release (in log scale). (b) The locations of the bikeshare stations in the three outcome units. (c) Wildfire smoke coverage on August 31, 2021 as measured by HMS, where yellow represents light, moderate or heavy smoke.

potential outcomes in Section 3.2, define causal estimands for the immediate and carryover effect in Section 3.3, and establish the identifying assumptions in Section 3.4.

3.1 Exposure and carryover mappings

The outcome unit does not receive the intervention itself, it instead experiences the treatment through its connections with potentially treated interventional units. We formalize this using exposure mappings. The function $h_t : \mathcal{A}^N \times \mathcal{G} \rightarrow \mathcal{E}$ maps the interventional units' treatment assignment and the outcome unit's bipartite connection vector at time t to the outcome unit's exposure value at the same time, where \mathcal{E} denotes the set of possible exposure values. Then, $E_t = h_t(\mathbf{A}_t, \mathbf{G}_t)$ is the realized exposure at time t . The function $h_t(\cdot)$ might return a scalar such as the proportion of interventional units with which m is connected that are treated. It can also be completely general, specified to return the vector of treatment levels for all connected interventional units, or it can be extended to incorporate covariates.

In our study, we acquire daily smoke exposure from the National Oceanic and Atmospheric Ad-

ministration’s Hazard Mapping System (HMS). HMS uses satellite imagery to track smoke plumes originating from wildfires and integrates information on fire activity, \mathbf{A}_t , and smoke transport, \mathbf{G}_t , to infer potential smoke exposure in each region on day t , E_t . This structure aligns naturally with our bipartite framework. HMS reports the observed smoke thickness in a given region reflecting the cumulative contribution of smoke. In our study, we consider a binary exposure mapping, $\mathcal{E} = \{0, 1\}$, where a populated area is considered exposed ($E_t = 1$) under light or heavier smoke thickness according to HMS, and unexposed ($E_t = 0$) otherwise. Overall, San Francisco and the East Bay experienced 147 days with smoke, while San Jose experienced 137. Figure 1c shows smoke exposure on August 31, 2021 when two of the areas are exposed.

In our time series setting, we further introduce a function of the L past exposures, termed carryover mapping. Specifically, we specify $h_t^c : \mathcal{E}^L \rightarrow \mathcal{R}$ that maps the vector of the exposures during the past L time periods to a summary value. Similarly to the exposure mapping, the carryover mapping can be arbitrarily complex; it might return a scalar, or be completely general and return the vector of past exposures. We use $R_t = h_t^c(\bar{E}_{t-1, L-1})$ for the observed carryover value at time t , with realization r_t . In our study, we consider a binary carryover mapping defined based on whether at least four days in the past week are exposed, $R_t = I(\sum_{l=1}^7 E_{t-l} \geq 4)$ where $I(\cdot)$ is the indicator function. Under this definition, carryover exposure occurred on 115 days in San Francisco, 166 days in the East Bay, and 104 days in San Jose.

3.2 Potential outcomes under exposure mapping assumptions

Let $Y_t(\bar{\mathbf{a}}_t, \bar{\mathbf{g}}_t)$ denote the potential outcome for unit m at time t had the treatment path of the N interventional units been $\bar{\mathbf{a}}_t$, and under bipartite connection path $\bar{\mathbf{g}}_t$. The observed outcome corresponds to the potential outcome under the observed treatment and network, $Y_t = Y_t(\bar{\mathbf{A}}_t, \bar{\mathbf{G}}_t)$. We include the bipartite graph in the notation for potential outcomes to establish that the graph plays a role in how the potential outcomes vary with the interventional units’ treatment, but we do not assume that the network is manipulable. Potential outcomes are allowed to depend on the most recent and past treatments of the interventional units. The following assumption encodes that the treatment of interventional units and the bipartite network drive the potential outcomes only through the exposure and carryover values.

Assumption 1. For each $t \in \mathcal{T}$, the following holds. Let $\mathbf{a}_s, \mathbf{a}'_s \in \mathcal{A}^N$ and $\mathbf{g}_s, \mathbf{g}'_s \in \mathcal{G}$ be vectors with corresponding exposures $h_s(\mathbf{a}_s, \mathbf{g}_s) = e_s$ and $h_s(\mathbf{a}'_s, \mathbf{g}'_s) = e'_s$ for $s = t, t-1, \dots, t-L$, and carryover exposures $h_t^c(\bar{e}_{t-1, L-1}) = r_t$ and $h_t^c(\bar{e}'_{t-1, L-1}) = r'_t$. If it holds that $e_t = e'_t$ and $r_t = r'_t$, then $Y_t(\bar{\mathbf{a}}_t, \bar{\mathbf{g}}_t) = Y_t(\bar{\mathbf{a}}'_t, \bar{\mathbf{g}}'_t)$, and the potential outcome can be denoted as $Y_t(e_t, r_t)$.

Under Assumption 1, potential outcomes depend on the most recent exposure value, e_t , and the

summarized carryover exposure, r_t . The carryover exposure is allowed to depend on the exposure values during the most recent L time periods. The collection of all potential outcomes for outcome unit m at time t is the set $\mathcal{Y}_t(\cdot) = \{Y_t(e_t, r_t), \text{ for } e_t \in \mathcal{E} \text{ and } r_t \in \mathcal{R}\}$.

In cross-sectional settings, assumptions like Assumption 1 which reduce potential outcomes based on exposure mappings have been discussed in the unipartite [Aronow and Samii, 2017, Forastiere et al., 2021] and bipartite [Zigler et al., 2025, Harshaw et al., 2023, Doudchenko et al., 2020] interference literature. Sävje [2024] discusses the implications of using exposure mappings in the definition of estimands and as assumptions on potential outcomes, providing interesting distinctions between the two.

3.3 Causal estimands for the immediate and carryover effects

We define time-specific estimands for the outcome unit m that represent the immediate and carryover effect of the most recent and past exposures, respectively. Specifically, let $e, e' \in \mathcal{E}$ and $r, r' \in \mathcal{R}$ represent possible values for the exposure and carryover mappings at time t . Then, we define

$$\tau_t^{\text{imm}}(e, e'; r) = Y_t(e, r) - Y_t(e', r), \quad \text{and} \quad \tau_t^{\text{car}}(r, r'; e) = Y_t(e, r) - Y_t(e, r'),$$

representing the effect at time t of switching the most recent exposure from e to e' when the carryover exposure is set to r , and the effect of switching the carryover exposure from r to r' when the most recent exposure is equal to e , respectively.

The time-specific estimands cannot be estimated without parametric assumptions. Instead, we consider target estimands that represent temporally-averaged causal effects. Specifically, we use \mathcal{T}_e to denote the subset of \mathcal{T} with $E_t = e$, and \mathcal{T}_r to denote the subset of \mathcal{T} with $R_t = r$. We define

$$\begin{aligned} \tau^{\text{imm}}(e, e') &= \frac{1}{|\mathcal{T}_e|} \sum_{t \in \mathcal{T}_e} \tau_t^{\text{imm}}(e, e'; R_t) = \frac{1}{|\mathcal{T}_e|} \sum_{t \in \mathcal{T}_e} (Y_t - Y_t(e', R_t)), \quad \text{and} \\ \tau^{\text{car}}(r, r') &= \frac{1}{|\mathcal{T}_r|} \sum_{t \in \mathcal{T}_r} \tau_t^{\text{car}}(r, r'; E_t) = \frac{1}{|\mathcal{T}_r|} \sum_{t \in \mathcal{T}_r} (Y_t - Y_t(E_t, r')), \end{aligned} \tag{1}$$

where we have used that the observed outcome is equal to the potential outcome under the observed exposures, $Y_t = Y_t(E_t, R_t)$. Under the following assumption, these quantities have a causal interpretation as immediate and carryover effect, respectively.

Assumption 2. The immediate and carryover treatment effects are constant in the carryover and most recent exposure value, respectively, i.e., for $t \in \mathcal{T}$ and any $e, e' \in \mathcal{E}$ and $r, r' \in \mathcal{R}$, it holds that $\tau_t^{\text{imm}}(e, e'; r) = \tau_t^{\text{imm}}(e, e'; r')$, and $\tau_t^{\text{car}}(r, r'; e) = \tau_t^{\text{car}}(r, r'; e')$.

We maintain Assumption 2 throughout as it allows us to gain estimation efficiency in estimating immediate effects by pulling information across time periods with different values of the carryover exposure, and similarly for estimating carryover effects. However, we note here that Assumption 2 is *not* necessary. We discuss alternative estimands and estimation strategies that bypass this assumption in Supplement C.3.

Since these estimands represent contrasts of potential outcomes among time periods with a fixed exposure value, they resemble temporal versions of the sample average treatment effect on the treated in the cross-sectional literature without interference. In the presence of multiple outcome units, the estimands in (1) can be averaged across units to represent population-level effects. Alternative estimands tied to the treatment of the interventional units can also be considered, as the impact of changes in the exposure for specific changes in the treatment vector of the interventional units.

The temporally-averaged estimands defined in (1) involve potential outcomes under exposure values that are not observed. Specifically, they involve potential outcomes of the form $Y_t(e', R_t)$ for time periods t with $E_t = e$, and potential outcomes of the form $Y_t(E_t, r')$ for time periods t with $R_t = r$. In principle, to avoid positivity violations, one can assume that all exposure levels considered in the estimands are possible for all time periods [Han et al., 2024]. Instead, if the exposure value e' is impossible for some time period $t \in \mathcal{T}_e$, or the carryover exposure value r' is impossible for some time period $t \in \mathcal{T}_r$, then we assume that this time period is excluded from the corresponding estimand. This is relevant in studies with non-stationarity in the exposure variable where the outcome units are guaranteed to experience the exposure during certain time windows. However, this is not expected to be an issue in our study, where it is always possible that the outcome units do not experience smoke from wildfires.

The estimands presented here represent contrasts of potential outcomes for a single outcome unit averaged over time. In Section 4.4, we discuss how focusing on temporally-average estimands might lead to weaker confounding adjustment requirements compared to estimands that average across units.

3.4 Ignorable assignments: assumptions and results

We establish unconfoundedness assumptions that allow us to estimate the immediate and carryover effects. Our assumptions pertain to the interventional units' treatment assignment and the random bipartite network.

Assumption 3. (Unconfoundedness of the treatment and network assignment). The interventional units' treatment assignment and the network formation at times $t, t-1, \dots, t-L$ is independent of the potential outcomes $\mathcal{Y}_t(\cdot)$, conditional on the value of a function of time at time t , $f(t)$, time-invariant

covariates, and time-varying covariates of the interventional units, the outcome unit, and the network at times $t, t-1, \dots, t-S$, i.e., $P(\bar{\mathbf{A}}_{t,L}, \bar{\mathbf{G}}_{t,L} \mid \mathcal{Y}_t(\cdot), f(t), \bar{\mathbf{X}}_{t,S}, \mathbf{X}_0) = P(\bar{\mathbf{A}}_{t,L}, \bar{\mathbf{G}}_{t,L} \mid f(t), \bar{\mathbf{X}}_{t,S}, \mathbf{X}_0)$.

Under Assumption 3, the treatment level of interventional units can be driven by the characteristics of the outcome unit of interest and general temporal trends such as those that alter the overall prevalence of treatment. Therefore, the allowed treatment assignment mechanisms accommodate complex bipartite dependencies between interventional and outcome units. In particular, this formulation recognizes that confounding may stem not only from the covariates of the interventional units, but also from features of the network and the outcome unit that influence treatment assignment. Furthermore, Assumption 3 allows the formation of connections between the outcome unit and interventional units to depend on temporal trends, as well as on past characteristics of the interventional units, the outcome unit and the network. It can also depend on the realized treatment level, which is relevant in applications where the overall treatment prevalence might lead to higher or lower outreach of the interventional units. The probabilistic formalization of unconfoundedness in Assumption 3 implicitly assumes a random network generation. That said, confounding can also arise in scenarios with a known and fixed network as illustrated in Doudchenko et al. [2020], therefore our results are also applicable in that case.

Below, we establish that Assumption 3 implies that the recent and carryover exposure that the outcome unit receives from the interventional units' treatment through the bipartite network is unconfounded. (The proof is in Supplement B.)

Proposition 1. (Exposure unconfoundedness). If Assumption 3 holds, then the outcome unit's most recent and carryover exposure is independent of the potential outcomes $\mathcal{Y}_t(\cdot)$ conditional on the temporal trend at time t , $f(t)$, and covariate information, i.e., $P(E_t, R_t \mid \mathcal{Y}_t(\cdot), f(t), \bar{\mathbf{X}}_{t,S}, \mathbf{X}_0) = P(E_t, R_t \mid f(t), \bar{\mathbf{X}}_{t,S}, \mathbf{X}_0)$.

This result holds for exposure mappings that are arbitrarily complex. The exposure unconfoundedness statement in Proposition 1 has been evoked as an assumption in previous work on bipartite interference in cross-sectional settings [Zigler et al., 2025, Doudchenko et al., 2020]. Here, exposure unconfoundedness is established while acknowledging that, in a bipartite interference context, the exposure experienced by an outcome unit is governed by mechanisms operating at the treatment and network levels. This has important implications for practice. Assumption 3 yields practical insights for identifying confounders that exist in the treatment-outcome or network-outcome relationships. This is particularly relevant in bipartite interference contexts for which we have a clear grasp of the physical

or mechanistic processes driving the network structure. Therefore, this assumption provides guidance that renders confounding adjustment more tangible, nuanced and actionable within the bipartite setting.

The unconfoundedness result in Proposition 1 means that we can acquire unbiased estimators of the temporally-averaged immediate causal effect, $\tau^{\text{imm}}(e, e')$, in the following manner: Compare outcomes of time periods with similar values of the carryover exposure and covariates in the conditioning set, and different values of their exposure [see Forastiere et al., 2021, for a related discussion], and average over the covariate distribution among time periods with $E_t = e$ [Abadie and Imbens, 2006]. We can similarly acquire unbiased estimators for the carryover effect $\tau^{\text{car}}(r, r')$. Importantly, the covariates \mathbf{X}_0 are constant across time. Therefore, they are implicitly *always* conditioned on when studying the same outcome unit across time. This implies that the time-invariant covariates that create differences in the assignment mechanism of treatment *across* interventional units, or the assignment mechanism of bipartite connections *across* pairs, *need not be measured* when focusing on estimands that average over time. Instead, we need to control for time-varying information only to estimate causal effects. We discuss this further in Section 4.4. Furthermore, as we discuss in Section 4, the temporal trend function $f(t)$ does not need to be known or specified by the analyst.

4 Estimation

Temporally-averaged causal effects can be estimated by controlling for time-varying information for exposure mappings of arbitrary complexity. In our study of the effects of smoke from wildfires, a region’s exposure is binary indicating the presence or absence of smoke exposure for the population residing in the area. Also, we consider a binary carryover exposure based on whether the region had smoke exposure during at least four out of the last seven days. Therefore, from here onwards, we focus on the estimation of causal effects under binary exposure and carryover mappings.

Viewing the time periods as the elementary unit of observation, in Section 4.1 we introduce algorithms for estimating the immediate and carryover effects that match time periods with different exposure values under balance constraints for time-varying information. In Section 4.2, we define the corresponding causal effect estimators and we show, under assumptions on the potential outcome model, that the estimators’ bias is bounded and can be controlled by the algorithmic tuning parameters. We discuss an inferential approach in Section 4.3. Lastly, in Section 4.4, we discuss estimation advantages that arise by focusing on estimands that average over time for a specific outcome unit, over estimands that average across units.

4.1 Algorithms for estimating immediate and carryover effects

We propose algorithms for estimating the immediate and carryover effects. We focus here on the immediate effect among time periods with exposure, $\tau^{\text{imm}}(1, 0)$ in (1). For each exposed time period ($t \in \mathcal{T}_1$ with $E_t = 1$), the algorithm “searches” for a corresponding unexposed time period ($t \in \mathcal{T}_0$ with $E_t = 0$) in close temporal proximity to create a match, such that the matches satisfy overall balance constraints on time-varying information. These algorithms are constructed as integer programming optimization problems with the objective of maximizing the number of matched exposed time periods, under constraints at the level of each time period, each match, and across all matches.

Specifically, let $t_e \in \mathcal{T}_1 = \{t : E_t = 1\}$ and $t_u \in \mathcal{T}_0 = \{t : E_t = 0\}$ denote an exposed and an unexposed time period, respectively. We introduce binary indicators $a_{t_e t_u}$ for each pair of exposed and unexposed time periods such that $a_{t_e t_u} = 1$ if the time periods are matched, and $a_{t_e t_u} = 0$ if not. The objective of the optimization problem is to maximize

$$\max_{\mathbf{a}} \sum_{t_e, t_u} a_{t_e t_u}, \quad (2)$$

over all possible indicators $\mathbf{a} \in \{0, 1\}^{|\mathcal{T}_1| \times |\mathcal{T}_0|}$, where \sum_{t_e, t_u} denotes the summation over both sets of indices, $\sum_{t_e \in \mathcal{T}_1} \sum_{t_u \in \mathcal{T}_0}$. Each time period, exposed or unexposed, can be part of at most one match,

$$\sum_{t_u} a_{t_e t_u} \leq 1, \quad \forall t_e \in \mathcal{T}_1, \quad \text{and} \quad \sum_{t_e} a_{t_e t_u} \leq 1, \quad \forall t_u \in \mathcal{T}_0.$$

The objective in (2) along with the constraint that an exposed time period can be part of at most one match implies that the optimization problem is formulated to maximize the number of matched exposed time periods. In principle, an unexposed time period could be involved in more than one match. However, we have found that in practice doing so leads to inaccurate variance estimation and inference.

We impose constraints that target the balance of temporal trends, the time-varying carryover exposure, and time-varying covariates. In reality little (if any) information is known about the temporal trends $f(t)$. We balance temporal trends indirectly by specifying that the average difference in time of exposed and unexposed time periods across all matches is at most $\delta \geq 0$,

$$\left| \sum_{t_e, t_u} a_{t_e t_u} (t_e - t_u) \right| \leq \delta \sum_{t_e, t_u} a_{t_e t_u}. \quad (3)$$

This constraint does not necessarily imply that *each* of the matched pairs is close in time, rather than they are close *on average*. In order to improve the balance of local temporal trends and to reduce the computationally intensive search for possible match combinations, we also impose that each matched pair of time periods is at most ϵ apart in time,

$$|a_{t_e t_u}(t_e - t_u)| \leq \epsilon, \quad \forall t_e \in \mathcal{T}_1, \forall t_u \in \mathcal{T}_0.$$

Moreover, we specify that the carryover exposure is balanced on average across matched pairs up to some $\delta' \geq 0$,

$$\left| \sum_{t_e, t_u} a_{t_e t_u} (R_{t_e} - R_{t_u}) \right| \leq \delta' \sum_{t_e, t_u} a_{t_e t_u}. \quad (4)$$

We specify a balance constraint on the time-varying covariates between exposed and unexposed matched time periods up to lag S , as

$$\left| \sum_{t_e, t_u} a_{t_e t_u} (\bar{\mathbf{X}}_{t_e, S} - \bar{\mathbf{X}}_{t_u, S}) \right| \leq \mathbf{1}_{(S+1)(Np^{\text{int}} + Np^{\text{net}} + p^{\text{out}})} \cdot \delta' \sum_{t_e, t_u} a_{t_e t_u}, \quad (5)$$

where $\mathbf{1}_n$ is the n -vector of 1s. This balance constraint states that the temporal covariates are on average balanced in matched exposed and unexposed time periods. We discuss the choice of algorithmic parameters ϵ , δ and δ' in Section 4.2.

The covariate vector \mathbf{X}_t includes Np^{int} interventional unit covariates, and Np^{net} network level covariates. If N is large, the constraint in (5) would be high-dimensional, which could drastically reduce the number of matches. In such cases, we propose replacing this balance constraint on the individual values of interventional and network covariates with summaries of the corresponding covariates across interventional units. To create such summaries, consider a vector $\mathbf{q} = (q_1, q_2, \dots, q_N)^\top$. We define $X_{td}^{\text{int, sum.}} = \mathbf{q}^\top (X_{t1d}^{\text{int}}, X_{t2d}^{\text{int}}, \dots, X_{tNd}^{\text{int}})^\top$ as the summary of the d^{th} interventional covariate across units at time t , for $d = 1, 2, \dots, p^{\text{int}}$. Then, $\mathbf{X}_t^{\text{int, sum.}} = (X_{t1}^{\text{int, sum.}}, X_{t2}^{\text{int, sum.}}, \dots, X_{tp^{\text{int}}}^{\text{int, sum.}})^\top$ denotes the \mathbf{q} -summaries of all the interventional units' covariates. We similarly define $X_{td}^{\text{net, sum.}} = \mathbf{q}^\top (X_{t1d}^{\text{net}}, X_{t2d}^{\text{net}}, \dots, X_{tNd}^{\text{net}})^\top$ as a summary of the d^{th} network covariate across interventional units for $d = 1, 2, \dots, p^{\text{net}}$, and $\mathbf{X}_t^{\text{net, sum.}} = (X_{t1}^{\text{net, sum.}}, X_{t2}^{\text{net, sum.}}, \dots, X_{tp^{\text{net}}}^{\text{net, sum.}})^\top$. Finally, we use $\mathbf{X}_t^{\text{sum.}} = (\mathbf{X}_t^{\text{int, sum.}\top}, \mathbf{X}_t^{\text{net, sum.}\top}, \mathbf{X}_t^{\text{out}\top})^\top$ where $X_{td}^{\text{sum.}}$ denotes the d^{th} covariate in $\mathbf{X}_t^{\text{sum.}}$. The balance constraint is placed on the vector $\bar{\mathbf{X}}_{t, S}^{\text{sum.}}$ which includes summaries of the interventional and network covariates,

and the outcome unit covariates over the $S + 1$ time periods $t, t - 1, \dots, t - S$, as

$$\left| \sum_{t_e, t_u} a_{t_e t_u} (\overline{\mathbf{X}}_{t_e, S}^{\text{sum.}} - \overline{\mathbf{X}}_{t_u, S}^{\text{sum.}}) \right| \leq \mathbf{1}_{(S+1)(p^{\text{int}} + p^{\text{net}} + p^{\text{out}})} \cdot \delta' \sum_{t_e, t_u} a_{t_e t_u}.$$

The vector \mathbf{q} controls which covariate summary should be balanced, and its choice will be driven by the problem at hand. For example, by setting $q_i = \frac{1}{n}$ for all i , the algorithm balances the average covariate value across interventional units for matched time periods. Alternatively, q_i could give different weights to the covariate value of interventional units based on their geographic proximity to the outcome unit, or the frequency with which they are connected. Different vectors \mathbf{q} can be used for different covariates, and multiple summaries of the same covariate under different vectors \mathbf{q} could be balanced.

A visualization of the algorithm is in Figure 2. For each exposed time period (green circle), an available unexposed time period (blue circle) is searched within the light blue shaded area, such that the resulting set of exposed and matched unexposed time periods satisfy overall balance constraints. The arrows indicate the resulting matched pairs.

Our approach combines principles from matching [e.g. Rubin, 1973, 1980, Stuart, 2010, Imai et al., 2023] and covariate balancing [Hainmueller, 2012, Imai and Ratkovic, 2014, Zubizarreta, 2015, Li et al., 2018]. As in matching, some constraints are imposed on each pair and restrict which unexposed time periods can be paired with each exposed one. Then, as in covariate balancing methodology, some constraints specify conditions on the overall resulting data set, irrespective of who is paired with whom. Integer programming optimization algorithms have been previously used in the causal inference literature [Zubizarreta, 2012, Zubizarreta et al., 2013, Keele et al., 2014]. Our formalization is different since the fundamental unit of observation is time (rather than physical units) and the confounders correspond to time-varying information. By harvesting the temporal dimension of the data and by investigating the problem through its true bipartite lens, confounding adjustment for interventional, outcome, and network covariates becomes more transparent. For example, as we discuss in the context of our study in Section 6, time-varying confounding due to interventional unit and network covariates might not exist. Such understanding of the needs of confounding adjustment would not be obvious if addressing the same study question by projecting it on a unipartite framework.

For the carryover effect, the proposed algorithm is defined similarly, balancing the most recent exposure in (4) instead of the carryover exposure. The algorithm is discussed in Supplement C.2. Moreover, the algorithm discussed here finds a single unexposed time period as a match to each exposed time period. We additionally designed algorithms which match an exposed time period to two

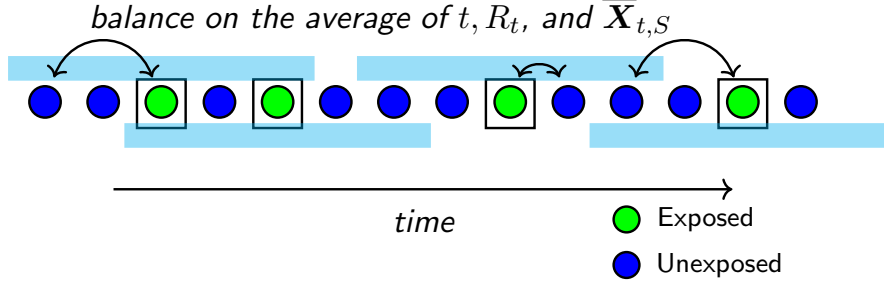


Figure 2: Illustration of the algorithm for the immediate effect. Out of 14 time periods, four are exposed (green circles) and ten are unexposed (blue circles). Available matches for each exposed time period are shaded light blue with the corresponding exposed time period in the middle. In this illustration, $\epsilon = 2$. Out of the possible available unexposed time periods, matches are acquired by maximizing the number of matches subject to balance constraints on t , R_t , and $\bar{X}_{t,S}$.

or one-or-two unexposed time periods. We defer these algorithms to Supplement C.1. Lastly, Assumption 2 of constant immediate and carryover effects is not necessary. However, for estimating the immediate effect, this assumption allows us to pull information across time periods with different carryover exposures and, therefore, gain estimation efficiency, and similarly for estimating the carryover effect. In Supplement C.3, we discuss alternative estimands and estimation procedures for immediate and carryover effects that do not rely on this assumption.

4.2 The matching estimators and theoretical guarantees

The matches produced by these algorithms are the basis for estimating the immediate and carryover causal effects, $\tau^{\text{imm}}(1, 0)$ and $\tau^{\text{car}}(1, 0)$. We focus here on the immediate effect, but the estimator for the carryover effect and its theoretical guarantees are similar (see Supplement C.2).

Let $\mathcal{T}_1^* = \{t : E_t = 1 \text{ and } a_{t_e t_u} = 1 \text{ for some } t_u\}$ denote the set of matched exposed time periods. For $t_e \in \mathcal{T}_1^*$, $Y_{t_e}^*$ is the observed outcome value for its matched unexposed time period which is equal to $\sum_{t_u} a_{t_e t_u} Y_{t_u}$. The estimator of the immediate effect is defined as

$$\hat{\tau}^{\text{imm}}(1, 0) = \frac{1}{|\mathcal{T}_1^*|} \sum_{t_e \in \mathcal{T}_1^*} (Y_{t_e} - Y_{t_e}^*). \quad (6)$$

We implicitly assume that \mathcal{T}_1^* is non-empty. Otherwise, if it is not possible to satisfy the balance constraints, drawing causal inferences from such data might not be trustworthy.

We show that the bias of this estimator is bounded. We consider cases where the outcome is a linear or non-linear function of the exposure, time, and time-varying covariates, in line with Zubizarreta [2015]. We clarify that our approach does not involve fitting an outcome model to the data, and that assuming an outcome model in the following results is to investigate the method's performance and

its reliance on the algorithmic tuning parameters. We first consider the linear case. The proofs are in Supplement D.

Theorem 1. If $Y_t(e, r) = \beta_0 + \beta_1 e + \beta_2 r + \beta_3 t + \beta_4^\top \overline{\mathbf{X}}_{t,S}^{\text{sum.}} + \epsilon_t(e, r)$ for all $t = 1, 2, \dots, T$, with $E(\epsilon_t(e, r) | E_t, t, \overline{\mathbf{X}}_{t,S}^{\text{sum.}}) = 0$, then $|E(\hat{\tau}^{\text{imm}}(1, 0) - \tau^{\text{imm}}(1, 0))| \leq \delta |\beta_3| + \delta' (|\beta_2| + \|\beta_4\|_1)$ where δ and δ' are the balance constraints tuning parameters.

According to Theorem 1, the bias of the matching estimators is bounded by algorithmic parameters controlling how well time-varying information is balanced, and the strength of time-varying confounding in the outcome structure. We note here that we interpret the expectation operator in these derivations by a model-based perspective by seeing the potential outcomes as random variables [Zigler et al., 2025]. An alternative bias bound that involves the tuning parameter ϵ is provided in Supplement D. We discuss the choice of algorithmic parameters at the end of this section.

The linear temporal trend assumption in Theorem 1 might not hold in many settings. However, even when the temporal trend is non-linear, a linear approximation might be relatively accurate in real-world settings where changes over time are expected to happen slowly and data are measured on a relatively short time window. In such cases, the bias of the estimator remains negligible. If temporal trends change more quickly over the study window, additional terms for time would need to be balanced as part of the proposed algorithms. We discuss these points in Supplement D and as part of the following extension where we allow for smooth, non-linear terms for all covariates, including the temporal trend function.

To accommodate non-linearity, we extend the algorithm to impose balance constraints for auxiliary variables targeting higher order and localized versions of time and the measured covariates. Consider a generic variable V_t measured over time. We define a localized version of this variable by breaking its support $[a, b]$ into $(b - a)/\ell$ intervals of length ℓ . The midpoint of the r^{th} interval is denoted by ϕ_r . Then, for each r , we construct the auxiliary variable V_{tr}^\dagger as $V_{tr}^\dagger = (V_t - \phi_r) I(V_t \in [\phi_r - \ell/2, \phi_r + \ell/2])$. We perform this procedure for time t and for the time-varying covariates in $\mathbf{X}_t^{\text{sum.}}$. We include balance constraints as in (5) for these auxiliary variables raised to the power of k for $k = 1, 2, \dots, K - 1$.

We show that the bias of the causal effect estimator is still bounded, where the bound is driven by algorithmic parameters and the smoothness of functions in the outcome model.

Theorem 2. Suppose that the potential outcomes satisfy $Y_t(e, r) = \theta + \beta_1 e + \beta_2 r + h_0(t) + \sum_{s=0}^S p^{\text{int}} + p^{\text{net}} + p^{\text{out}} \sum_{d=1} h_{sd}(X_{(t-s)d}^{\text{sum.}}) + \epsilon_t(e, r)$, with $E(\epsilon_t(e, r) | E_t, t, \overline{\mathbf{X}}_{t,S}^{\text{sum.}}) = 0$ and functions $h_0, h_{01}, h_{02}, \dots, h_{S(p^{\text{int}} + p^{\text{net}} + p^{\text{out}})}$ that are K -times differentiable on their support. If $h_0^{(k)}$ and $h_{sd}^{(k)}$ represent the k^{th} derivative of h_0 and h_{sd} respectively, and $|h_0^{(k)}(t)|, |h_{sd}^{(k)}(x)| \leq c$ for some $c > 0$ for all $s = 0, 1, \dots, S$, covariate $d =$

$1, 2, \dots, p^{\text{int}} + p^{\text{net}} + p^{\text{out}}, t, x$ in the functions' support, and $k = 1, 2, \dots, K$, then $|\mathbb{E}(\hat{\tau}^{\text{imm}} - \tau^{\text{imm}})| \leq C_T \delta + (|\beta_2| + C_X) \delta' + C_{TX} \ell^{K-1}$, where C_T, C_X and C_{TX} are constants proportional to c .

The constants C_T, C_X and C_{TX} depend on the smoothness of the functions with the corresponding indices, and their exact form is given in Supplement D. Importantly, other than smoothness assumptions, these results do not rely on restrictions on how temporal trends influence the outcome, and a non-stationary (such as monotonic) outcome poses no further challenges. Theorem 2 establishes that, by setting the algorithms' tuning parameters δ, δ' and ℓ to be small enough, the bias of the corresponding causal effect estimators can be guaranteed to be negligible. Since the most recent and carryover exposures are binary, the form $\beta_1 e + \beta_2 r$ in the outcome model does not impose any restriction other than the no-interaction Assumption 2. Extending our results to allow for interactions among the covariates would be theoretically straightforward. However, practically, the necessary additional balancing constraints might hinder our ability to find adequate matches.

The choice of $(\epsilon, \delta, \delta', \ell)$ has a direct impact on the resulting number of matches with smaller values imposing stricter constraints. Smaller values of δ and δ' imply a smaller maximum possible bias, and they can, in principle be set arbitrarily small, even to zero. In practice, using small values for δ, δ' might return a small number of matches and an estimated effect that is not representative of all exposed time periods. As with all matching procedures, the estimated immediate effect is representative of the matched exposed time periods only, $\tilde{\tau}^{\text{imm}}(1, 0) = \sum_{t_e \in \mathcal{T}_1^*} [Y_{t_e}(1, R_{t_e}) - Y_{t_e}(0, R_{t_e})] / |\mathcal{T}_1^*|$. When the proportion of matched exposed time periods is small, the estimate's interpretation might be complicated, and might differ from the effect on all the exposed time periods $\tau^{\text{imm}}(1, 0)$ in the presence of heterogeneity across time (see Supplement H).

Therefore, the choice of algorithmic tuning parameters should be guided by domain knowledge and the characteristics of the dataset. If the temporal trend is believed to change slowly over time, a larger ϵ value can be used to allow for more available unexposed time periods in forming each match. In the absence of other information, we recommend setting $\delta = \delta' = 0.05$ or 0.1 as a default for standardized covariates [Zubizarreta, 2015] and performing sensitivity analysis to such choices.

4.3 Inference

By viewing our algorithm as part of the design phase, we construct confidence intervals conditional on the resulting data set of matches [Ho et al., 2007]. As shown in (6), our estimators are averages of differences between a time period's observed outcome and the outcome of its match. We construct Wald-type confidence intervals using the standard deviation of the outcome differences. Specifically, for the immediate causal effect, we define $\hat{s}^2 = \sum_{t_e \in \mathcal{T}_1^*} (Y_{t_e} - Y_{t_e}^* - \hat{\tau}^{\text{imm}}(1, 0))^2 / (|\mathcal{T}_1^*| - 1)$, and we

construct an α -level confidence interval as $[\hat{\tau}^{\text{imm}}(1, 0) - z_{1-\alpha/2} \hat{s} / \sqrt{|\mathcal{T}_1^*|}, \hat{\tau}^{\text{imm}}(1, 0) + z_{1-\alpha/2} \hat{s} / \sqrt{|\mathcal{T}_1^*|}]$, where $z_{1-\alpha/2}$ is the $1 - \alpha/2$ quantile of the standard normal distribution. We similarly acquire a p-value for testing the null hypothesis of no causal effect on the outcome unit, $H_0 : \tau^{\text{imm}}(1, 0) = 0$ v.s. $H_A : \tau^{\text{imm}}(1, 0) \neq 0$ as $p = P(|Z| > \sqrt{|\mathcal{T}_1^*|} |\hat{\tau}^{\text{imm}}(1, 0)| / \hat{s})$, where $Z \sim N(0, 1)$. P-values in one-sided hypothesis tests can be obtained similarly. The inferential procedure for the carryover effect proceeds similarly using the matches acquired from the carryover algorithm.

In Supplement E we investigate the proposed inferential procedure. There, we show that the confidence intervals we construct are expected to cover the true value at least $(1 - \alpha)100\%$ of the time, under certain conditions. The extent of conservativeness depends on the magnitude of imbalance of time-varying information within each matched pair. As a result, the conservativeness of the inferential procedure would be alleviated if our estimator was based on matches from an alternative algorithm that balances covariates within each match. In practice, however, such alternative could return substantially fewer matches. There, we also discuss that the inferential approach performs well even with time series data that display temporal correlation. We illustrate these points in simulations in Supplement H.

In the presence of multiple outcome units, we discuss hypothesis testing for whether the exposure has an effect on any outcome unit in Supplement C.4.

4.4 The potential advantages of temporal analyses in bipartite settings

Here, we discuss the case with multiple outcome units measured over time and the potential advantages of focusing on time series data for an outcome unit, instead of the cross-sectional approach of focusing on a collection of units measured at a given time period.

In this setting, cross-sectional estimands that average across outcome units for each time period could be considered. An example of cross-sectional immediate effect is $\gamma_t(e, e'; r) = \frac{1}{M} \sum_{j=1}^M [Y_{tj}(e, r) - Y_{tj}(e', r)]$ which averages across M outcome units for a given time period, where we have extended the notation to include the subscript j corresponding to outcome unit $m_j \in \{m_1, m_2, \dots, m_M\}$. Estimation of cross-sectional estimands requires that we measure and adjust for all meaningful differences across units that confound the exposure-outcome relationship, which can be complex and high-dimensional. For example, in the study of [Zigler and Papadogeorgou \[2021\]](#), the treatment assignment of power plants and population health can vary across the United States in intricate ways, all of which would need to be measured and adjusted. In our study of Section 2 with three outcome units, confounding adjustment for estimating cross-sectional estimands would be impossible.

In this setting, our approach would harvest the time series aspect of the data and be applied to each outcome unit separately. Estimation of the temporally-average causal effects for each outcome unit

requires that we account for time-varying confounding only, which might be simpler to understand and measure, an observation that was also noted in the interrupted time series literature [Rockers et al., 2015] and in the causal inference literature [Imai and Kim, 2021]. For example, consider the case where the interventional units’ treatment is constant over time. Our results show that confounding would only be due to covariates that predict the network and the outcome. If the random network depends only on the units’ time-invariant characteristics like their geographic distance, no confounding adjustment would be necessary to estimate interpretable and policy-relevant estimands. Alternatively, if the network is driven by naturally-occurring processes with temporal variation such as meteorology, one would only need to account for those for causal effect estimation, which are simpler to understand and measure. Furthermore, if confounding variables show relatively smooth temporal trends during the time window under study, such as weather variables, collecting them is unnecessary since they are indirectly balanced in our algorithms (Theorems 1 and 2).

The inherent bipartite nature of the data suggests that temporal confounding is likely to display smoother trends compared to unipartite scenarios. In bipartite settings, the separation of physical units implies that decisions affecting one set of units may not immediately manifest and impact the other. Consequently, if an interventional unit variable influences the outcome units, it might be due to its overall trend over time, such as its average over preceding time periods. In that case, this ‘moving average’ covariate value will be relatively smooth across time. If left unmeasured, the bias occurring due to its non-temporal component is expected to be small. We illustrate this in the simulations of Section 5.

5 Simulation Study

We perform simulations to investigate the performance of our estimators and the properties of our inferential procedure.

5.1 Simulation setup

We generate data that closely resemble the data from our study described in Section 2 in the following ways. First, we consider a time window of $T = 1,003$ time periods, which is of equal length to the temporal window in our study. Second, we generate time-varying covariates with realizations that closely resemble the pattern of the time-varying covariates in our data. We provide an overview of our simulation setup here, with additional information on how the data are generated and the different simulation scenarios deferred to Supplement F.

We consider $N = 50$ interventional units. For each interventional unit n_i , we generate a unit-

Table 1: Table of the five confounding scenarios considered in our simulations, in which the treatment \mathbf{A} , the network \mathbf{G} , and the observed outcome \mathbf{Y} are generated based on the covariates marked with \times .

Scenario	Smooth time			Location-varying			Time-varying		
	t	f^{int}	f^{out}	loc	$\mathbf{X}_0^{\text{int}}$	$\mathbf{X}_0^{\text{out}}$	$\mathbf{X}_{t_i}^{\text{int}}$	$\mathbf{X}_{t_j}^{\text{out}}$	R_t
(a) No confounders	\mathbf{A}								
	\mathbf{G}								
	\mathbf{Y}					\times			
(b) Time-smooth confounders	\mathbf{A}	\times							
	\mathbf{G}			\times					
	\mathbf{Y}		\times						
(c) Location-varying confounders	\mathbf{A}				\times				
	\mathbf{G}			\times					
	\mathbf{Y}					\times			
(d) Time-varying confounders	\mathbf{A}						\times		\times
	\mathbf{G}	\times							
	\mathbf{Y}							\times	\times
(e) All confounders	\mathbf{A}		\times		\times		\times		\times
	\mathbf{G}	\times		\times					
	\mathbf{Y}		\times			\times		\times	\times

specific temporal trend, $f_i^{\text{int}}(t)$. The temporal trend for the outcome unit m , $f^{\text{out}}(t)$, is set equal to the trend of its geographically-closest interventional unit. For each interventional unit n_i , we also consider $p_0^{\text{int}} = 1$ time-invariant covariate X_{0i}^{int} , and $p^{\text{int}} = 5$ time-varying covariates $\mathbf{X}_{t_i}^{\text{int}} = (X_{t_i1}^{\text{int}}, X_{t_i2}^{\text{int}}, \dots, X_{t_i5}^{\text{int}})^\top$. Similarly, an outcome unit m has $p_0^{\text{out}} = 1$ and $p^{\text{out}} = 5$ time-invariant and time-varying covariates denoted by X_0^{out} and $\mathbf{X}_t^{\text{out}} = (X_{t1}^{\text{out}}, X_{t2}^{\text{out}}, \dots, X_{t5}^{\text{out}})^\top$, respectively. Time-varying covariates include location-specific variation, and hypothetical seasonality and extreme weather trends in order to capture our observed data for temperature, humidity, precipitation, wind speed, and wind direction. In Supplement F, we illustrate that the covariates in our simulated data match the observed covariates closely. In order to evaluate an approach that uses information across outcome units instead of time (see our discussion in Section 4.4), we generate 200 outcome units using this setup, though our approach is only fit on one of them.

We consider five data generative models corresponding to settings with different confounding structure. Under the different scenarios, the treatment assignment for interventional unit n_i is allowed to depend on smooth temporal trends through $f_i^{\text{int}}(t)$ and on covariates through X_{0i}^{int} and $\mathbf{X}_{t_i}^{\text{int}}$. The entries of the bipartite network are generated independently from Bernoulli distributions with probability that might depend on time, location, and units' spatial proximity. The exposure of unit m at time t is specified as $E_t = I(\sum_{i=1}^N A_{ti}G_{tij} \geq d)$, where d is chosen such that the proportion of time periods with exposure is approximately 20%. The carryover exposure is defined as whether the majority of the pre-

vious seven time periods are exposed or not, $R_t = I(\frac{1}{7} \sum_{s=t-7}^{t-1} E_s \geq 4)$, as in our study. The outcome is allowed to depend on the exposure, the carryover exposure, the smooth temporal trend $f^{\text{out}}(t)$, and the covariates X_0^{out} and $\mathbf{X}_t^{\text{out}}$.

Table 1 shows the variables that are used in each data generative model component across the different scenarios. These five scenarios correspond to five different confounding structures for the exposure-outcome relationship: (a) no confounding, (b) confounding by smooth temporal variables, (c) confounding by location-varying variables, (d) confounding by time-varying covariates, and (e) all types of confounding. Confounding arises if a predictor of the outcome is correlated with a predictor of the treatment assignment, the bipartite network, or both. For example, in scenario (b) the temporal trend components $f_i^{\text{int}}(t)$ and $f^{\text{out}}(t)$ induce confounding due to their common smooth temporal trend, and in scenario (d) the time-varying covariates for the interventional and outcome units, which are defined based on one another, induce confounding of the exposure-outcome relationship.

5.2 Estimation

We estimate the temporally-averaged causal effect specific to an outcome unit. We fit our algorithms that match an exposed time period to one (Section 4), one-or-two or two (Supplement C.1) unexposed time periods, and we denote them as 1-1, 1-1/2, and 1-2 in the results, respectively. We employ balance constraints on the time-varying covariates $\mathbf{X}_t^{\text{out}}$. Since $f_i^{\text{int}}(t)$ and $f^{\text{out}}(t)$ represent smooth temporal trends, we do *not* consider balance constraints on them, illustrating that the constraints on time suffice. For a consistent choice of tuning parameter δ' across the time-varying covariates, we standardize each one of them using the pooled standard deviation of exposed and unexposed time periods [Rosenbaum and Rubin, 1985]. Specifically, the entries of the d^{th} covariate $\mathbf{X}_{.d}^{\text{out}} = (X_{1d}^{\text{out}}, X_{2d}^{\text{out}}, \dots, X_{Td}^{\text{out}})^{\top}$ are divided by $\sqrt{(\text{Var}(\mathbf{X}_{(e=1)d}^{\text{out}}) + \text{Var}(\mathbf{X}_{(e=0)d}^{\text{out}}))/2}$, where $\text{Var}(\mathbf{X}_{(e=1)d})$ and $\text{Var}(\mathbf{X}_{(e=0)d})$ is the variance of the covariate among exposed and unexposed time periods, respectively. Therefore, δ' denotes the allowed covariate imbalance as the proportion of the covariate standard deviation. We consider three sets of tuning parameters $(\delta, \delta', \epsilon)$. The results shown here correspond to values (2, 0.05, 6). Alternative choices for the tuning parameters are discussed in Section 5.4. We estimate the causal effect using (6), and acquire 95% confidence intervals as detailed in Section 4.3.

Since there do not exist alternative approaches in the literature for estimating causal effects in bipartite time series settings, we implement three naïve approaches, and estimators based on linear regression, and inverse propensity weighting (IPW). `Naïve-t` uses temporal information for the single outcome unit and estimates an effect as the difference of mean outcomes between exposed and unexposed time periods. `Naïve-j` uses information across the 200 outcome units for a single time period

and estimates an effect as the difference of mean outcomes between exposed and unexposed outcome units. `Naïve-all` estimates an effect as the overall difference of mean outcomes in exposed and unexposed time periods across units. `Naïve-j` and `Naïve-all` are the only two approaches that use information across outcome units. The linear regression estimator (`Reg`) corresponds to the coefficients of the exposure and the carryover exposure in a model that incorporates all covariates linearly. For the IPW estimator (`IPW`), we consider a logistic propensity score model for the exposure on the covariates, and estimate the causal effect based on the average of the inverse-propensity weighted outcomes. Additional details on all approaches are included in Supplement G.

5.3 Simulation results

Table 2 shows the estimation and inferential results for estimating the immediate and carryover effect for one outcome unit using the three naïve approaches, the estimator based on linear regression, the IPW estimator, and the three proposed estimators. For each estimator we report bias, mean squared error, and coverage of 95% intervals. For the proposed algorithms, we further report the proportion of exposed time periods that were matched, and the success rate that the optimization problem was solved.

We focus first on the immediate causal effect. In the absence of confounding factors (scenario (a)), all estimators are unbiased. In the presence of location-varying confounding (scenario (c)), the `Naïve-j` and `Naïve-all` estimators are the only ones exhibiting bias, illustrating that estimators that focus on a specific outcome unit are robust to location-varying confounding (see Section 4.4). The `Naïve-t` estimator is biased with 95% intervals that cover the true value less than 95% of the time in the presence of temporal confounding (scenarios (b) and (d)). The regression and IPW estimators are biased when time-varying confounders exist (scenarios (d) and (e)). In contrast, the proposed estimators perform well in terms of bias and coverage of intervals across all confounding scenarios. Interestingly, even though the theoretical guarantees of the proposed estimator (Section 4.2) rely on the outcome model that the regression estimator fits, the proposed approach, which combines principles of matching and calibration, is more robust to outcome misspecification. These results are in line with existing results in the literature on the relative merits of matching, calibration, and regression approaches [e.g., Imai et al., 2023]. Lastly, the proposed algorithms successfully return matches across at least 97% of data sets, indicating that our optimization formulation is not overly restrictive and is practical for general use.

For the carryover effect, all alternative estimation strategies show varying degrees of bias and undercoverage depending on the confounding structure, suggesting higher sensitivity to model as-

assumptions. In comparison, the proposed estimators remain close to unbiased with coverage that is approximately or higher than nominal. However, compared to the immediate effect algorithms, the algorithm for the carryover effect returns a solution to the optimization problem in a smaller proportion

Table 2: Bias, mean squared error (MSE), coverage of 95% intervals (%), proportion of exposed time points matched (%), and proportion of simulations with a solution to the optimization problem (%). We consider the 3 naïve approaches denoted with ‘N’, regression (Reg), inverse propensity weighting (IPW), and the three proposed estimators. The simulation scenarios correspond to (a) No confounders, (b) Time-smooth confounders, (c) Location-varying confounders, (d) Time-varying confounders, and (e) All confounders.

		Immediate effect					Carryover effect				
		Bias	MSE	Cover	Prop	Success	Bias	MSE	Cover	Prop	Success
(a)	N-t	0.002	0.008	94.2	-	-	0.032	0.105	95.5	-	-
	N-j	0.022	0.306	91.4	-	-	0.072	0.263	98.2	-	-
	N-all	0.001	0.000	96.4	-	-	0.005	0.013	70.2	-	-
	Reg	0.002	0.008	94	-	-	0.010	0.095	96	-	-
	IPW	0.002	0.008	93.8	-	-	0.009	0.105	91.8	-	-
	1-1	0.011	0.013	95.8	100	100	0.033	0.160	93.8	96.5	87.6
	1-1/2	0.010	0.013	95.2	100	100	0.042	0.162	93.4	96.8	91.2
	1-2	0.009	0.010	95.1	98.3	100	0.030	0.141	95.3	81.5	85.6
(b)	N-t	0.031	0.018	85.6	-	-	0.060	0.123	73	-	-
	N-j	0.001	0.037	94	-	-	-0.081	0.064	91.2	-	-
	N-all	0.008	0.002	26.6	-	-	-0.041	0.007	21.6	-	-
	Reg	0.020	0.011	92.6	-	-	0.037	0.088	82.8	-	-
	IPW	0.019	0.011	92.8	-	-	0.024	0.074	82.2	-	-
	1-1	0.015	0.011	94.4	98.7	100	0.028	0.060	95	92.7	87.2
	1-1/2	0.015	0.011	94.8	98.7	99.8	0.039	0.054	94.1	92.7	88.4
	1-2	0.021	0.010	94.2	87.5	97	0.036	0.056	95.3	62.9	84.8
(c)	N-t	0.001	0.008	96.2	-	-	0.022	0.112	94.5	-	-
	N-j	0.106	0.074	92.6	-	-	0.238	0.145	83.6	-	-
	N-all	0.113	0.019	7.4	-	-	0.563	0.354	0	-	-
	Reg	0.000	0.008	96.2	-	-	-0.010	0.133	94.3	-	-
	IPW	0.000	0.009	95.4	-	-	-0.010	0.145	87.9	-	-
	1-1	0.008	0.014	95.4	100	100	0.016	0.107	95.7	96.7	69.8
	1-1/2	0.011	0.014	95.4	100	100	0.026	0.113	94.6	96.7	73.6
	1-2	0.013	0.011	94.8	96.9	99.8	0.019	0.089	94.3	81.5	66.2
(d)	N-t	4.782	23.094	0	-	-	5.028	25.583	0	-	-
	N-j	0.022	0.115	94.2	-	-	0.005	0.163	96.2	-	-
	N-all	4.841	23.487	0	-	-	5.086	25.938	0	-	-
	Reg	0.211	0.061	57.4	-	-	0.393	0.183	26.6	-	-
	IPW	0.422	0.224	39.6	-	-	0.367	0.207	62.2	-	-
	1-1	0.056	0.038	98.4	96.4	100	0.069	0.062	98.6	79.7	100
	1-1/2	0.062	0.038	97.6	96.4	100	0.069	0.067	99	79.7	100
	1-2	0.040	0.037	98.8	69.3	100	0.057	0.093	98.9	33.6	99.8
(e)	N-t	4.342	19.074	0	-	-	4.694	22.416	0.2	-	-
	N-j	0.559	0.614	73.6	-	-	1.167	1.802	37.6	-	-
	N-all	4.670	21.884	0	-	-	5.108	26.204	0	-	-
	Reg	0.149	0.037	72	-	-	0.413	0.209	17.2	-	-
	IPW	-0.480	0.300	35.8	-	-	-0.511	0.497	56.3	-	-
	1-1	0.052	0.030	97.4	81.3	99.8	0.085	0.049	99.2	54.6	98.4
	1-1/2	0.043	0.032	97.4	81.4	100	0.083	0.048	99	54.7	98.6
	1-2	0.025	0.031	97.7	53.5	97	0.049	0.096	99.4	20.1	96

of data sets, and it maintains a smaller proportion of time periods with carryover exposure. This results from the frequency and density of the carryover exposure compared to the most recent exposure, which illustrates that different exposure structures might alter the performance of the algorithm.

Lastly, the $1-1$ and $1-1/2$ algorithms yield the same proportion of matched exposed time periods. This alignment is logical as the objective of the optimization problem is to maximize the number of matched exposed time periods, with the matches acquired under the $1-1$ algorithm also possible under the $1-1/2$ algorithm. As expected, the $1-2$ algorithm yields the lowest proportion of matched exposed periods due to its requirement to find two relevant unexposed periods. Despite that, the corresponding estimator performs comparably to the estimators corresponding to the two other algorithms. We recommend that the $1-2$ algorithm is preferred when it returns a similar proportion of matched exposed time periods compared to the $1-1$ and $1-1/2$ algorithms.

5.4 Additional simulations

We investigate the performance of the proposed algorithms with additional simulations in Supplement H, with details on the data generative mechanism in Supplement H.1. In Supplement H.2, we compare the three proposed algorithms and corresponding estimators under different sparsity levels of the exposure. In Supplement H.3, we consider estimation and inference in the presence of multiple outcome units. In Supplement H.4, we show that the matching estimators *without* any adjustment for measured covariates are unbiased under temporally-smooth confounding, illustrating that smooth temporal trends are implicitly adjusted through the time constraints and need *not* be measured. In Supplement H.5, we assess the performance of matching methods with alternative tuning parameter values. Results are generally robust to the choice of δ and ϵ , and despite some residual bias under larger δ' values in some scenarios, interval coverage is close to nominal across all cases. In Supplement H.6, we illustrate that applying constraints on the covariates within *each* match alleviates the overcoverage of 95% intervals, supporting the discussion in Section 4.3. All the simulations are under a homogeneous treatment effect to separate the evaluation of estimation efficiency from the discussion on targeted estimand, and ease comparison of estimators. In Supplement H.7, we show that under treatment effect heterogeneity, results from the proposed estimators are representative of the matched population of exposed time periods. Lastly, in Supplement H.8, we demonstrate that temporal correlation in the outcome has minimal effect on the performance of our inferential procedure and we compare it to an approach that uses the Newey-West variance estimator [Newey and West, 1986].

6 The Impact of Wildfire Smoke Exposure on Bikeshare Hours

Traditional unit-to-unit cross-sectional analyses would be infeasible in our study as it would be impossible to control for attributes of interventional and outcome units with only three outcome units (see discussion in Section 4.4). However, given daily data on 1,003 days, approximately 140 of which are exposed across the three areas, our approach can be applied to estimate the effect of smoke exposure on each outcome area, without the need to consider location-varying covariates, and controlling for time-varying confounding only.

The proposed algorithms balance daily temperature, humidity, precipitation, wind speed, and wind direction as potential time-varying confounders, while smooth seasonal trends are balanced implicitly. We find it plausible that no further covariates are necessary beyond weather-related data to meet the unconfoundedness assumptions. This reasoning stems from our understanding of the bipartite structure of the problem: factors (other than weather conditions) influencing wildfire occurrence and smoke dispersion patterns are unlikely to impact biking activity in distant locations, and economic indices fluctuating over time that might affect biking activity are likely unrelated to wildfire presence in North American forests. Therefore, even though our analysis is performed at the level of the outcome unit without using interventional unit information explicitly, the appropriateness of the estimation approach is based on the investigation of unconfoundedness from a bipartite perspective. Consequently, even though implementation does not necessarily differ, there exist subtle, yet important differences in how confounding might be investigated under a bipartite lens.

We estimate the immediate and carryover effects for each area separately using the Naïve- t estimator described in Section 5 and the estimators based on the proposed algorithms that match one exposed time period to one (Section 4), two or one-or-two (Supplement C.1) unexposed time periods. We set the tuning parameters of the proposed algorithms as $(\delta, \delta', \epsilon) = (2, 0.1, 6)$.

Table 3 shows the causal effect estimates, p-values, and the number of exposed time periods used by each approach. Effect estimates are in hours of bikeshare rentals. The naïve approach, which uses all the exposed (and unexposed) time periods, estimates that both the immediate and the carryover effect is positive (albeit, not statistically significant). These results under the naïve approach imply that the most recent and past smoke exposure increase biking activity. This unrealistic result is likely due to temporal confounding since exposure is more common during the late summer and fall months when there is also more biking activity.

Instead, effect estimates from the proposed algorithms and estimators return more realistic results. We estimate that smoke exposure reduces biking activity in San Francisco, while it does not have an

impact in the East Bay and San Jose areas. These results are statistically significant at the 0.05 level for San Francisco for the estimator corresponding to the algorithm that matches one exposed time period to one or one-or-two unexposed time periods (1-1, and 1-1/2). Since exposure is relatively dense during the summer and fall months, the algorithm that searches for two unexposed time periods for each exposed one returns approximately half the number of matches compared to the other two algorithms, which might explain the larger p-values. Based on the algorithm’s constraints, the proposed estimator uses unexposed time periods during the summer and fall months only (see Supplement I.2 for an illustration).

For the carryover effect, none of the estimates are statistically significant at the 0.05 level, with point estimates generally close to 0. This suggests that smoke exposure during the previous week does not have an impact on current biking activity. However, the proportions of time periods with carryover exposure that were matched are relatively low, especially for the 1–2 algorithm. This is due to the dense carryover exposure conditions in summer and fall and a small number of unexposed time periods which restricts the quantity of available matches.

We conducted a sensitivity analysis to the definition of exposure, and performed the same analysis when an area is categorized as exposed during a given day under medium or high smoke thickness, and unexposed under no or light smoke thickness (see Supplement I.3). We find that all effect estimates are negative and similar or larger in magnitude in that case, even though most results are not statistically significant, likely due to the small number of days with exposure (40 or less).

Table 3: The immediate and carryover effect estimates of wildfire smoke on hours of bikeshare rentals in San Francisco, East Bay, and San Jose for Naïve- t and the matching estimators. For each region, the three columns correspond to the estimate, p-value (bold font if below 0.05), and number of matches.

	San Francisco			East Bay			San Jose		
	Est	p-value	#Exp	Est	p-value	#Exp	Est	p-value	#Exp
	<u>Immediate effect</u>								
Naïve- t	268.520	(1.000)	147	24.542	(1.000)	147	10.635	(1.000)	137
1-1	-107.457	(0.016)	101	-1.218	(0.340)	103	-0.055	(0.491)	99
1-1/2	-85.293	(0.028)	101	0.621	(0.586)	103	-1.815	(0.239)	99
1-2	-58.845	(0.117)	56	2.266	(0.736)	59	0.384	(0.514)	59
	<u>Carryover effect</u>								
Naïve- t	318.650	(1.000)	115	25.129	(1.000)	166	17.249	(1.000)	104
1-1	-14.092	(0.441)	71	-4.423	(0.102)	72	3.671	(0.869)	65
1-1/2	-7.649	(0.456)	71	-3.551	(0.135)	72	3.423	(0.853)	65
1-2	39.725	(0.970)	31	-0.228	(0.476)	32	1.922	(0.856)	31

7 Discussion

In this manuscript, we introduced a causal inference framework for time series data with bipartite interference, a random network, and carryover effects. Focusing on time-averaged estimands, we showed that controlling for time-varying information allows us to attribute outcome differences to exposure’s causal effects. We introduce algorithms that combine notions from matching and covariate balancing, with corresponding estimators which perform well across various scenarios. In our study, we find some evidence that smoke from wildfires reduces population mobility.

Alternative estimation approaches from the causal inference literature can be adapted to our framework. Weighting or matching on the propensity of exposure is one such alternative. However, since the exposure is defined based on the interventional units’ treatments and the network, the exposure propensity score would require that we model the high-dimensional treatment and network assignment incorporating potential time-invariant confounders, which is practically difficult to do accurately. At the same time, outcome modeling approaches like panel regression [[Arkhangelsky et al., 2024](#), [Imai and Kim, 2021](#)] would require correct specification of the confounding adjustment functional form, which is particularly complicated in bipartite settings where confounding relates to both the treatment and the network. Balancing methods [[Hainmueller, 2012](#), [Fong et al., 2018](#)] and methods from the econometrics literature [[Imai and Kim, 2021](#)] may assign weights to unexposed periods that are temporally distant from the exposed periods, and therefore might be susceptible to confounding by temporal trends. Our proposed approach which combines matching and covariate balancing bypasses these issues.

Despite the merits of the proposed framework, several open questions remain. First, future work can extend our estimation framework to time series settings under more complicated exposure mappings. In principle, even in the case where the exposure is not binary, matching and balancing algorithms designed for binary exposures can still be useful for estimating interpretable effects. For instance, in the setting of [Pouget-Abadie et al. \[2019\]](#), [Doudchenko et al. \[2020\]](#), [Brennan et al. \[2022\]](#), and [Harshaw et al. \[2023\]](#) where an outcome unit’s exposure ranges from 0 to 1, the proposed algorithms can be extended to accommodate a categorized exposure. Second, future work can investigate the impact of misspecification of the exposure and carryover mapping functions to matching or balancing estimators, bipartite interference settings, or observational data following the work for Horvitz-Thompson estimators under exposure misspecification in the unipartite literature [[Sävje, 2024](#), [Leung, 2022](#), [Weinstein and Nevo, 2026](#)].

Third, in future work it is interesting to investigate how to tailor bipartite methodology to specific

study designs and construct estimators with robustness properties to model misspecification. For example, in settings where the propensity score is known or can be estimated reliably, one can draw from the literature with independent data to construct doubly robust estimators by incorporating constraints on the propensity score in the algorithm of Section 4 or by matching on both the propensity and the prognostic score [Antonelli et al., 2018]. In shift-share study designs for observational settings with exogenous shocks, it is interesting to investigate how to design alternative, robust estimators by controlling for the expected exposures derived from multiple exposure candidate models [Borusyak and Hull, 2023], or by employing ensemble approaches that combine estimators with complementary failure modes [Gulek and Vives-i Bastida, 2025]. Lastly, it is interesting to consider extending synthetic control approaches, such as matrix completion [Athey et al., 2021] and the augmented synthetic control method [Ben-Michael et al., 2021], to the bipartite setting. However, it is unclear how the methodology can incorporate spatial correlation across units [Grossi et al., 2025], where nearby similar areas might experience the exposure simultaneously, while distant areas may have less relevance to the target, rendering it difficult to identify a valid donor pool. Alternatively, future work can investigate how outcome autoregressive models can be employed for the estimation of causal effects in bipartite settings with time series data and carryover exposures, which would likely require additional assumptions [Antonelli et al., 2024]. Investigating, adapting and extending these approaches to the bipartite setting where interventional and outcome units are separate remains a promising area for future work.

Acknowledgements

We thank Corwin Zigler, Fabrizia Mealli, Lucas Henneman, Jean Pouget-Abadie, and Jennifer Brennan for their useful comments in the preparation of this manuscript.

Funding

The authors are grateful for support from the National Science Foundation under Grant No 2124124.

References

- Alberto Abadie and Matias D Cattaneo. Econometric methods for program evaluation. *Annual Review of Economics*, 10:465–503, 2018.
- Alberto Abadie and Guido W Imbens. Large sample properties of matching estimators for average treatment effects. *Econometrica*, 74(1):235–267, 2006.
- Anish Agarwal, Sarah H Cen, Devavrat Shah, and Christina Lee Yu. Network synthetic interventions: A causal framework for panel data under network interference. 2023.

- Joseph Antonelli, Matthew Cefalu, Nathan Palmer, and Denis Agniel. Doubly robust matching estimators for high dimensional confounding adjustment. *Biometrics*, 74(4):1171–1179, 2018.
- Joseph Antonelli, Max Rubinstein, Denis Agniel, Rosanna Smart, Elizabeth Stuart, Matthew Cefalu, Terry Schell, Joshua Eagan, Elizabeth Stone, Max Griswold, et al. Autoregressive models for panel data causal inference with application to state-level opioid policies. *arXiv preprint arXiv:2408.09012*, 2024.
- Dmitry Arkhangelsky, Guido W Imbens, Lihua Lei, and Xiaoman Luo. Design-robust two-way-fixed-effects regression for panel data. *Quantitative Economics*, 15(4):999–1034, 2024.
- Peter M. Aronow and Cyrus Samii. Estimating average causal effects under general interference, with application to a social network experiment. *Annals of Applied Statistics*, 11:1912–1947, 12 2017.
- Susan Athey, Mohsen Bayati, Nikolay Doudchenko, Guido Imbens, and Khashayar Khosravi. Matrix completion methods for causal panel data models. *Journal of the American Statistical Association*, 116(536):1716–1730, 2021.
- Eli Ben-Michael, Avi Feller, and Jesse Rothstein. The augmented synthetic control method. *Journal of the American Statistical Association*, 116(536):1789–1803, 2021.
- Yoav Benjamini and Yosef Hochberg. Controlling the false discovery rate: a practical and powerful approach to multiple testing. *Journal of the Royal statistical society: series B (Methodological)*, 57(1):289–300, 1995.
- Iavor Bojinov and Neil Shephard. Time series experiments and causal estimands: Exact randomization tests and trading. *Journal of the American Statistical Association*, 114:1665–1682, 10 2019.
- Iavor Bojinov, David Simchi-Levi, and Jinglong Zhao. Design and analysis of switchback experiments. *Management Science*, 69(7):3759–3777, 2023.
- Kirill Borusyak and Peter Hull. Nonrandom exposure to exogenous shocks. *Econometrica*, 91(6):2155–2185, 2023.
- Jennifer Brennan, Vahab Mirrokni, and Jean Pouget-Abadie. Cluster randomized designs for one-sided bipartite experiments. *Advances in Neural Information Processing Systems*, 35:37962–37974, 2022.
- Jianfei Cao and Connor Dowd. Estimation and inference for synthetic control methods with spillover effects. *arXiv preprint arXiv:1902.07343*, 2019.
- Ambarish Chattopadhyay, Kosuke Imai, and José R Zubizarreta. Design-based inference for generalized network experiments with stochastic interventions. *arXiv preprint arXiv:2312.03268*, 2023.

- Bin Chen, Yufang Jin, Erica Scaduto, Max A Moritz, Michael L Goulden, and James T Randerson. Climate, fuel, and land use shaped the spatial pattern of wildfire in california’s sierra nevada. *Journal of Geophysical Research: Biogeosciences*, 126(2):e2020JG005786, 2021.
- Duncan A Clark and Mark S Handcock. An approach to causal inference over stochastic networks. *arXiv preprint arXiv:2106.14145*, 2021.
- Roberta Di Stefano and Giovanni Mellace. The inclusive synthetic control method. *Discussion Papers on Business and Economics, University of Southern Denmark*, 14, 2020.
- Annie Doubleday, Youngjun Choe, Tania M Busch Isaksen, and Nicole A Errett. Urban bike and pedestrian activity impacts from wildfire smoke events in seattle, wa. *Journal of Transport & Health*, 21:101033, 2021.
- Nick Doudchenko, Minzhengxiong Zhang, Evgeni Drynkin, Edoardo Airoldi, Vahab Mirrokni, and Jean Pouget-Abadie. Causal inference with bipartite designs. 10 2020.
- Christian Fong, Chad Hazlett, and Kosuke Imai. Covariate balancing propensity score for a continuous treatment: Application to the efficacy of political advertisements. *The Annals of Applied Statistics*, 12(1):156–177, 2018.
- Laura Forastiere, Edoardo M Airoldi, and Fabrizia Mealli. Identification and estimation of treatment and interference effects in observational studies on networks. *Journal of the American Statistical Association*, 116(534):901–918, 2021.
- Giulio Grossi, Patrizia Lattarulo, Marco Mariani, Alessandra Mattei, and O Oner. Synthetic control group methods in the presence of interference: The direct and spillover effects of light rail on neighborhood retail activity. *arXiv preprint arXiv:2004.05027*, 2020.
- Giulio Grossi, Alessandra Mattei, and Georgia Papadogeorgou. Spatial vertical regression for spatial panel data: Evaluating the effect of the florentine tramway’s first line on commercial vitality. *arXiv preprint arXiv:2505.00450*, 2025.
- Ahmet Gulek and Jaume Vives-i Bastida. Synthetic IV estimation in panels. Technical report, MIT, 2025. Job Market Paper.
- Jens Hainmueller. Entropy balancing for causal effects: A multivariate reweighting method to produce balanced samples in observational studies. *Political analysis*, 20(1):25–46, 2012.
- Kevin Han, Guillaume Basse, and Iavor Bojinov. Population interference in panel experiments. *Journal of Econometrics*, 238(1):105565, 2024.

- Christopher Harshaw, Fredrik Sävje, David Eisenstat, Vahab Mirrokni, and Jean Pouget-Abadie. Design and analysis of bipartite experiments under a linear exposure-response model. *Electronic Journal of Statistics*, 17(1):464–518, 2023.
- Daniel E Ho, Kosuke Imai, Gary King, and Elizabeth A Stuart. Matching as nonparametric preprocessing for reducing model dependence in parametric causal inference. *Political analysis*, 15(3):199–236, 2007.
- Yuchen Hu and Stefan Wager. Switchback experiments under geometric mixing. *arXiv preprint arXiv:2209.00197*, 2022.
- Kosuke Imai and In Song Kim. On the use of two-way fixed effects regression models for causal inference with panel data. *Political Analysis*, 29(3):405–415, 2021.
- Kosuke Imai and Marc Ratkovic. Covariate balancing propensity score. *Journal of the Royal Statistical Society Series B: Statistical Methodology*, 76(1):243–263, 2014.
- Kosuke Imai, In Song Kim, and Erik H Wang. Matching methods for causal inference with time-series cross-sectional data. *American Journal of Political Science*, 67(3):587–605, 2023.
- Guido W Imbens. Causal inference in the social sciences. *Annual Review of Statistics and Its Application*, 11, 2024.
- Luke Keele, Rocío Titiunik, and José R Zubizarreta. Enhancing a geographic regression discontinuity design through matching to estimate the effect of ballot initiatives on voter turnout. *Journal of the Royal Statistical Society, Series A*, 178:223–239, 2014.
- Michael P Leung. Causal inference under approximate neighborhood interference. *Econometrica*, 90(1):267–293, 2022.
- Fan Li, Kari Lock Morgan, and Alan M Zaslavsky. Balancing covariates via propensity score weighting. *Journal of the American Statistical Association*, 113(521):390–400, 2018.
- Sizhu Lu, Lei Shi, Yue Fang, Wenxin Zhang, and Peng Ding. Design-based causal inference in bipartite experiments. *arXiv preprint arXiv:2501.09844*, 2025.
- Fiammetta Menchetti and Iavor Bojinov. Estimating causal effects in the presence of partial interference using multivariate bayesian structural time series models. *Harvard Business School Technology & Operations Mgt. Unit Working Paper*, (21-048), 2020.
- Whitney K Newey and Kenneth D West. A simple, positive semi-definite, heteroskedasticity and autocorrelationconsistent covariance matrix. 1986.

- Georgia Papadogeorgou, Zhaoyan Song, Guido Imbens, and Fabrizia Mealli. Causal inference when intervention units and outcome units differ. *arXiv preprint arXiv:2507.20231*, 2025.
- Jean Pouget-Abadie, Kevin Aydin, Warren Schudy, Kay Brodersen, and Vahab Mirrokni. Variance reduction in bipartite experiments through correlation clustering. *Advances in Neural Information Processing Systems*, 32, 2019.
- Colleen E Reid, Michael Brauer, Fay H Johnston, Michael Jerrett, John R Balmes, and Catherine T Elliott. Critical review of health impacts of wildfire smoke exposure. *Environmental health perspectives*, 124(9):1334–1343, 2016.
- Peter C Rockers, John-Arne Røttingen, Ian Shemilt, Peter Tugwell, and Till Bärnighausen. Inclusion of quasi-experimental studies in systematic reviews of health systems research. *Health Policy*, 119(4):511–521, 2015.
- Paul R Rosenbaum and Donald B Rubin. Constructing a control group using multivariate matched sampling methods that incorporate the propensity score. *The American Statistician*, 39(1):33–38, 1985.
- David G Rosenthal, Eric Vittinghoff, Geoffrey H Tison, Mark J Pletcher, Jeffrey E Olgin, Donald J Grandis, and Gregory M Marcus. Assessment of accelerometer-based physical activity during the 2017-2018 california wildfire seasons. *JAMA Network Open*, 3(9):e2018116–e2018116, 2020.
- Donald B Rubin. Matching to remove bias in observational studies. *Biometrics*, pages 159–183, 1973.
- Donald B Rubin. Bias reduction using mahalanobis-metric matching. *Biometrics*, pages 293–298, 1980.
- Fredrik Sävje. Causal inference with misspecified exposure mappings: separating definitions and assumptions. *Biometrika*, 111(1):1–15, 2024.
- Elizabeth A Stuart. Matching methods for causal inference: A review and a look forward. *Statistical science: a review journal of the Institute of Mathematical Statistics*, 25(1):1, 2010.
- Bar Weinstein and Daniel Nevo. Causal inference with misspecified network interference structure. *Biometrics*, 82(1):ujag023, 03 2026. ISSN 0006-341X. doi: 10.1093/biomtc/ujag023. URL <https://doi.org/10.1093/biomtc/ujag023>.
- Nathan B Wikle and Corwin M Zigler. Causal health impacts of power plant emission controls under modeled and uncertain physical process interference. *arXiv preprint arXiv:2306.05665*, 2023.
- Tianhui Zhou, Guangyu Tong, Fan Li, Laine E. Thomas, and Fan Li. Psweight: An r package for propensity score weighting analysis. *The R Journal*, 14:282–300, 2022. ISSN 2073-4859. doi: 10.32614/RJ-2022-011. <https://doi.org/10.32614/RJ-2022-011>.

- Corwin Zigler, Vera Liu, Fabrizia Mealli, and Laura Forastiere. Bipartite interference and air pollution transport: estimating health effects of power plant interventions. *Biostatistics*, 26(1):kxae051, 2025.
- Corwin M Zigler and Georgia Papadogeorgou. Bipartite causal inference with interference. *Statistical science: a review journal of the Institute of Mathematical Statistics*, 2021.
- José R Zubizarreta. Using mixed integer programming for matching in an observational study of kidney failure after surgery. *Journal of the American Statistical Association*, 107(500):1360–1371, 2012.
- José R Zubizarreta, Dylan S Small, Neera K Goyal, Scott Lorch, and Paul R Rosenbaum. Stronger instruments via integer programming in an observational study of late preterm birth outcomes. *The Annals of Applied Statistics*, pages 25–50, 2013.
- José R. Zubizarreta. Stable weights that balance covariates for estimation with incomplete outcome data. *Journal of the American Statistical Association*, 110:910–922, 7 2015.

Supplementary materials

Table of Contents

A Glossary	3
B Proof of exposure unconfoundedness	5
C Estimation	5
C.1 Alternative algorithms with 1-2 or 1-‘1 or 2’ matching	5
C.2 Algorithms for estimating the carryover effect	9
C.3 Estimands and estimation in the absence of Assumption 2	10
C.4 Testing a null hypothesis of no causal effect with multiple outcome units	11
D Proofs of bounded bias of causal estimators	12
D.1 Linear potential outcome model	12
D.2 Nonlinear potential outcome model	17
E Variance estimation	19
E.1 Setup and notation	20
E.2 Variance estimation when matching exactly within each pair	21
E.3 Variance estimation for the causal effect estimator based on our algorithms	22
E.4 Temporal correlation in the outcome model residuals	23
E.5 Our causal estimator within a regression framework on the matched sample	24
F A Synthetic Dataset on Wildfire Exposure	26
F.1 Generating the temporal trends and covariates for the interventional and outcome units	27

F.2	The treatment assignment, bipartite network, and outcome	29
G	Description for alternative approaches	31
G.1	The naïve approaches	31
G.2	Linear regression estimator	32
G.3	IPW estimator	33
H	Additional Simulations	33
H.1	Data generation	33
H.2	Single-unit estimation and inference across different exposure sparsity levels	39
H.3	Testing the global null hypothesis	42
H.4	Algorithms balancing time but not the time-varying covariates	43
H.5	Analysis of tuning parameters	45
H.6	Modification of the algorithms to impose constraints within each match	47
H.7	Simulations under heterogeneous treatment effects	48
H.8	The impact of outcome temporal correlation on inference	50
I	Additional study information	52
I.1	Additional information on the study data set	52
I.2	Illustrations of resulting data for San Francisco based on the proposed algorithms	53
I.3	Results under alternative definition of exposure	54

A Glossary

In Table S.4, we include a glossary of the notation used in the manuscript.

Table S.4: Table of notation

Symbol	Description
\mathcal{N}	The set of interventional units, $\mathcal{N} = \{n_1, n_2, \dots, n_N\}$ where n_i denotes the i^{th} unit
m	The outcome unit
\mathcal{T}	The set of time periods, $\mathcal{T} = \{1, 2, \dots, T\}$
A_{ti}, \mathbf{A}_t	A_{ti} is treatment of interventional unit n_i at time t and \mathbf{A}_t is the vector of treatments across all units at time t
G_{ti}, \mathbf{G}_t	G_{ti} is the connectivity measurement of interventional unit n_i with outcome unit m at time t , and \mathbf{G}_t is the vector of these measurements across interventional units
$\mathbf{X}_{0i}^{\text{int}}, \mathbf{X}_0^{\text{out}}, \mathbf{X}_{0i}^{\text{net}}$	Time-invariant covariates of dimension $p_0^{\text{int}}, p_0^{\text{out}}, p_0^{\text{net}}$ for the interventional unit n_i , the outcome unit m , and their relationship, respectively
$\mathbf{X}_{ti}^{\text{int}}, \mathbf{X}_t^{\text{out}}, \mathbf{X}_{ti}^{\text{net}}$	Time-varying covariates of dimension $p^{\text{int}}, p^{\text{out}}, p^{\text{net}}$ for the interventional unit n_i , the outcome unit m , and their relationship, respectively, at time t . Specifically, $\mathbf{X}_{ti}^{\text{int}} = (X_{ti1}^{\text{int}}, X_{ti2}^{\text{int}}, \dots, X_{tip^{\text{int}}}^{\text{int}})^{\top}$, and similarly for $\mathbf{X}_{ti}^{\text{net}}$
$\mathbf{X}_0, \mathbf{X}_t$	Vectors including all time-invariant and time-varying covariates, respectively
\bar{V}_t	The history of a covariate over times $1, 2, \dots, t$. Specifically, $\bar{V}_t = (V_t, V_{t-1}, \dots, V_1)^{\top}$
$\bar{V}_{t,S}$	The history of a covariate over times $t-S, t-S+1, \dots, t$. Specifically, $\bar{V}_{t,S} = (V_t, V_{t-1}, \dots, V_{t-S})^{\top}$

Symbol	Description
h_t	The exposure mapping $h_t : \mathcal{A}^N \times \mathcal{G} \rightarrow \mathcal{E}$ reflects the exposure function at time t that maps the interventional units' treatment and the bipartite connectivity network to the outcome unit exposure
h_t^c	The carryover mapping $h_t^c : \mathcal{E}^L \rightarrow \mathcal{R}$ reflects the function that summarizes the exposure values during time periods $t - L, t - L + 1, \dots, t - 1$
E_t	The exposure of the outcome unit m at time t . It is defined based on the function h_t applied on $\mathbf{A}_t, \mathbf{G}_t$
R_t	The carryover exposure of outcome unit m at time t . It is defined as the value of the function h_t^c on the exposures $\bar{E}_{t-1, L-1} = (E_{t-1}, E_{t-2}, \dots, E_{t-L})^\top$
Y_t	The observed outcome for the outcome unit at time t
$Y_t(\bar{\mathbf{a}}_t, \bar{\mathbf{g}}_t), Y_t(e_t, r_t)$	The potential outcome of the outcome unit at time t with and without the exposure mapping Assumption 1
$\mathcal{Y}_t(\cdot)$	The collection of the outcome unit's all potential outcomes for time t
$\tau_t^{\text{imm}}(e, e'; r)$	The immediate effect at time t for a change in the most recent exposure, $\tau_t^{\text{imm}}(e, e'; r) = Y_t(e, r) - Y_t(e', r)$
$\tau_t^{\text{car}}(r, r'; e)$	The carryover effect at time t for a change in the carryover exposure, $\tau_t^{\text{car}}(r, r'; e) = Y_t(e, r) - Y_t(e, r')$
$\mathcal{T}_e, \mathcal{T}_r$	Subsets of \mathcal{T} with exposure $E_t = e$ or carryover exposure $R_t = r$, respectively
$\tau^{\text{imm}}(e, e')$	Immediate effect averaged over time periods with $E_t = e$, $\tau^{\text{imm}}(e, e') = \frac{1}{ \mathcal{T}_e } \sum_{t \in \mathcal{T}_e} \tau_t^{\text{imm}}(e, e'; R_t)$
$\tau^{\text{car}}(r, r')$	Carryover effect averaged over time periods with $R_t = r$, $\tau^{\text{car}}(r, r') = \frac{1}{ \mathcal{T}_r } \sum_{t \in \mathcal{T}_r} \tau_t^{\text{car}}(r, r'; E_t)$.

B Proof of exposure unconfoundedness

Proof of Proposition 1. First, since \mathbf{X}_0 are time-invariant, we can treat them as constants in the condition and thus omit them for simplicity. Then,

$$\begin{aligned}
& P(E_t = e, R_t = r | \mathcal{Y}_t(\cdot), f(t), \bar{\mathbf{X}}_{t,S}) \\
&= \sum_{\forall \bar{\mathbf{g}}_{t,L}, \bar{\mathbf{a}}_{t,L}} P(E_t = e, R_t = r | \bar{\mathbf{G}}_{t,L} = \bar{\mathbf{g}}_{t,L}, \bar{\mathbf{A}}_{t,L} = \bar{\mathbf{a}}_{t,L}, \mathcal{Y}_t(\cdot), f(t), \bar{\mathbf{X}}_{t,S}) \\
&\quad P(\bar{\mathbf{G}}_{t,L} = \bar{\mathbf{g}}_{t,L}, \bar{\mathbf{A}}_{t,L} = \bar{\mathbf{a}}_{t,L} | \mathcal{Y}_t(\cdot), f(t), \bar{\mathbf{X}}_{t,S}) \\
&= \sum_{\forall \bar{\mathbf{g}}_{t,L}, \bar{\mathbf{a}}_{t,L}} I(h_t(\mathbf{a}_t, \mathbf{g}_t) = e) \cdot I(h_t^c(\bar{\mathbf{h}}_{t-1,L-1}(\bar{\mathbf{a}}_{t-1,L-1}, \bar{\mathbf{g}}_{t-1,L-1})) = r) \\
&\quad P(\bar{\mathbf{G}}_{t,L} = \bar{\mathbf{g}}_{t,L}, \bar{\mathbf{A}}_{t,L} = \bar{\mathbf{a}}_{t,L} | f(t), \bar{\mathbf{X}}_{t,S}) \\
&= \sum_{\forall \bar{\mathbf{g}}_{t,L}, \bar{\mathbf{a}}_{t,L}} P(E_t = e, R_t = r | \bar{\mathbf{G}}_{t,L} = \bar{\mathbf{g}}_{t,L}, \bar{\mathbf{A}}_{t,L} = \bar{\mathbf{a}}_{t,L}, f(t), \bar{\mathbf{X}}_{t,S}) \\
&\quad P(\bar{\mathbf{G}}_{t,L} = \bar{\mathbf{g}}_{t,L}, \bar{\mathbf{A}}_{t,L} = \bar{\mathbf{a}}_{t,L} | f(t), \bar{\mathbf{X}}_{t,S}) \\
&= P(E_t = e, R_t = r | f(t), \bar{\mathbf{X}}_{t,S})
\end{aligned}$$

where $\bar{\mathbf{h}}_{t-1,L-1}(\bar{\mathbf{a}}_{t-1,L-1}, \bar{\mathbf{g}}_{t-1,L-1})$ is equal to

$$(h_{t-1}(\mathbf{a}_{t-1}, \mathbf{g}_{t-1}), h_{t-2}(\mathbf{a}_{t-2}, \mathbf{g}_{t-2}), \dots, h_{t-L}(\mathbf{a}_{t-L}, \mathbf{g}_{t-L}))^\top.$$

The first equation holds as a result of the law of total probability. In the second equation, the first component is simply the indicator function for whether the exposure and carryover exposure take the target values or not. In the second term, the potential outcomes $\mathcal{Y}_t(\cdot)$ drop out using Assumption 3. Then, the same expansion can be written without conditioning on potential outcomes in the third and fourth equations. □

C Estimation

C.1 Alternative algorithms with 1-2 or 1-‘1 or 2’ matching

C.1.1 Algorithm with matching 1-2

We propose an alternate algorithm which matches an exposed time point to *two* unexposed time points, one occurring temporally *before* and one *after*, while maintaining balance constraints on time-varying

information across matches. Consider indicators $a_{t_e t_{u_1} t_{u_2}}$ for whether the exposed time $t_e \in \mathcal{T}_1$ is matched to the unexposed timestamps $t_{u_1}, t_{u_2} \in \mathcal{T}_0$. The objective function of the optimization algorithm is to maximize

$$\max_{\mathbf{a}} \sum_{t_e, t_{u_1}, t_{u_2}} a_{t_e t_{u_1} t_{u_2}}. \quad (\text{S.7})$$

The constraints are similar in spirit to the ones for algorithm (2), but they are adapted to accommodate the ‘1-2’ matches. Exposed and unexposed time periods can be used in a match at most once, though if an exposed time period is matched, it is matched to two unexposed ones:

$$\begin{aligned} \sum_{t_{u_1}, t_{u_2}} a_{t_e t_{u_1} t_{u_2}} &\leq 1, \quad \forall t_e \in \mathcal{T}_1. \\ \sum_{t_e, t_{u_1}, t_{u_2}} a_{t_e t_{u_1} t_{u_2}} I(t_{u_1} = t_u) + \sum_{t_e, t_{u_1}, t_{u_2}} a_{t_e t_{u_1} t_{u_2}} I(t_{u_2} = t_u) &\leq 1, \quad \forall t_u \in \mathcal{T}_0. \end{aligned}$$

Therefore, the objective of the optimization problem is to maximize the number of matched exposed time periods, with a match being of the form (t_e, t_{u_1}, t_{u_2}) .

We impose constraints that balance time, the carryover exposure, and time-varying covariates. These constraints are imposed on value of the variable for the exposed unit compared to the average value of the corresponding variable for its two unexposed time periods. Specifically, the constraint in (S.8) balances, *on average*, the time of the exposed time period compared to the average time of its unexposed matches,

$$\left| \sum_{t_e, t_{u_1}, t_{u_2}} a_{t_e t_{u_1} t_{u_2}} \left(t_e - \frac{t_{u_1} + t_{u_2}}{2} \right) \right| \leq \delta \sum_{t_e, t_{u_1}, t_{u_2}} a_{t_e t_{u_1} t_{u_2}}, \quad (\text{S.8})$$

but it does not restrict the time difference for each match. The constraint in (S.9) restricts the temporal difference and order of time periods for each individual match, as

$$\begin{aligned} |a_{t_e t_{u_1} t_{u_2}} (t_e - t_{u_i})| &\leq \epsilon, \quad \text{for } i = 1, 2 \\ a_{t_e t_{u_1} t_{u_2}} (t_e - t_{u_1}) &\geq 0, \quad \text{and} \quad a_{t_e t_{u_1} t_{u_2}} (t_{u_2} - t_e) \geq 0, \end{aligned} \quad (\text{S.9})$$

for all $t_e \in \mathcal{T}_1$, and $t_{u_1}, t_{u_2} \in \mathcal{T}_0$. The first line imposes that the time difference between an exposed time period and each of its matched unexposed ones cannot exceed ϵ . The second line forces a temporal sequence within each match, requiring the exposed period to fall within the unexposed ones.

For balancing the carryover exposure, the constraint takes the form

$$\left| \sum_{t_e, t_{u_1}, t_{u_2}} a_{t_e t_{u_1} t_{u_2}} \left(R_{t_e} - \frac{R_{t_{u_1}} + R_{t_{u_2}}}{2} \right) \right| \leq \delta' \sum_{t_e, t_{u_1}, t_{u_2}} a_{t_e t_{u_1} t_{u_2}}. \quad (\text{S.10})$$

In addition, the average value of time-varying covariates is balanced when comparing an exposed time periods with the average covariate value of its matches. Specifically,

$$\left| \sum_{t_e, t_{u_1}, t_{u_2}} a_{t_e t_{u_1} t_{u_2}} \left(\bar{\mathbf{X}}_{t_e, S} - \frac{\bar{\mathbf{X}}_{t_{u_1}, S} + \bar{\mathbf{X}}_{t_{u_2}, S}}{2} \right) \right| \leq \mathbf{1}_{(S+1)(Np^{\text{int}} + Np^{\text{net}} + p^{\text{out}})} \cdot \delta' \sum_{t_e, t_{u_1}, t_{u_2}} a_{t_e t_{u_1} t_{u_2}}.$$

Since this constraint can be high-dimensional, for a large number of interventional units N , we instead propose balancing summary values of the interventional and network covariates as

$$\left| \sum_{t_e, t_{u_1}, t_{u_2}} a_{t_e t_{u_1} t_{u_2}} \left(\bar{\mathbf{X}}_{t_e, S}^{\text{sum.}} - \frac{\bar{\mathbf{X}}_{t_{u_1}, S}^{\text{sum.}} + \bar{\mathbf{X}}_{t_{u_2}, S}^{\text{sum.}}}{2} \right) \right| \leq \mathbf{1}_{(S+1)(p^{\text{int}} + p^{\text{net}} + p^{\text{out}})} \cdot \delta' \sum_{t_e, t_{u_1}, t_{u_2}} a_{t_e t_{u_1} t_{u_2}},$$

Matching algorithms seek control units that resemble the treated units in order to predict what would have happened to the treated units had they been control. Therefore, here, matching one exposed time period to two unexposed ones can improve the accuracy of imputing an exposed time period's missing potential outcome, over matching one to one. Ensuring that the exposed period falls between matched unexposed ones in (S.9) is expected to improve balance of the temporal trends. For instance, monotonic temporal trends would be more effectively balanced when matching an exposed period with unexposed periods both before and after. Therefore, this 1-2 algorithm can be more accurate in imputing missing potential outcomes for exposed time periods, and more efficient in estimating causal effects, compared to the 1-1 algorithm.

C.1.2 Algorithm with matching 1-1/2

While the algorithm that matches one exposed time period to two unexposed time periods in Supplement C.1.1 might provide more accurate imputations of missing potential outcomes in some cases, it might lead to fewer matched exposed units than the 1-1 algorithm in Section 4, especially in scenarios with a relatively high proportion of exposed time periods. Here, we introduce an approach that combines the previous two, and allows an exposed time period to be matched to one *or* two unexposed time periods.

Specifically, we consider binary matching indicators of the form $a_{t_e t_u}$ and $a_{t_e t_{u_1} t_{u_2}}$ where $a_{t_e t_u} =$

1 denotes that exposed time period t_e is matched only to one unexposed time period t_u , whereas $a_{t_e t_{u_1} t_{u_2}} = 1$ denotes that t_e is matched to two unexposed time periods t_{u_1} and t_{u_2} . The target is to maximize the number of matched exposed time periods as

$$\max_{\mathbf{a}} \left(\sum_{t_e, t_u} a_{t_e t_u} + \sum_{t_e, t_{u_1}, t_{u_2}} a_{t_e t_{u_1} t_{u_2}} \right).$$

The constraints we impose are similar in spirit to those in optimization problems (2) and (S.7), but they are re-designed to account for the presence of two types of matches. Each time period can be involved in either a match of type 1-1 or 1-2, and at most once,

$$\begin{aligned} \sum_{t_u} a_{t_e t_u} + \sum_{t_{u_1}, t_{u_2}} a_{t_e t_{u_1} t_{u_2}} &\leq 1, \\ \sum_{t_e, t_u} a_{t_e t_u} I(t_u = \tilde{t}_u) + \sum_{t_e, t_{u_1}, t_{u_2}} a_{t_e t_{u_1} t_{u_2}} I(t_{u_1} = \tilde{t}_u) + \sum_{t_e, t_{u_1}, t_{u_2}} a_{t_e t_{u_1} t_{u_2}} I(t_{u_2} = \tilde{t}_u) &\leq 1, \end{aligned}$$

for all $t_e \in \mathcal{T}_1$. and $\tilde{t}_u \in \mathcal{T}_0$. Moreover, the average time difference between an exposed time period and its one or two matches is bounded by the constant $\delta \geq 0$, as

$$\left| \sum_{t_e, t_u} a_{t_e t_u} (t_e - t_u) + \sum_{t_e, t_{u_1}, t_{u_2}} a_{t_e t_{u_1} t_{u_2}} \left(t_e - \frac{t_{u_1} + t_{u_2}}{2} \right) \right| \leq \delta \left(\sum_{t_e, t_u} a_{t_e t_u} + \sum_{t_e, t_{u_1}, t_{u_2}} a_{t_e t_{u_1} t_{u_2}} \right).$$

Furthermore, the time difference between matched exposed and unexposed time periods is bounded by ϵ in 1-1 or 1-2 matches, and in 1-2 matches the exposed time period lies temporally between the two matched unexposed ones, as

$$\begin{aligned} |a_{t_e t_u} (t_e - t_u)| &\leq \epsilon, & |a_{t_e t_{u_1} t_{u_2}} (t_e - t_{u_i})| &\leq \epsilon, \text{ for } i = 1, 2 \\ a_{t_e t_{u_1} t_{u_2}} (t_e - t_{u_1}) &\geq 0, & \text{and } a_{t_e t_{u_1} t_{u_2}} (t_{u_2} - t_e) &\geq 0. \end{aligned}$$

Finally, we impose constraints that balance the carryover exposure and time-varying covariates across the resulting data set of matches. Specifically, for the carryover exposure, we specify

$$\begin{aligned} \left| \sum_{t_e, t_u} a_{t_e t_u} (R_{t_e} - R_{t_u}) + \sum_{t_e, t_{u_1}, t_{u_2}} a_{t_e t_{u_1} t_{u_2}} \left(R_{t_e} - \frac{R_{t_{u_1}} + R_{t_{u_2}}}{2} \right) \right| \\ \leq \delta' \left(\sum_{t_e, t_u} a_{t_e t_u} + \sum_{t_e, t_{u_1}, t_{u_2}} a_{t_e t_{u_1} t_{u_2}} \right). \end{aligned} \tag{S.11}$$

For the time-varying covariates, we specify the balance constraint on the complete vector as

$$\left| \sum_{t_e, t_u} a_{t_e t_u} (\bar{\mathbf{X}}_{t_e, S} - \bar{\mathbf{X}}_{t_u, S}) + \sum_{t_e, t_{u_1}, t_{u_2}} a_{t_e t_{u_1} t_{u_2}} \left(\bar{\mathbf{X}}_{t_e, S} - \frac{\bar{\mathbf{X}}_{t_{u_1}, S} + \bar{\mathbf{X}}_{t_{u_2}, S}}{2} \right) \right| \leq \mathbf{1}_{(S+1)(Np^{\text{int}} + Np^{\text{net}} + p^{\text{out}})} \cdot \delta' \left(\sum_{t_e, t_u} a_{t_e t_u} + \sum_{t_e, t_{u_1}, t_{u_2}} a_{t_e t_{u_1} t_{u_2}} \right),$$

or only on the summary values of covariates across interventional units as

$$\left| \sum_{t_e, t_u} a_{t_e t_u} (\bar{\mathbf{X}}_{t_e, S}^{\text{sum.}} - \bar{\mathbf{X}}_{t_u, S}^{\text{sum.}}) + \sum_{t_e, t_{u_1}, t_{u_2}} a_{t_e t_{u_1} t_{u_2}} \left(\bar{\mathbf{X}}_{t_e, S}^{\text{sum.}} - \frac{\bar{\mathbf{X}}_{t_{u_1}, S}^{\text{sum.}} + \bar{\mathbf{X}}_{t_{u_2}, S}^{\text{sum.}}}{2} \right) \right| \leq \mathbf{1}_{(S+1)(p^{\text{int}} + p^{\text{net}} + p^{\text{out}})} \cdot \delta' \left(\sum_{t_e, t_u} a_{t_e t_u} + \sum_{t_e, t_{u_1}, t_{u_2}} a_{t_e t_{u_1} t_{u_2}} \right).$$

This 1-1/2 algorithm is expected to yield more matches than the 1-2 algorithm since it allows some exposed time points to be matched to a single unexposed one. At the same time, when possible, it allows for exposed time periods to be matched to two unexposed ones, which can improve the balance of temporal trends and improve accuracy in imputing the missing potential outcomes for exposed time periods.

C.1.3 The matching estimators for the 1-2 and 1-1/2 algorithms

When an exposed time period t_e is matched with two unexposed periods, t_{u_1} and t_{u_2} , $Y_{t_e}^*$ is set as the average of the two unexposed outcomes, $Y_{t_e}^* = (Y_{t_{u_1}} + Y_{t_{u_2}})/2$. The corresponding estimator of the immediate causal effect is the same as in (6) with these values of $Y_{t_e}^*$ for the matched exposed time periods.

For the 1-2 algorithm, the set of matched exposed time periods is $\mathcal{T}_1^* = \{t : E_t = 1 \text{ and } a_{t_e t_{u_1} t_{u_2}} = 1 \text{ for some } t_u\}$, and similarly for the 1-1/2 algorithm.

C.2 Algorithms for estimating the carryover effect

We detail the three algorithms for estimating the carryover effect that correspond to the 1-1, 1-2, and 1-1/2 algorithms in Section 4, Supplement C.1.1 and Supplement C.1.2, respectively.

We adopt the same index notation for the binary indicators $a_{t_e t_u}$ and $a_{t_e t_{u_1} t_{u_2}}$ where now t_e corresponds to a time period with carryover exposure, and t_u, t_{u_1} and t_{u_2} correspond to time periods without carryover exposure. The objective of the optimization problem for maximizing the number of matches, as well as the constraints that each time period can be part of at most one match, and the balance constraints on time and the time-varying covariates remain the same as described in Section

4.1, Supplement C.1.1 and Supplement C.1.2. We update the constraint in (4), (S.10) and (S.11) to specify balance of the most recent exposure (instead of the carryover exposure). The specific form of this constraint is

$$\left| \sum_{t_e, t_u} a_{t_e t_u} (E_{t_e} - E_{t_u}) \right| \leq \delta \sum_{t_e, t_u} a_{t_e t_u},$$

$$\left| \sum_{t_e, t_{u_1}, t_{u_2}} a_{t_e t_{u_1} t_{u_2}} \left(E_{t_e} - \frac{E_{t_{u_1}} + E_{t_{u_2}}}{2} \right) \right| \leq \delta \sum_{t_e, t_{u_1}, t_{u_2}} a_{t_e t_{u_1} t_{u_2}}.$$

and

$$\begin{aligned} \left| \sum_{t_e, t_u} a_{t_e t_u} (E_{t_e} - E_{t_u}) + \sum_{t_e, t_{u_1}, t_{u_2}} a_{t_e t_{u_1} t_{u_2}} \left(E_{t_e} - \frac{E_{t_{u_1}} + E_{t_{u_2}}}{2} \right) \right| \\ \leq \delta \left(\sum_{t_e, t_u} a_{t_e t_u} + \sum_{t_e, t_{u_1}, t_{u_2}} a_{t_e t_{u_1} t_{u_2}} \right), \end{aligned}$$

for the 1-1 algorithm in Section 4, the 1-2 algorithm in Supplement C.1.1, and the 1-1/2 algorithm in Supplement C.1.2, respectively.

Lastly, exactly like for the immediate effect, the causal estimator for the carryover effect is of the same form as in (6) for $Y_{t_e}^* = Y_{t_u}$ for 1-1 matches, and $Y_{t_e}^* = (Y_{t_{u_1}} + Y_{t_{u_2}})/2$ for 1-2 matches. In Supplement D we show that the causal estimators for the carryover effect have bounded bias.

C.3 Estimands and estimation in the absence of Assumption 2

Under Assumption 2, in the definition of the immediate effect in (1), we average over time periods with exposure $E_t = e$, and carryover exposure equal to its observed value R_t . Then, for accurate estimation of the immediate effect, the impact of the carryover exposure on the outcome is “controlled” by balancing the observed carryover exposure over the matched sample in the constraints (4), (S.10) or (S.11). Therefore, this assumption allows us to use time periods with different values of observed carryover exposure.

Here, we discuss estimands and estimation of immediate and carryover effects in the absence of Assumption 2. We alter the definition of estimands in (1) to specify the exposure and carryover value of the time periods that are averaged over. Specifically, if \mathcal{T}_{er} denotes the subset of \mathcal{T} for which $E_t = e$

and $R_t = r$, we consider

$$\tau^{\text{imm}}(e, e'; r) = \frac{1}{|\mathcal{T}_{er}|} \sum_{t \in \mathcal{T}_{er}} \tau_t^{\text{imm}}(e, e'; r), \quad \text{and} \quad \tau^{\text{car}}(r, r'; e) = \frac{1}{|\mathcal{T}_{er}|} \sum_{t \in \mathcal{T}_{er}} \tau_t^{\text{car}}(r, r'; e). \quad (\text{S.12})$$

Accurate estimation of the immediate causal effect requires that we match exactly on the carryover exposure and we only use time periods with the specific carryover exposure value. Specifically, to estimate the immediate effect for carryover exposure equal to r , we substitute the constraints in (4), (S.10), or (S.11) with

$$R_{t_e} = R_{t_u} = r,$$

$$R_{t_e} = R_{t_{u_1}} = R_{t_{u_2}} = r,$$

and

$$R_{t_e} = R_{t_u} = R_{t_{u_1}} = R_{t_{u_2}} = r$$

for the algorithm in Section 4, Supplement C.1.1, and Supplement C.1.2, respectively.

Similar reasoning applies to the estimation of carryover effects in (S.12). When Assumption 2 is relaxed, $\tau^{\text{car}}(r, r'; e)$ is identified by fixing the current exposure to e in matched periods in the algorithm detailed in Supplement C.2.

C.4 Testing a null hypothesis of no causal effect with multiple outcome units

Our matching algorithms and estimators are designed to evaluate the immediate or carryover effect of the treatment on each outcome unit separately. In the presence of multiple outcome units, and when making general policy evaluations, we might be interested in studying whether the exposure has an effect on *any* of them. We use the immediate effect as an example. Suppose a collection of outcome units $\mathcal{M} = \{m_1, m_2, \dots, m_M\}$. For each outcome unit m_j we use τ_j^{imm} to denote the immediate effect on this unit. We wish to test the hypothesis that

$$\mathbf{H}_0 : \tau_j^{\text{imm}} = 0, \quad \forall j = 1, 2, \dots, M \quad \text{v.s.}$$

$$\mathbf{H}_A : \text{There exists at least one } j \text{ such that } \tau_j^{\text{imm}} \neq 0,$$

We acquire a p-value for testing the null hypothesis of no effect on unit m_j , according to Section 4.3, for all outcome units. We adjust these p-values by performing a false discovery rate (FDR) correction for multiple comparisons [Benjamini and Hochberg, 1995]. Then, we compare the adjusted p-values to the pre-specified α -level. If all adjusted p-values are greater than α , we fail to reject the null hypothesis H_0 . Otherwise, we reject the null hypothesis and identify the affected units as those with adjusted p-values less than α .

D Proofs of bounded bias of causal estimators

D.1 Linear potential outcome model

We re-state Theorem 1 to include the statements for all three estimators and both the immediate and the carryover effect.

Theorem S.3. If $Y_t(e, r) = \beta_0 + \beta_1 e + \beta_2 r + \beta_3 t + \beta_4^\top \overline{\mathbf{X}}_{t,S}^{\text{sum.}} + \epsilon_t(e, r)$ for all $t = 1, 2, \dots, T$, with $E(\epsilon_t(e, r) | E_t, t, \overline{\mathbf{X}}_{t,S}^{\text{sum.}}) = 0$, then $|E(\hat{\tau}^{\text{imm}}(1, 0) - \tau^{\text{imm}}(1, 0))| \leq \delta |\beta_3| + \delta' (|\beta_2| + \|\beta_4\|_1)$ for the estimators of the immediate effect resulting from the 1-1, 1-2, or 1-1/2 algorithms, and $|E(\hat{\tau}^{\text{car}}(1, 0) - \tau^{\text{car}}(1, 0))| \leq \delta |\beta_3| + \delta' (|\beta_1| + \|\beta_4\|_1)$ for all estimators of the carryover effect, where δ and δ' are the balance constraints tuning parameters.

Proof of Theorem S.3. We consider the case of bounding the bias of the matching algorithms when the outcome model has a linear form in the exposures, time, and time-varying covariates. Define I_1 as the set of matched pairs (t_e, t_u) and I_2 as the set of matched triplets (t_e, t_{u_1}, t_{u_2}) . Let $\mathbf{E} = (E_1, E_2, \dots, E_T)^T$ denote the observed exposure across time, and $\mathbf{t} = (1, 2, \dots, T)^T$ the sequence of time points. Let $\beta_{4,s,d}$ denote the coefficient for the d -th covariate at lag s , where $s \in \{0, 1, \dots, S\}$.

- For the algorithm that matches one exposed time period to one unexposed time period:

$$\begin{aligned}
& |E(\hat{\tau}^{\text{imm}} - \tau^{\text{imm}})| \\
&= \left| E \left(E \left(\frac{1}{|I_1|} \sum_{(t_e, t_u) \in I_1} Y_{t_e} - Y_{t_u} \right) - E[(Y_t(1, R_t) - Y_t(0, R_t)) I(E_t = 1)] | \mathbf{E}, \mathbf{t}, \overline{\mathbf{X}}_{t,S}^{\text{sum.}} \right) \right| \\
&= \left| \frac{1}{|I_1|} \sum_{(t_e, t_u) \in I_1} \left(\beta_1 + \beta_2 R_{t_e} - \beta_2 R_{t_u} + \beta_3 t_e - \beta_3 t_u + \beta_4^\top \overline{\mathbf{X}}_{t_e,S}^{\text{sum.}} - \beta_4^\top \overline{\mathbf{X}}_{t_u,S}^{\text{sum.}} \right) - \beta_1 \right| \\
&\leq \frac{1}{|I_1|} |\beta_2| \left| \sum_{(t_e, t_u) \in I_1} (R_{t_e} - R_{t_u}) \right| + \frac{1}{|I_1|} |\beta_3| \left| \sum_{(t_e, t_u) \in I_1} (t_e - t_u) \right| +
\end{aligned}$$

$$\begin{aligned} & \frac{1}{|I_1|} \left| \sum_s \sum_d \beta_{4,s,d} \sum_{(t_e, t_u) \in I_1} (X_{(t_e-s)d}^{\text{sum.}} - X_{(t_u-s)d}^{\text{sum.}}) \right| \\ & \leq \delta' |\beta_2| + \delta |\beta_3| + \delta' \|\beta_4\|_1. \end{aligned}$$

- For the algorithm that matches one exposed time period to two unexposed time periods:

$$\begin{aligned} & |E(\hat{\tau}^{\text{imm}} - \tau^{\text{imm}})| \\ & = \left| E \left(E \left(\frac{1}{|I_2|} \sum_{(t_e, t_{u_1}, t_{u_2}) \in I_2} Y_{t_e} - \frac{1}{2} (Y_{t_{u_1}} + Y_{t_{u_2}}) \right) - E[(Y_t(1, R_t) - Y_t(0, R_t)) I(E_t = 1)] \mid \mathbf{E}, \mathbf{t}, \bar{\mathbf{X}}_{t,S}^{\text{sum.}} \right) \right| \\ & = \left| \frac{1}{|I_2|} \sum_{(t_e, t_{u_1}, t_{u_2}) \in I_2} \left(\beta_1 + \beta_2 R_{t_e} - \frac{\beta_2}{2} (R_{t_{u_1}} + R_{t_{u_2}}) + \beta_3 t_e - \frac{\beta_3}{2} (t_{u_1} + t_{u_2}) + \right. \right. \\ & \quad \left. \left. \beta_4^\top \bar{\mathbf{X}}_{t_e,S}^{\text{sum.}} - \frac{\beta_4^\top}{2} (\bar{\mathbf{X}}_{t_{u_1},S}^{\text{sum.}} + \bar{\mathbf{X}}_{t_{u_2},S}^{\text{sum.}}) \right) - \beta_1 \right| \\ & \leq \frac{1}{|I_2|} |\beta_2| \left| \sum_{(t_e, t_{u_1}, t_{u_2}) \in I_2} \left(R_{t_e} - \frac{1}{2} (R_{t_{u_1}} + R_{t_{u_2}}) \right) \right| + \frac{1}{|I_2|} |\beta_3| \left| \sum_{(t_e, t_{u_1}, t_{u_2}) \in I_2} \left(t_e - \frac{1}{2} (t_{u_1} + t_{u_2}) \right) \right| + \\ & \quad \frac{1}{|I_2|} \left| \sum_s \sum_d \beta_{4,s,d} \sum_{(t_e, t_{u_1}, t_{u_2}) \in I_2} X_{(t_e-s)d}^{\text{sum.}} - \frac{1}{2} (X_{(t_{u_1}-s)d}^{\text{sum.}} + X_{(t_{u_2}-s)d}^{\text{sum.}}) \right| \\ & \leq \delta' |\beta_2| + \delta |\beta_3| + \delta' \|\beta_4\|_1. \end{aligned}$$

- For the algorithm that matches one exposed time period to one or two unexposed time periods:

$$\begin{aligned} & |E(\hat{\tau}^{\text{imm}} - \tau^{\text{imm}})| \\ & = \left| E \left(E \left(\frac{1}{|I_1| + |I_2|} \sum_{(t_e, t_u) \in I_1} (Y_{t_e} - Y_{t_u}) + \sum_{(t_e, t_{u_1}, t_{u_2}) \in I_2} \left(Y_{t_e} - \frac{1}{2} (Y_{t_{u_1}} + Y_{t_{u_2}}) \right) \right) - \right. \\ & \quad \left. - E[(Y_t(1, R_t) - Y_t(0, R_t)) I(E_t = 1)] \mid \mathbf{E}, \mathbf{t}, \bar{\mathbf{X}}_{t,S}^{\text{sum.}} \right) \right| \\ & = \left| \frac{1}{|I_1| + |I_2|} \sum_{(t_e, t_u) \in I_1} \left(\beta_1 + \beta_2 R_{t_e} - \beta_2 R_{t_u} + \beta_3 t_e - \beta_3 t_u + \beta_4^\top \bar{\mathbf{X}}_{t_e,S}^{\text{sum.}} - \beta_4^\top \bar{\mathbf{X}}_{t_u,S}^{\text{sum.}} \right) + \right. \\ & \quad \sum_{(t_e, t_{u_1}, t_{u_2}) \in I_2} \left(\beta_1 + \beta_2 R_{t_e} - \frac{\beta_2}{2} (R_{t_{u_1}} + R_{t_{u_2}}) + \beta_3 t_e - \frac{\beta_3}{2} (t_{u_1} + t_{u_2}) + \right. \\ & \quad \left. \left. \beta_4^\top \bar{\mathbf{X}}_{t_e,S}^{\text{sum.}} - \frac{\beta_4^\top}{2} (\bar{\mathbf{X}}_{t_{u_1},S}^{\text{sum.}} + \bar{\mathbf{X}}_{t_{u_2},S}^{\text{sum.}}) \right) - \beta_1 \right| \\ & \leq \frac{1}{|I_1| + |I_2|} |\beta_2| \left| \sum_{(t_e, t_u) \in I_1} (R_{t_e} - R_{t_u}) + \sum_{(t_e, t_{u_1}, t_{u_2}) \in I_2} \left(R_{t_e} - \frac{1}{2} (R_{t_{u_1}} + R_{t_{u_2}}) \right) \right| + \end{aligned}$$

$$\begin{aligned}
& \frac{1}{|I_1| + |I_2|} |\beta_3| \left| \sum_{(t_e, t_u) \in I_1} (t_e - t_u) + \sum_{(t_e, t_{u_1}, t_{u_2}) \in I_2} \left(t_e - \frac{1}{2}(t_{u_1} + t_{u_2}) \right) \right| + \\
& \frac{1}{|I_1| + |I_2|} \left| \sum_s \sum_d \beta_{4,s,d} \left(\sum_{(t_e, t_u) \in I_1} X_{(t_e-s)d}^{\text{sum.}} - X_{(t_u-s)d}^{\text{sum.}} + \right. \right. \\
& \quad \left. \left. \sum_{(t_e, t_{u_1}, t_{u_2}) \in I_2} X_{(t_e-s)d}^{\text{sum.}} - \frac{1}{2}(X_{(t_{u_1}-s)d}^{\text{sum.}} + X_{(t_{u_2}-s)d}^{\text{sum.}}) \right) \right| \\
& \leq \delta' |\beta_2| + \delta |\beta_3| + \delta' \|\beta_4\|_1.
\end{aligned}$$

□

Remark 1 (An alternative upper bound under linear model). In the proposed algorithm, Constraint (3) restricts the within-pair time difference to a maximum distance of ϵ . Similar constraints apply to the 1-2 and 1-'1 or 2' algorithms discussed in Supplement C.1. Using the 1-1 algorithm of Section 4 here, we derive an alternative bias bound. Specifically,

$$\begin{aligned}
|E(\widehat{\tau}^{\text{imm}} - \tau^{\text{imm}})| & \leq \frac{1}{|I_1|} |\beta_2| \left| \sum_{(t_e, t_u) \in I_1} (R_{t_e} - R_{t_u}) \right| + \frac{1}{|I_1|} |\beta_3| \left| \sum_{(t_e, t_u) \in I_1} (t_e - t_u) \right| + \\
& \quad \frac{1}{|I_1|} \left| \sum_s \sum_d \beta_{4,s,d} \sum_{(t_e, t_u) \in I_1} (X_{(t_e-s)d}^{\text{sum.}} - X_{(t_u-s)d}^{\text{sum.}}) \right| \\
& \leq \delta' |\beta_2| + \frac{1}{|I_1|} |\beta_3| \left| \sum_{(t_e, t_u) \in I_1} (t_e - t_u) \right| + \delta' \|\beta_4\|_1
\end{aligned}$$

Because Constraint (3) dictates that

$$\frac{1}{|I_1|} |\beta_3| \left| \sum_{(t_e, t_u) \in I_1} (t_e - t_u) \right| \leq \frac{1}{|I_1|} |\beta_3| \sum_{(t_e, t_u) \in I_1} |t_e - t_u| \leq |\beta_3| \epsilon,$$

an alternative upper bound for the bias is $\delta' |\beta_2| + \epsilon |\beta_3| + \delta' \|\beta_4\|_1$.

The upper bound in Theorem 1 is $\delta' |\beta_2| + \delta |\beta_3| + \delta' \|\beta_4\|_1$. Since ϵ is a strictly positive integer, this new bound does not provide guidance for reducing the bias bound, which can instead be made small based on small values for δ, δ' . That said, this result shows that the bias bound is equal to $\delta' |\beta_2| + \min(\epsilon, \delta) |\beta_3| + \delta' \|\beta_4\|_1$.

Remark 2 (Bias of estimators in the presence of non-linear temporal trends). The model on the po-

tential outcomes in Theorems 1 and S.3 specifies a linear temporal trend. This specification can be realistic and represent potential outcomes (close to) accurately in situations where temporal trends change slowly and are smooth over time, or when the observed temporal window is relatively short. In Theorems 2 and S.4 we show that, when we extend the proposed algorithms to balance additional terms, our estimators have bounded bias in the presence of non-linear temporal (and covariate) terms in the potential outcome model.

Here, we address a related but different question. We consider the case where a general temporal trend function $f(t)$ is included in the model for the potential outcomes, instead of simply a term that is linear in t . We assume that this function is K -times differentiable for $K \geq 2$, and $f^{(k)}$ stands for the k^{th} derivative of f . For this scenario, we evaluate the bias of our estimator when our balance constraints are placed only on the average time of matches as in (3), instead of including the additional terms.

We consider the case of the Algorithm 1-1. In the proof of the bias bound in Theorem S.3, the term

$$\frac{1}{|I_1|} |\beta_3| \left| \sum_{(t_e, t_u) \in I_1} (t_e - t_u) \right|$$

is now equal to

$$\frac{1}{|I_1|} \left| \sum_{(t_e, t_u) \in I_1} (f(t_e) - f(t_u)) \right|.$$

Let t_{mid} be the midpoint of the $[1, T]$ time window, with $t_{\text{mid}} = \frac{1+T}{2}$. Using Taylor' expansion of f around t_{mid} , we can write

$$\begin{aligned} f(t_e) - f(t_u) = & \\ & \sum_{k=1}^{K-1} \frac{f^{(k)}(t_{\text{mid}})}{k!} (t_e - t_{\text{mid}})^k + \text{RE}_{t_e, K} - \sum_{k=1}^{K-1} \frac{f^{(k)}(t_{\text{mid}})}{k!} (t_u - t_{\text{mid}})^k - \text{RE}_{t_u, K} \end{aligned}$$

where

$$\text{RE}_{t_e, K} = \frac{f^{(K)}(\xi_{t_e})}{K!} (\xi_{t_e} - t_{\text{mid}})^K \quad \text{and} \quad \text{RE}_{t_u, K} = \frac{f^{(K)}(\xi_{t_u})}{K!} (\xi_{t_u} - t_{\text{mid}})^K$$

with $\xi_{t_e} \in [\min(t_e, t_{\text{mid}}), \max(t_e, t_{\text{mid}})]$ and $\xi_{t_u} \in [\min(t_u, t_{\text{mid}}), \max(t_u, t_{\text{mid}})]$. Then, returning to the

term we want to bound, using the triangle inequality we write

$$\begin{aligned}
& \frac{1}{|I_1|} \left| \sum_{(t_e, t_u) \in I_1} f(t_e) - f(t_u) \right| \\
& \leq \frac{1}{|I_1|} \sum_{k=1}^{K-1} \frac{|f^{(k)}(t_{\text{mid}})|}{k!} \left| \sum_{(t_e, t_u) \in I_1} ((t_e - t_{\text{mid}})^k - (t_u - t_{\text{mid}})^k) \right| \\
& \quad + \frac{1}{|I_1|} \sum_{(t_e, t_u) \in I_1} \frac{|f^{(K)}(\xi_{t_e})| + |f^{(K)}(\xi_{t_u})|}{K!} \left(\frac{T-1}{2} \right)^K.
\end{aligned} \tag{S.13}$$

Therefore, we notice the following that are of interest.

- For $K = 2$, the bound in (S.13) reduces to

$$\frac{1}{|I_1|} |f'(t_{\text{mid}})| \left| \sum_{(t_e, t_u) \in I_1} (t_e - t_u) \right| + \frac{1}{|I_1|} \sum_{(t_e, t_u) \in I_1} \frac{|f''(\xi_{t_e})| + |f''(\xi_{t_u})|}{2} \left(\frac{T-1}{2} \right)^2$$

which based on the constraint on the average time periods of matched pairs in (3) also reduces to

$$\delta |f'(t_{\text{mid}})| + \frac{1}{|I_1|} \sum_{(t_e, t_u) \in I_1} \frac{|f''(\xi_{t_e})| + |f''(\xi_{t_u})|}{2} \left(\frac{T-1}{2} \right)^2.$$

- When the function $f(t)$ is linear and $f(t) = \beta_3 t$, this bound (for $K = 2$) reduces exactly to $|\beta_3| \delta$ as in Theorems 1 and S.3.
- When the function is non-linear, but it changes very slowly as a function of time (with small second-derivative) then the additional bias remains small. Specifically, if $|f'(t_{\text{mid}})| < \infty$ and the second derivative $|f''(\xi)| \leq c \left(\frac{2}{T-1} \right)^2 \delta$ for all $\xi \in [1, T]$ and some $c > 0$, then the bound reduces to

$$\delta |f'(t_{\text{mid}})| + c\delta.$$

- In general, if the second derivative cannot be assumed small, but the K^{th} derivative can for $K \geq 3$, we can extend the algorithm to balance $K - 2$ additional terms and guarantee small bias. Specifically, we would balance $(t_e - t_{\text{mid}})^k$ for $k = 2, 3, \dots, K - 1$. Then the bound in (S.13) becomes

$$\delta \sum_{k=1}^{K-1} \frac{|f^{(k)}(t_{\text{mid}})|}{k!} + \frac{1}{|I_1|} \sum_{(t_e, t_u) \in I_1} \frac{|f^{(K)}(\xi_{t_e})| + |f^{(K)}(\xi_{t_u})|}{K!} \left(\frac{T-1}{2} \right)^K.$$

Following a similar thought process to the previous bound, as long as $f^{(K)}(\xi) < c \left(\frac{T-1}{2}\right)^K \delta$ for all $\xi \in [1, T]$, then the bias due to the function of time is bounded by a term that is controlled by the algorithmic parameter δ .

D.2 Nonlinear potential outcome model

We extend Theorem 2 to incorporate all three estimators derived from the 1-1, 1-2, and 1-1/2 algorithms, for both the immediate and the carryover effect.

Theorem S.4. Suppose that the potential outcomes satisfy $Y_t(e, r) = \theta + \beta_1 e + \beta_2 r + h_0(t) + \sum_{s=0}^S \sum_{d=1}^{p^{\text{int}}+p^{\text{net}}+p^{\text{out}}} h_{sd}(X_{(t-s)d}^{\text{sum.}}) + \epsilon_t(e, r)$, with $E(\epsilon_t(e, r) | E_t, t, \bar{\mathbf{X}}_{t,S}^{\text{sum.}}) = 0$ and functions $h_0, h_{01}, h_{02}, \dots, h_{S(p^{\text{int}}+p^{\text{net}}+p^{\text{out}})}$ that are K -times differentiable on their support. If $h_0^{(k)}$ and $h_{sd}^{(k)}$ represent the k^{th} derivative of h_0 and h_{sd} respectively, and $|h_0^{(k)}(t)|, |h_{sd}^{(k)}(x)| \leq c$ for some $c > 0$ for all $s = 0, 1, \dots, S$, covariate $d = 1, 2, \dots, p^{\text{int}} + p^{\text{net}} + p^{\text{out}}$, t, x in the function's support, and $k = 1, 2, \dots, K$, then the bias for the proposed estimator of the immediate effect under all three algorithms satisfies $|E(\hat{\tau}^{\text{imm}}(1, 0) - \tau^{\text{imm}}(1, 0))| \leq C_T \delta + (|\beta_2| + C_X) \delta' + C_{TX} \ell^{K-1}$. Similarly, the bias for the estimator of the carryover effect satisfies $|E(\hat{\tau}^{\text{car}}(1, 0) - \tau^{\text{car}}(1, 0))| \leq C_T \delta + (|\beta_1| + C_X) \delta' + C_{TX} \ell^{K-1}$, where C_T, C_X and C_{TX} are constants proportional to c that depend on the smoothness of the functions with the corresponding indices.

Proof of Theorem S.4. Our proof proceeds similarly to the proof in Theorem S.3. We focus here on the estimator for the immediate effect based on the algorithm that matches an exposed time period to one unexposed time period. The proof for the bias bound for the causal estimator based on the algorithms that match one exposed time period to two, or one-or-two unexposed time periods detailed in Supplement C.1, and the proof for the bias bound for the estimator of the carryover effect follow similarly to the proof below and the proof of Theorem S.3, and are therefore omitted.

In non-linear settings, balance constraints are imposed on additional variables. For the variable $X_{(t-s)d}^{\text{sum.}}$, we partition its support $[a_{sd}, b_{sd}]$ into disjoint intervals of length ℓ . The total number of intervals is $(b_{sd} - a_{sd})/\ell$. If ϕ_{sdr} is the midpoint of the r -th interval, our algorithm includes balance constraints on the localized auxiliary variable at the k -th power as

$$(X_{(t-s)d}^{\text{sum.}})^{k,\dagger} = (X_{(t-s)d}^{\text{sum.}} - \phi_{sdr})^k I \left(X_{(t-s)d}^{\text{sum.}} \in [\phi_{sdr} - \ell/2, \phi_{sdr} + \ell/2] \right),$$

for $k = 1, 2, \dots, K - 1$.

Then, to derive a bound for the bias, we first derive a bound for the quantity $h_{sd}(X_{(t-s)d}^{\text{sum.}}) -$

$h_{sd}(X_{(t_u-s)d}^{\text{sum}})$, as follows.

$$\begin{aligned}
& \left| \sum_{(t_e, t_u) \in I_1} h_{sd}(X_{(t_e-s)d}^{\text{sum}}) - h_{sd}(X_{(t_u-s)d}^{\text{sum}}) \right| \\
&= \left| \sum_{r=1}^{(b_{sd}-a_{sd})/\ell} \sum_{(t_e, t_u) \in I_1} \left[\left(\sum_{k=1}^{K-1} \gamma_{sdrk} (X_{(t_e-s)d}^{\text{sum}})^{k,\dagger} + \text{RE}_{t_e-s,d,r,K} \right) - \right. \right. \\
&\quad \left. \left. \left(\sum_{k=1}^{K-1} \gamma_{sdrk} (X_{(t_u-s)d}^{\text{sum}})^{k,\dagger} + \text{RE}_{t_u-s,d,r,K} \right) \right] \right| \\
&\leq \sum_{r=1}^{(b_{sd}-a_{sd})/\ell} \left(\sum_{k=1}^{K-1} |\gamma_{sdrk}| \left| \sum_{(t_e, t_u) \in I_1} (X_{(t_e-s)d}^{\text{sum}})^{k,\dagger} - (X_{(t_u-s)d}^{\text{sum}})^{k,\dagger} \right| \right. \\
&\quad \left. + |I_1| \frac{|h_{sd}^{(K)}(\xi_{(t_e-s)d})| + |h_{sd}^{(K)}(\xi_{(t_u-s)d})|}{K!} (\ell/2)^K \right) \\
&\leq |I_1| \left(\sum_{r=1}^{(b_{sd}-a_{sd})/\ell} \left(\sum_{k=1}^{K-1} \delta' |\gamma_{sdrk}| + \frac{|h_{sd}^{(K)}(\xi_{(t_e-s)d})| + |h_{sd}^{(K)}(\xi_{(t_u-s)d})|}{K!} (\ell/2)^K \right) \right) \\
&\leq |I_1| \left((b_{sd} - a_{sd})/\ell \left(\sum_{k=1}^{K-1} \delta' c/k! + 2 \frac{c}{K!} (\ell/2)^K \right) \right)
\end{aligned}$$

where

- $\gamma_{sdrk} := \frac{h_{sd}^{(k)}(\phi_{sdr})}{k!}$ is the coefficient of the k^{th} order in the Taylor expansion for function h_{sd} around ϕ_{sdr} , where $\frac{|h_{sd}^{(k)}(\phi_{sdr})|}{k!} \leq \frac{c}{k!}$,
- $\text{RE}_{t-s,d,r,K}$ is the residual of the Taylor expansion of the function h_{sd} such that $|\text{RE}_{t-s,d,r,K}| \leq \frac{|h_{sd}^{(K)}(\xi_{(t-s)d})|}{K!} (\ell/2)^K \leq \frac{c}{K!} (\ell/2)^K$, and
- $\xi_{(t-s)d}$ is a value between $\min(X_{(t-s)d}^{\text{sum}}, I(X_{(t-s)d}^{\text{sum}}) \in [\phi_{sdr} - \ell/2, \phi_{sdr} + \ell/2])$, ϕ_{sdr} and $\max(X_{(t-s)d}^{\text{sum}}, I(X_{(t-s)d}^{\text{sum}}) \in [\phi_{sdr} - \ell/2, \phi_{sdr} + \ell/2])$, ϕ_{sdr} .

Therefore, for the causal estimator of the immediate effect we can show that

$$\begin{aligned}
& |E(\widehat{\tau}^{\text{imm}}(1, 0) - \tau^{\text{imm}}(1, 0))| \\
&= \left| E \left(\frac{1}{|I_1|} \sum_{(t_e, t_u) \in I_1} Y_{t_e} - Y_{t_u} \right) - E[(Y_t(1, R_t) - Y_t(0, R_t)) I(E_t = 1)] \mid \mathbf{E}, \mathbf{t}, \overline{\mathbf{X}}_{t,S}^{\text{sum}} \right| \\
&= \left| \frac{1}{|I_1|} \sum_{(t_e, t_u) \in I_1} \left(\theta + \beta_1 + \beta_2(R_{t_e} - R_{t_u}) + (h_0(t_e) - h_0(t_u)) + \right. \right.
\end{aligned}$$

$$\begin{aligned}
& \left. \sum_{s=0}^S \sum_{d=1}^{p^{\text{int}}+p^{\text{net}}+p^{\text{out}}} (h_{sd}(X_{(t_e-s)d}^{\text{sum.}}) - h_{sd}(X_{(t_u-s)d}^{\text{sum.}})) \right) - \beta_1 \Big| \\
& \leq |\beta_2| \delta' + \left(\frac{T-1}{\ell} \left(\sum_{k=1}^{K-1} \frac{\delta c}{k!} + 2 \frac{c}{K!} (\ell/2)^K \right) \right) + \\
& \quad \sum_s \sum_d \left(\frac{b_{sd} - a_{sd}}{\ell} \left(\sum_{k=1}^{K-1} \frac{\delta' c}{k!} + 2 \frac{c}{K!} (\ell/2)^K \right) \right) \\
& \leq C_T \delta + (|\beta_2| + C_X) \delta' + C_{TX} \ell^{K-1}.
\end{aligned}$$

where the values of the constants are

$$\begin{aligned}
C_T &= \sum_{k=1}^{K-1} \frac{(T-1)c}{\ell k!}, \\
C_X &= \sum_{s=0}^S \sum_{d=1}^{p^{\text{int}}+p^{\text{net}}+p^{\text{out}}} \sum_{k=1}^{K-1} \frac{(b_{sd} - a_{sd})c}{\ell k!}, \\
C_{TX} &= \left(\frac{1}{2} \right)^{K-1} \left(\frac{(T-1)c}{K!} + \sum_{s=0}^S \sum_{d=1}^{p^{\text{int}}+p^{\text{net}}+p^{\text{out}}} \frac{(b_{sd} - a_{sd})c}{K!} \right).
\end{aligned}$$

□

E Variance estimation

We consider the case of estimating the immediate effect when we match an exposed time period to one unexposed time period (detailed in Section 4). The arguments follow similarly for the algorithms of estimating the immediate effect that match an exposed time period to two or one-or-two time periods (detailed in Supplement C.1), or for the algorithms for estimating the carryover effect (detailed in Supplement C.2).

Here, we consider a simplified setting where all exposed time periods are matched, $|\mathcal{T}_1^*| = |\mathcal{T}_1|$, and the number of exposed time periods is fixed, so $|\mathcal{T}_1^*|$ does not vary across data sets. This could be the case when the number of unexposed time periods is large relative to the number of exposed ones, and the number of exposed is fixed by design. Therefore, we do not consider the general case where $|\mathcal{T}_1^*|$ has inherent variability that will have to be considered.

For the derivations below, we assume that the error terms in the potential outcome model of Theorem 1 and Theorem 2 have finite second moment. For simplicity, we also assume that this variance is constant, i.e., $\text{Var}(e_t(e, r)) = \sigma^2$, for some $\sigma^2 > 0$.

E.1 Setup and notation

Here, it is useful to introduce some notation. For what follows we use k to denote the k^{th} match, where $k = 1, 2, \dots, \mathcal{T}_1$, and for which time period $t_{e,k}$ is matched to time period $t_{u,k}$. This match contributes $Z_k = Y_{t_{e,k}} - Y_{t_{u,k}}$ to the estimator, which can be written as

$$\hat{\tau}^{\text{imm}} = \frac{1}{|\mathcal{T}_1|} \sum_{k=1}^{|\mathcal{T}_1|} Z_k.$$

We study the form of Z_k and the linear and nonlinear models of Theorems 1 and 2. Under the linear model, Z_k is equal to

$$\begin{aligned} Z_k &= \beta_0 + \beta_1 + \beta_2 R_{t_{e,k}} + \beta_3 t_{e,k} + \beta_4^\top \bar{\mathbf{X}}_{t_{e,k},S}^{\text{sum.}} + \epsilon_{t_{e,k}}(1, R_{t_{e,k}}) - \\ &\quad \left(\beta_0 + \beta_2 R_{t_{u,k}} + \beta_3 t_{u,k} + \beta_4^\top \bar{\mathbf{X}}_{t_{u,k},S}^{\text{sum.}} + \epsilon_{t_{u,k}}(0, R_{t_{u,k}}) \right) \\ &= \beta_1 + \left[\beta_2 (R_{t_{e,k}} - R_{t_{u,k}}) + \beta_3 (t_{e,k} - t_{u,k}) + \beta_4^\top \left(\bar{\mathbf{X}}_{t_{e,k},S}^{\text{sum.}} - \bar{\mathbf{X}}_{t_{u,k},S}^{\text{sum.}} \right) \right] + \\ &\quad \epsilon_{t_{e,k}}(1, R_{t_{e,k}}) - \epsilon_{t_{u,k}}(0, R_{t_{u,k}}). \end{aligned}$$

We use imb_k to denote the magnitude of the overall imbalance within match k (weighted by each variable's importance in the outcome model) where

$$\text{imb}_k = \beta_2 (R_{t_{e,k}} - R_{t_{u,k}}) + \beta_3 (t_{e,k} - t_{u,k}) + \beta_4^\top \left(\bar{\mathbf{X}}_{t_{e,k},S}^{\text{sum.}} - \bar{\mathbf{X}}_{t_{u,k},S}^{\text{sum.}} \right),$$

and eDiff_k to denote the difference of the error terms within the match defined as

$$\text{eDiff}_k = \epsilon_{t_{e,k}}(1, R_{t_{e,k}}) - \epsilon_{t_{u,k}}(0, R_{t_{u,k}}).$$

Then,

$$Z_k = \beta_1 + \text{imb}_k + \text{eDiff}_k.$$

Under the non-linear model in Theorem 2, everything follows similarly, except the definition of the imbalance term imb_k includes the term $h_0(t_{e,k}) - h_0(t_{u,k})$ instead of $\beta_3(t_{e,k} - t_{u,k})$, and the term $\sum_{s=0}^S p^{\text{int}} + \sum_{d=1}^{p^{\text{net}} + p^{\text{out}}} \left[h_{sd}(X_{(t_{e,k}-s)d}^{\text{sum.}}) - h_{sd}(X_{(t_{u,k}-s)d}^{\text{sum.}}) \right]$ instead of $\beta_4^\top \left(\bar{\mathbf{X}}_{t_{e,k},S}^{\text{sum.}} - \bar{\mathbf{X}}_{t_{u,k},S}^{\text{sum.}} \right)$.

Under this setup, we can write the true variance of the estimator as

$$\text{Var}(\hat{\tau}^{\text{imm}}) = \text{Var}\left(\frac{1}{|\mathcal{T}_{1\cdot}|} \sum_{k=1}^{|\mathcal{T}_{1\cdot}|} Z_k\right) = \text{Var}\left(\frac{1}{|\mathcal{T}_{1\cdot}|} \sum_{k=1}^{|\mathcal{T}_{1\cdot}|} (\text{imb}_k + \text{eDiff}_k)\right).$$

When balance is specified to be exact by setting $\delta = \delta' = 0$, we have that $\frac{1}{|\mathcal{T}_{1\cdot}|} \sum_{k=1}^{|\mathcal{T}_{1\cdot}|} \text{imb}_k = 0$, and the true variance of our estimator simplifies to

$$\text{Var}(\hat{\tau}^{\text{imm}}) = \text{Var}\left(\frac{1}{|\mathcal{T}_{1\cdot}|} \sum_{k=1}^{|\mathcal{T}_{1\cdot}|} \text{eDiff}_k\right) = \sigma_{\text{eDiff}}^2 / |\mathcal{T}_{1\cdot}|, \quad (\text{S.14})$$

since the error terms are assumed independent.

Finally, our estimator for the variance can be written as

$$\widehat{\text{Var}}(\hat{\tau}^{\text{imm}}) = \frac{1}{|\mathcal{T}_{1\cdot}| - 1} \sum_{k=1}^{|\mathcal{T}_{1\cdot}|} (Z_k - \hat{\tau}^{\text{imm}})^2. \quad (\text{S.15})$$

E.2 Variance estimation when matching exactly within each pair

We consider first an alternative algorithm that ensures that all temporal information within *each matched pair* is identical. We note that this is *not* the proposed estimator in Section 4, the variance of which is considered in Supplement E.3.

Under this alternative algorithm, $\text{imb}_k = 0$ for all matches $k = 1, 2, \dots, \mathcal{T}_{1\cdot}$. Consider the resulting estimator $\hat{\tau}^{\text{imm}}$ based on the acquired matches from such algorithm which can be written as

$$\hat{\tau}^{\text{imm}} = \frac{1}{|\mathcal{T}_{1\cdot}|} \sum_{k=1}^{|\mathcal{T}_{1\cdot}|} Z_k = \beta_1 + \frac{1}{|\mathcal{T}_{1\cdot}|} \sum_{k=1}^{|\mathcal{T}_{1\cdot}|} \text{eDiff}_k.$$

In this case, our variance estimator in (S.15) is equal to

$$\frac{1}{|\mathcal{T}_{1\cdot}| - 1} \sum_{k=1}^{|\mathcal{T}_{1\cdot}|} \left[\text{eDiff}_k - \left(\frac{1}{|\mathcal{T}_{1\cdot}|} \sum_{k=1}^{|\mathcal{T}_{1\cdot}|} \text{eDiff}_k \right) \right]^2$$

and it is, therefore, unbiased for $\text{Var}(\hat{\tau}^{\text{imm}})$ in (S.14).

There are a few notes worth making here. If the temporal trend exists and is linear ($\beta_3 \neq 0$ in the model of Theorem 1) it is impossible to balance time exactly within each match, and $\text{imb}_k \neq 0$

necessarily. Therefore, this approach works in the absence of a temporal trend (i.e., $\beta_3 = 0$ in the linear model of Theorem 1), or when the temporal trend follows a nonlinear function (such as $h_0(t)$ in Theorem 2) which is *measured* and matched on exactly. As a result, the requirements over the temporal trend term for unbiased estimation of the variance are relatively strong. If none of these hold, some imbalance within each pair will remain, which is studied in the next section. Finally, when matching exactly within each pair, unless the number of unexposed time periods far surpass the number of exposed ones, it is expected that there will be exposed time periods for which a match will not exist, and $|\mathcal{T}_{1.}| < |\mathcal{T}_{1.}|$. This is not a case we consider here.

E.3 Variance estimation for the causal effect estimator based on our algorithms

In this case, the algorithms do not match time-varying information exactly within each pair as in Supplement E.2, rather than impose overall balance constraints (Section 4). The variance estimator in (S.15) can be re-written as

$$\begin{aligned}\widehat{\text{Var}}(\widehat{\tau}^{\text{imm}}) &= \frac{1}{|\mathcal{T}_{1.}| - 1} \sum_{k=1}^{|\mathcal{T}_{1.}|} \left[\beta_1 + \text{imb}_k + \text{eDiff}_k - \frac{1}{|\mathcal{T}_{1.}|} \sum_{k=1}^{|\mathcal{T}_{1.}|} (\beta_1 + \text{imb}_k + \text{eDiff}_k) \right]^2 \\ &= \frac{1}{|\mathcal{T}_{1.}| - 1} \sum_{k=1}^{|\mathcal{T}_{1.}|} \left[\text{imb}_k + \text{eDiff}_k - \frac{1}{|\mathcal{T}_{1.}|} \sum_{k=1}^{|\mathcal{T}_{1.}|} (\text{imb}_k + \text{eDiff}_k) \right]^2,\end{aligned}$$

which, since the average time and time-varying covariates are balanced exactly across matched pairs with $\delta = \delta' = 0$, is also equal to

$$= \frac{1}{|\mathcal{T}_{1.}| - 1} \sum_{k=1}^{|\mathcal{T}_{1.}|} \left[\text{imb}_k + \text{eDiff}_k - \frac{1}{|\mathcal{T}_{1.}|} \sum_{k=1}^{|\mathcal{T}_{1.}|} \text{eDiff}_k \right]^2.$$

Then, we can write $\text{E} \left[\widehat{\text{Var}}(\widehat{\tau}^{\text{imm}}) \right]$ as

$$\begin{aligned}& \frac{1}{|\mathcal{T}_{1.}| - 1} \sum_{k=1}^{|\mathcal{T}_{1.}|} \text{E}(\text{imb}_k^2) + \frac{2}{|\mathcal{T}_{1.}| - 1} \sum_{k=1}^{|\mathcal{T}_{1.}|} \text{E} \left[\text{imb}_k * \left(\text{eDiff}_k - \frac{1}{|\mathcal{T}_{1.}|} \sum_{k=1}^{|\mathcal{T}_{1.}|} \text{eDiff}_k \right) \right] \\ & \quad + \frac{1}{|\mathcal{T}_{1.}| - 1} \sum_{k=1}^{|\mathcal{T}_{1.}|} \text{E} \left[\left(\text{eDiff}_k - \frac{1}{|\mathcal{T}_{1.}|} \sum_{k=1}^{|\mathcal{T}_{1.}|} \text{eDiff}_k \right)^2 \right] \\ & = \frac{1}{|\mathcal{T}_{1.}| - 1} \sum_{k=1}^{|\mathcal{T}_{1.}|} \text{E}(\text{imb}_k^2) + \sigma_{\text{eDiff}}^2 / |\mathcal{T}_{1.}|,\end{aligned}$$

where the equality holds because the errors (and therefore the error differences) are independent of all information including the covariates, which implies that

$$\begin{aligned} E \left[\text{imb}_k \left(\text{eDiff}_k - \frac{1}{|\mathcal{T}_{1\cdot}|} \sum_{k=1}^{|\mathcal{T}_{1\cdot}|} \text{eDiff}_k \right) \right] &= \\ E [\text{imb}_k] \cdot E \left[\text{eDiff}_k - \frac{1}{|\mathcal{T}_{1\cdot}|} \sum_{k=1}^{|\mathcal{T}_{1\cdot}|} \text{eDiff}_k \right] &= 0. \end{aligned}$$

This demonstrates that the variance estimator is, in expectation, larger than the true variance, by a term that depends on the expected magnitude of imbalance within each match. Therefore using our variance estimator for inference would result in $(1 - \alpha)100\%$ intervals that cover the true value at least that proportion of time.

E.4 Temporal correlation in the outcome model residuals

In time series settings, it might be the case that outcomes are autocorrelated across time, even beyond what can be explained by measured covariates. In time series analyses of an outcome Y_t that exhibits temporal autocorrelation, researchers often adopt a model on the first differences $Z_t = Y_t - Y_{t-1}$ instead of a model directly on Y_t . That is because, often, the first differences Z_t will exhibit much less (if any) temporal autocorrelation.

In our simulations, we have found that our inferential approach is rather robust to temporal autocorrelation of the error terms of the outcome model (see Supplement H.8). We conjecture that this performance might have links to the fact that, in our estimator and its variance, the error terms appear only through the differences eDiff_k . Note that an exposed time period is required to be temporally close to its matched unexposed time period (no more than ϵ -apart). Therefore, even when the errors are temporally autocorrelated, the error differences might exhibit much less autocorrelation across matches, which makes our inferential procedure robust to temporal correlation of the error terms. Future work can evaluate this connection even further.

In Supplement H.8, we also consider an alternative inferential procedure based on the Newey-West variance estimator [Newey and West, 1986]. In Supplement E.5 we discuss how our point estimator can be acquired as the OLS estimator of a regression on the time periods matched by our algorithm, which will allow us to employ the Newey-West variance estimator.

E.5 Our causal estimator within a regression framework on the matched sample

In the presence of autocorrelated outcomes across time (such as in the case when the error terms are autocorrelated in the outcome models of Theorem 1 or Theorem 2), an alternative inferential strategy might employ the Newey-West variance estimator [Newey and West, 1986]. This estimator accounts for serial correlation in the outcomes, and often provides a more reliable, if not conservative, inference in time-series settings.

To use the Newey-West variance estimator, our first step is to rewrite our point estimator within a regression framework. Specifically, we employ regression of the outcome on the exposure on the time periods that are matched following the design phase (the optimization step in Section 4.1). Then, the ordinary least squares (OLS) estimator for the coefficient of the exposure is the point estimator, with regression-based standard errors to quantify uncertainty. Here, we illustrate that the OLS estimator is numerically equivalent to our proposed estimator in (6). Also, we note that the Wald-type standard errors we employ in Section 4.3 differ from the vanilla regression-based standard errors (from the regression that also assumes independent error terms) by a term of order $O(|\mathcal{T}_1|^{-1})$ which diminishes with the number of matched exposed time periods. We return to our implementation of the Newey-West variance estimator in Supplement H.8 where we evaluate its performance in simulations.

E.5.1 Equivalence of point estimates of the proposed causal estimator and the OLS estimator in the outcome on exposure regression

For simplicity, we focus on the algorithm and estimator for the immediate effect. We consider the time periods that have been part of a match. Specifically, we consider the time periods $t_e \in \mathcal{T}_1$ such that $a_{t_e t_u} = 1$ for some $t_u \in \mathcal{T}_0$, and the time periods $t_u \in \mathcal{T}_0$ such that $a_{t_e t_u} = 1$ for some $t_e \in \mathcal{T}_1$. Since there are $|\mathcal{T}_1|$ matched exposed time periods, and each time period can be part of at most one match, the number of time periods we consider is $2|\mathcal{T}_1|$. We construct the data set using these time periods only, and use Y_k and E_k to denote the outcome and exposure value for k th time period in ascending order in this data set, where $k = 1, 2, \dots, 2|\mathcal{T}_1|$. On this data set, we consider a simple linear regression of Y_k on E_k and we use the estimated coefficient of the exposure and associated confidence interval as the estimate and confidence interval of the immediate effect.

First, it is easy to show that this regression estimator is numerically equivalent to the $\hat{\tau}^{\text{imm}}$ intro-

duced in Section 4.2. To see this, recall from (6) that the proposed estimator is given by:

$$\hat{\tau}^{\text{imm}} = \frac{1}{|\mathcal{T}_1|} \sum_{t_e \in \mathcal{T}_1} (Y_{t_e} - Y_{t_e}^*).$$

Let $\bar{E} = \frac{1}{2|\mathcal{T}_1|} \sum_{k=1}^{2|\mathcal{T}_1|} E_k$ be the mean value of the exposure in the matched data set, so $\bar{E} = 0.5$. The OLS estimate for the coefficient of the exposure is equal to

$$\frac{\sum_{k=1}^{2|\mathcal{T}_1|} (E_k - \bar{E}) Y_k}{\sum_{k=1}^{2|\mathcal{T}_1|} (E_k - \bar{E})^2} = \frac{1}{0.5|\mathcal{T}_1|} \left(\sum_{t_e \in \mathcal{T}_1} 0.5 Y_{t_e} - 0.5 Y_{t_e}^* \right) = \hat{\tau}^{\text{imm}}.$$

Furthermore, letting $\bar{Y} = \frac{1}{2|\mathcal{T}_1|} \sum_{k=1}^{2|\mathcal{T}_1|} Y_k$, the OLS estimate of the regression intercept is equal to $\bar{Y} - 0.5\hat{\tau}^{\text{imm}}$.

E.5.2 Differences in inferences when viewing causal estimator through a regression lens

Here, we compare the standard error of the regression estimator with the proposed standard error under the Wald-type construction in Section 4.3.

Based on the results above about the estimated regression coefficients, the fitted values from the regression are equal to

$$\hat{Y}_k = (\bar{Y} - 0.5\hat{\tau}^{\text{imm}}) + \hat{\tau}^{\text{imm}} E_k.$$

Then, the sum of squared errors (SSE) can be written as

$$\begin{aligned} \text{SSE} &= \sum_{t_e \in \mathcal{T}_1} \left[\left(Y_{t_e} - \hat{Y}_{t_e} \right)^2 + \left(Y_{t_e}^* - \hat{Y}_{t_e}^* \right)^2 \right] \\ &= \sum_{t_e \in \mathcal{T}_1} \left[\left(Y_{t_e} - (\bar{Y} - 0.5\hat{\tau}^{\text{imm}}) - \hat{\tau}^{\text{imm}} \right)^2 + \left(Y_{t_e}^* - (\bar{Y} - 0.5\hat{\tau}^{\text{imm}}) \right)^2 \right] \\ &= \sum_{t_e \in \mathcal{T}_1} \left[\left(Y_{t_e} - \bar{Y} - 0.5\hat{\tau}^{\text{imm}} \right)^2 + \left(Y_{t_e}^* - \bar{Y} + 0.5\hat{\tau}^{\text{imm}} \right)^2 \right] \\ &= \sum_{t_e \in \mathcal{T}_1} \left[\left(Y_{t_e} - \frac{\sum Y_{t_e}}{|\mathcal{T}_1|} \right)^2 + \left(Y_{t_e}^* - \frac{\sum Y_{t_e}^*}{|\mathcal{T}_1|} \right)^2 \right]. \end{aligned}$$

Based on this residual variance estimate from the regression, denoted as MSE, is equal to

$$\text{MSE} = \frac{\sum_{t_e \in \mathcal{T}_1} \left[\left(Y_{t_e} - \frac{\sum Y_{t_e}}{|\mathcal{T}_1|} \right)^2 + \left(Y_{t_e}^* - \frac{\sum Y_{t_e}^*}{|\mathcal{T}_1|} \right)^2 \right]}{2|\mathcal{T}_1| - 2},$$

Hence the standard error for the coefficient of the exposure, denoted as $\hat{\sigma}_{\text{OLS}}^2$, is

$$\hat{\sigma}_{\text{OLS}}^2 = \frac{\text{MSE}}{\sum_{k=1}^{2|\mathcal{T}_{1\cdot}|} (E_k - \bar{E})^2} = \frac{\text{MSE}}{0.5|\mathcal{T}_{1\cdot}|} = \frac{\sum_{t_e \in \mathcal{T}_{1\cdot}} \left[\left(Y_{t_e} - \frac{\sum Y_{t_e}}{|\mathcal{T}_{1\cdot}|} \right)^2 + \left(Y_{t_e}^* - \frac{\sum Y_{t_e}^*}{|\mathcal{T}_{1\cdot}|} \right)^2 \right]}{|\mathcal{T}_{1\cdot}|(|\mathcal{T}_{1\cdot}| - 1)},$$

and the resulting confidence interval for the regression-based estimator of τ^{imm} is $[\hat{\tau}^{\text{imm}} - z_{1-\alpha/2} \hat{\sigma}_{\text{OLS}}, \hat{\tau}^{\text{imm}} + z_{1-\alpha/2} \hat{\sigma}_{\text{OLS}}]$.

We can write the variance estimator in our Wald-type inference described in Section 4.3 as

$$\begin{aligned} \hat{s}^2 &= \frac{\sum_{t_e \in \mathcal{T}_{1\cdot}} (Y_{t_e} - Y_{t_e}^* - \hat{\tau}^{\text{imm}})^2}{|\mathcal{T}_{1\cdot}| - 1} \\ &= \frac{\sum_{t_e \in \mathcal{T}_{1\cdot}} \left[\left(Y_{t_e} - \frac{\sum Y_{t_e}}{|\mathcal{T}_{1\cdot}|} \right) - \left(Y_{t_e}^* - \frac{\sum Y_{t_e}^*}{|\mathcal{T}_{1\cdot}|} \right) \right]^2}{|\mathcal{T}_{1\cdot}| - 1} \\ &= \frac{\sum_{t_e \in \mathcal{T}_{1\cdot}} \left[\left(Y_{t_e} - \frac{\sum Y_{t_e}}{|\mathcal{T}_{1\cdot}|} \right)^2 + \left(Y_{t_e}^* - \frac{\sum Y_{t_e}^*}{|\mathcal{T}_{1\cdot}|} \right)^2 - 2 \left(Y_{t_e} - \frac{\sum Y_{t_e}}{|\mathcal{T}_{1\cdot}|} \right) \left(Y_{t_e}^* - \frac{\sum Y_{t_e}^*}{|\mathcal{T}_{1\cdot}|} \right) \right]}{|\mathcal{T}_{1\cdot}| - 1}. \end{aligned}$$

Then, the difference between the standard error estimator in the regression-based confidence interval, $\hat{\sigma}_{\text{OLS}}^2$, and in the proposed Wald-type confidence interval in Section 4.3, $\hat{s}^2/|\mathcal{T}_{1\cdot}|$, is $2 \frac{\sum_{t_e \in \mathcal{T}_{1\cdot}} \left(Y_{t_e} - \frac{\sum Y_{t_e}}{|\mathcal{T}_{1\cdot}|} \right) \left(Y_{t_e}^* - \frac{\sum Y_{t_e}^*}{|\mathcal{T}_{1\cdot}|} \right)}{|\mathcal{T}_{1\cdot}|(|\mathcal{T}_{1\cdot}| - 1)}$. Because this term represents exactly twice the sample covariance of the outcomes in the exposed and unexposed time periods in the matched pairs $(Y_{t_e}$ and $Y_{t_e}^*)$, scaled by the sample size, this difference is of the order of $O(|\mathcal{T}_{1\cdot}|^{-1})$, and is therefore negligible.

F A Synthetic Dataset on Wildfire Exposure

We generate data over a rectangular region $[0, 1] \times [0, 4]$. We consider $N = 50$ interventional units, and $M = 200$ outcome units. We refer to the subset of our area $[0, 0.5] \times [1, 4]$ as the “urban” subregion, and we consider it to be more dense in outcome units than interventional units. The reverse is true for the remaining area which we refer to as the “rural” subregion. Specifically, we randomly generate the locations of 7 out of 50 interventional units and 150 out of 200 outcome units in the urban subregion, while the remaining interventional and outcome units are randomly positioned in the rural subregion. The outcome units are denoted by $\mathcal{M} = \{m_1, m_2, \dots, m_M\}$. Since we generate $M = 200$ outcome units, in what follows we use X_{0j}^{out} and $\mathbf{X}_{tj}^{\text{out}}$ to denote the time-invariant and time-varying covariates of outcome unit m_j , respectively, with $j = 1, 2, \dots, M$. For our simulations in Section 5, one randomly chosen outcome unit in the urban area is considered, whereas we use all M outcome units to evaluate

our multiple-testing inferential procedure detailed in Supplement C.4. To align with our real-world application, we set the total number of time periods to $T = 1003$.

F.1 Generating the temporal trends and covariates for the interventional and outcome units

We denote the smooth temporal trends as $f_i^{\text{int}}(t)$ and $f_j^{\text{out}}(t)$ for interventional unit n_i and outcome unit m_j , respectively. We generate the temporal trends to include the same increasing linear trend $\mu(t) = 0.0004t$, with temporally smooth unit-specific variation drawn from a Gaussian process with a Gaussian correlation kernel. Specifically, let f_i^{int} denote the value of the smooth temporal trend for interventional unit n_i across the T time periods as $\mathbf{f}_i^{\text{int}} = (f_i^{\text{int}}(1), \dots, f_i^{\text{int}}(T))^\top$. Similarly, we use $\boldsymbol{\mu}$ to denote the value of the overall temporal trend across the T time periods, as $\boldsymbol{\mu} = (\mu(1), \mu(2), \dots, \mu(T))^\top$. We draw $\mathbf{f}_i^{\text{int}} \sim N(\boldsymbol{\mu}, \Sigma)$ independently across interventional units, where the (t_1, t_2) entry of the covariance matrix Σ is $\Sigma_{t_1, t_2} = \frac{\exp(-(t_1 - t_2)^2)}{2 \cdot 100^2}$. If $\mathbf{f}_j^{\text{out}}$ denotes the temporal trend for outcome unit m_j at the T time periods, we set $\mathbf{f}_j^{\text{out}}$ equal to the value of $\mathbf{f}_i^{\text{int}}$ for the interventional unit n_i that is geographically closest to the outcome unit m_j .

We generate time-invariant covariates independently across units according to a different distribution for units located in the urban and rural subregions. Specifically, X_{0i}^{int} is drawn from a Beta(1, 9) distribution if n_i is located within the urban subregion $[0, 0.5] \times [1, 4]$, or a Beta(9, 1) distribution if it is located in the rural subregion. We generate the outcome unit time-invariant covariate in the same manner. Therefore, the time-invariant covariates of interventional and outcome units are more similar to one another when the units are located in the same subregion, with higher values in the rural compared to the urban region.

Finally, we generate $p^{\text{int}} = p^{\text{out}} = 5$ time-varying covariates for the interventional and the outcome units. These covariates are generated to resemble the observed values for temperature, humidity, precipitation, wind speed, and wind direction in our observed data. Below, we detail how each of the five covariates are generated for an outcome unit m_j with coordinates (x_j, y_j) , where $\mathbf{X}_{tj}^{\text{out}} = (X_{tj1}^{\text{out}}, X_{tj2}^{\text{out}}, \dots, X_{tj5}^{\text{out}})^\top$.

The first covariate X_{tj1}^{out} represents temperature for unit m_j over time. We set

$$X_{tj1}^{\text{out}} = \text{base_temperature}_j + \text{seasonal_effect}_t + \text{trend}_t + \\ + \text{daily_variation}_{tj},$$

where `base_temperature`, `seasonal_effect`, `trend`, and `daily_variation` are defined

as follows. We set $\text{base_temperature}_j = 20 - 3y_j + 5x_j$ with higher values for locations towards the bottom right corner of our geography (reflecting that the “southeast” area of our geography has warmer conditions). We set the seasonal variation as $\text{seasonal_effect}_t = 15 * \sin(\frac{2\pi}{365}(t - 150))$ which indicates annual temperature cycles, and $\text{trend}_t = t/5000$ represents a long-term warming trend. Lastly, we generate the day- and unit-specific errors as $\text{daily_variation}_{tj} \sim N(0, ([\log(|t - 500| + 2)]/1.5)^2)$, independently across units and time.

The second covariate X_{tj2}^{out} represents humidity patterns for the outcome unit m_j across time. This variable is generated based on two quantities, $\text{seasonal_effect}_{tj}$ and noise_{tj} which, in turn, are generated in two different ways depending on the outcome unit’s distance from 0 on the x-axis. (This design is such that locations that are close to 0 on the x-axis can be conceived as being “close to the coast” with higher humidity levels). If $x_j \leq 0.5$, the location is considered as being coastal, and the seasonal effect and noise are generated in the following manner. We specify $\text{seasonal_effect}_{tj} = 10 \sin(2\pi/365(t - 170)) + 5y_j - 20x_j + 65$, reflecting higher humidity during the summer, in areas closer to the sea (small x values) or in the north part of our geography (large y values). The noise term is generated as $\text{noise}_{tj} \sim N(0, 5^2)$ independently across time and units. If $x_j > 0.5$, the location is considered inland. The seasonal effect is simplified to be constant across coordinates in the inland area as $\text{seasonal_effect}_{tj} = 2 \sin(2\pi/365(t - 170)) + 10$. The noise term is generated as $\text{noise}_{tj} \sim N(0, 3^2)$ independently across times and units. Humidity is then generated from a truncated normal distribution with mean $\text{seasonal_effect}_{tj}$, standard deviation equal to 15, truncated below at 0, and above at the minimum of 100 and $\text{seasonal_effect}_{tj} + \text{noise}_{tj}$.

The precipitation covariate X_{tj3}^{out} is also generated differently based on the x -coordinate of each unit. For (coastal) outcome units with $x_j \leq 0.5$, we set $\text{seasonal_effect}_{tj} = 0.15 + y_j/100 - x_j/50 + 0.1 \sin\left(\frac{2\pi(t-180)}{365}\right)$ and we generate $\text{rain_indicator}_{tj}$ independently across units and time from a $\text{Ber}(\text{seasonal_effect}_{tj})$ distribution, with $\text{rain_indicator}_{tj} = 1$ reflecting rain at the location of outcome unit m_j at time t , and $= 0$ reflecting no rain. On days without rain, we set $X_{tj3}^{\text{out}} = 0$. On rainy days, we generate another Bernoulli draw as $\text{extreme_rain}_{tj} \sim \text{Ber}(0.01 \times \text{seasonal_effect}_{tj})$, with $\text{extreme_rain}_{tj} = 1$ reflecting heavy precipitation, and $= 0$ for moderate precipitation. This specification implies that heavy precipitation events are more likely during the summer. Then, for days with moderate rain, we generate $X_{tj3}^{\text{out}} \sim \text{Gamma}(0.05, 5)$, while on days with heavy rain we generate $X_{tj3}^{\text{out}} \sim \text{LogNormal}(2, 0.8^2)$. For (inland) outcome units with $x_j > 0.5$, we similarly generate $\text{rain_indicator}_{tj}$ independently across units and time from a $\text{Ber}(\text{seasonal_effect}_{tj})$ distribution where $\text{seasonal_effect}_{tj} = \max(0.1 \sin\left(\frac{2\pi(t-180)}{365}\right), 0)$. We set $X_{tj3}^{\text{out}} = 0$ if $\text{rain_indicator}_{tj} = 0$, and draw X_{tj3}^{out} from a $\text{Gamma}(2, 5)$ distribution if

`rain_indicatortj` = 1.

The covariate representing wind speed, X_{tj4}^{out} , is generated based on a smooth seasonal trend with heteroskedastic noise. For day t , the mean wind speed is specified as `mean_wind_speedt` = $10 + 20(1 - (\frac{1}{182}t - \frac{183}{182})^2)^{0.2}$ which forms a flattened parabolic dome centered at the middle of the year. We also specify `wind_speed_variancet` = $0.1\text{mean_wind_speed}_t - 1$. Then, the wind speed covariate is generated as $X_{tj4}^{\text{out}} \sim N(\text{mean_wind_speed}_{tj}, \text{wind_speed_variance}_t)$, independently across units and time. Lastly, to ensure sufficient variability across time, we add a random draw from the standard normal distribution $N(0, 1)$ to the X_{tj4}^{out} values which were generated with `wind_speed_variancet` < 0.1.

Lastly, the wind direction covariate X_{tj5}^{out} is generated to exhibit seasonal patterns. In January and December, it varies widely and is sampled uniformly on $[0, 1]$, whereas in other months, it remains relatively more constant and it is sampled uniformly on $[0.7, 0.9]$.

For an interventional unit n_i , their time-varying covariates are assigned to be equal to the time-varying covariates of the outcome unit m_j that is geographically closest. We scale the temporal trend variables and the time-varying covariates representing temperature, humidity, and wind speed for the interventional and outcome units to the $[0, 1]$ range by subtracting the minimum and dividing by the range of each variable across units. To ensure that most (over 95%) of values corresponding to the precipitation variable fall within the $[0, 1]$ interval, we apply a $\log(1 + x)$ transformation. Wind direction remains unchanged as it is naturally bounded within the $[0, 1]$ range.

The simulated covariates preserve similar fluctuation patterns compared to the observed covariates after re-scaling. As shown in Figure S.3, the temporal patterns in simulated temperature, humidity, precipitation, wind speed, and wind direction are very similar to those in our study data.

F.2 The treatment assignment, bipartite network, and outcome

We consider five scenarios that differ in their confounding structures. Each scenario defines a distinct way of generating treatment vectors for the interventional units over time. In the specifications below, when we write $A_{ti}, G_{tij} \sim (\text{Distribution})$ we implicitly specify the distribution of the variable conditional on all covariate information and temporal trends. In what follows, we define $\bar{R}_t = \frac{1}{M} \sum_{j=1}^M R_{tj}$.

(a) No confounders:

$$A_{ti} \sim \text{Ber}(0.3),$$

$$G_{tij} \sim \text{Ber}(0.3),$$

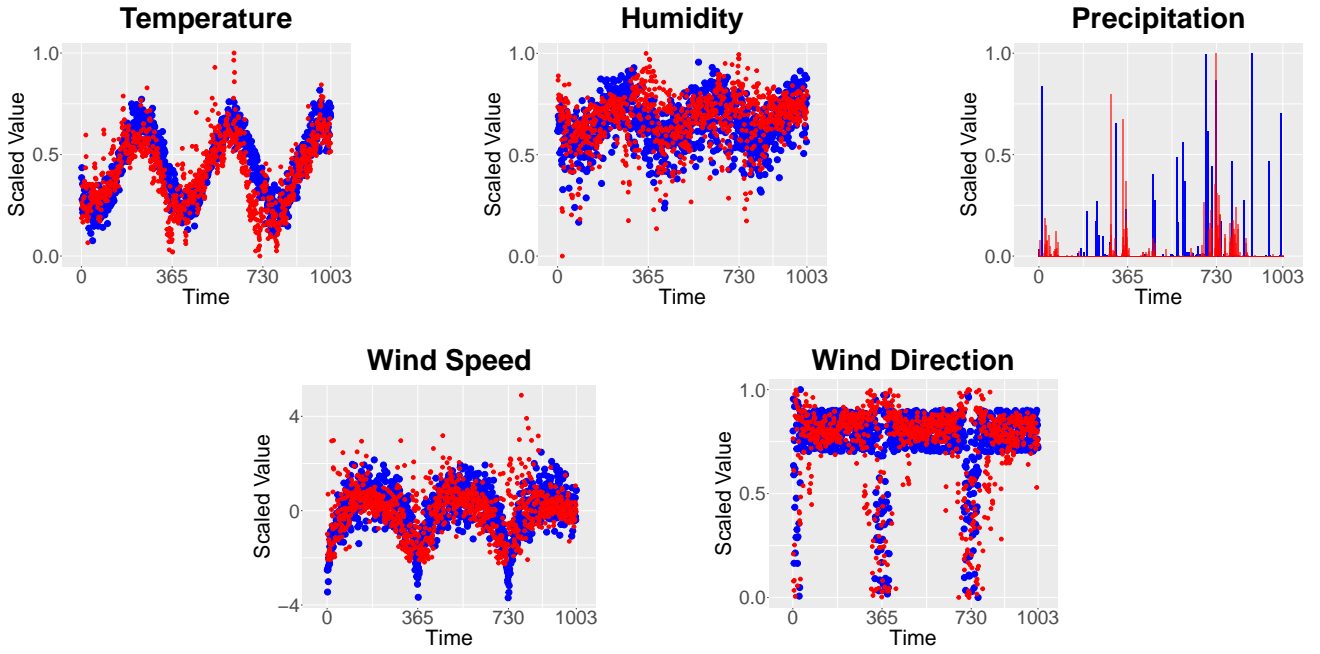


Figure S.3: The comparison between real covariates (in red) and simulated covariates (blue) under the same scale.

$$Y_{tj} = -E_{tj} - 0.5R_{tj} + 5X_{0j}^{\text{out}} + \epsilon_{tj}, \quad \text{where } E_{tj} = I\left(\sum_{i=1}^N A_{ti}G_{tij} \geq 7\right) \text{ and } \epsilon_{tj} \sim N(0, 1).$$

(b) Only time-smooth confounders exist:

$$A_{ti} \sim \text{Ber}(\exp \eta_{ti}/(1 + \exp \eta_{ti})), \quad \text{where } \eta_{ti} = 4.5(f_i^{\text{int}}(t) - 0.5),$$

$$G_{tij} \sim \text{Ber}(\rho), \quad \text{where } \rho = 1/(1 + \exp(\text{dist}(i, j)/4 * (1 + I(x_i < x_j))))),$$

$$Y_{tj} = -E_{tj} - 0.5R_{tj} + 2f_j^{\text{out}}(t) + \epsilon_{tj}, \quad \text{where } E_{tj} = I\left(\sum_{i=1}^N A_{ti}G_{tij} \geq 11\right) \text{ and } \epsilon_{tj} \sim N(0, 1).$$

(c) Only location-varying confounders exist:

$$A_{ti} \sim \text{Ber}(\exp \eta_{ti}/(1 + \exp \eta_{ti})), \quad \text{where } \eta_{ti} = X_{0i}^{\text{int}} - 0.5,$$

$$G_{tij} \sim \text{Ber}(\rho), \quad \text{where } \rho = 1/(1 + \exp(\text{dist}(i, j)/4 * (1 + I(x_i < x_j))))),$$

$$Y_{tj} = -E_{tj} - 0.5R_{tj} + 2X_{0j}^{\text{out}} + \epsilon_{tj}, \quad \text{where } E_{tj} = I\left(\sum_{i=1}^N A_{ti}G_{tij} \geq 13\right) \text{ and } \epsilon_{tj} \sim N(0, 1).$$

(d) Only time-varying confounders exist:

$$\begin{aligned}
A_{ti} &\sim \text{Ber}(\exp \eta_{ti}/(1 + \exp \eta_{ti})), & \text{where } \eta_{ti} &= 2X_{ti1}^{\text{int}} - X_{ti2}^{\text{int}} - 0.4X_{ti3}^{\text{int}} + 1.5X_{ti4}^{\text{int}} \\
& & & - 0.7X_{ti5}^{\text{int}} + 0.4\bar{R}_t - 0.6, \\
G_{tij} &\sim \text{Ber}(\rho_t), & \text{where } \rho_t &= 1/(1 + \exp\{0.6 \sin(2\pi(t + 50)/365)\}), \\
Y_{tj} &= -E_{tj} - 0.5R_{tj} + 4 \exp(2X_{tj1}^{\text{out}}) \\
&\quad + 1.2X_{tj2}^{\text{out}} - 2X_{tj3}^{\text{out}} + 2X_{tj4}^{\text{out}} \\
&\quad + X_{tj5}^{\text{out}} + \epsilon_{tj}, & \text{where } E_{tj} &= I\left(\sum_{i=1}^N A_{ti}G_{tij} \geq 15\right) \text{ and } \epsilon_{tj} \sim N(0, 1).
\end{aligned}$$

(e) All confounders exist:

$$\begin{aligned}
A_{ti} &\sim \text{Ber}(\exp \eta_{ti}/(1 + \exp \eta_{ti})), & \text{where } \eta_{ti} &= 0.4f_i^{\text{int}}(t) + 1.6X_{0i}^{\text{int}} + 1.6X_{ti1}^{\text{int}} - 0.8X_{ti2}^{\text{int}} \\
& & & - 0.32X_{ti3}^{\text{int}} + 1.2X_{ti4}^{\text{int}} - 0.56X_{ti5}^{\text{int}} \\
& & & + 0.015\bar{R}_t - 1.92, \\
G_{tij} &\sim \text{Ber}(\rho_{tij}), & \text{where } \rho_{tij} &= 1/(1 + \exp 0.6 \sin(2\pi(t + 50)/365) + \\
& & & \text{dist}(i, j)/4(1 + I(x_i < x_j))), \\
Y_{tj} &= -E_{tj} - 0.5R_{tj} + 1.8f_j^{\text{out}}(t) + 4 \exp X_{0j}^{\text{out}} \\
&\quad + 4 \exp X_{tj1}^{\text{out}} + 1.2X_{tj2}^{\text{out}} - 2X_{tj3}^{\text{out}} \\
&\quad + 2X_{tj4}^{\text{out}} + X_{tj5}^{\text{out}} + \epsilon_{tj}, & \text{where } E_{tj} &= I\left(\sum_{i=1}^N A_{ti}G_{tij} \geq 16\right) \text{ and } \epsilon_{tj} \sim N(0, 1).
\end{aligned}$$

G Description for alternative approaches

G.1 The naïve approaches

Implementing three naïve approaches requires a full dataset including exposure status E_t and outcomes Y_{tj} among all units m_1, m_2, \dots, m_M and all time points $t = 1, 2, \dots, T$. Naïve-all uses the full dataset, Naïve- t uses only the data from the first outcome unit across time, and Naïve- j uses the data across all outcome units but only for the first time point.

G.1.1 Estimator

For Naïve- t , we split the temporal data for the first outcome unit into two groups: the exposed time periods, $t \in \mathcal{T}_1$ if $E_{t1} = 1$, and the unexposed time periods, $t \in \mathcal{T}_0$ if $E_{t1} = 0$. Similarly, for Naïve- j , we split the data for the first time period in the exposed outcome units, $j \in \mathcal{J}_1$ if $E_{1j} = 1$,

and the unexposed outcome units, $j \in \mathcal{J}_0$, if $E_{1j} = 0$. For Naïve-all, we consider all units and time periods, and denote $(t, j) \in \mathcal{S}_1$ if the outcome unit-time period combination is exposed, $E_{tj} = 1$, and $(t, j) \in \mathcal{S}_0$ otherwise. We use the estimators $\hat{\tau}^{\text{Naïve}-t}$, $\hat{\tau}^{\text{Naïve}-j}$ and $\hat{\tau}^{\text{Naïve}-all}$ as follows:

$$\begin{aligned}\hat{\tau}^{\text{Naïve}-t} &= \frac{1}{|\mathcal{T}_1|} \sum_{t \in \mathcal{T}_1} Y_{t1} - \frac{1}{|\mathcal{T}_0|} \sum_{t \in \mathcal{T}_0} Y_{t1}, \\ \hat{\tau}^{\text{Naïve}-j} &= \frac{1}{|\mathcal{J}_1|} \sum_{j \in \mathcal{J}_1} Y_{1j} - \frac{1}{|\mathcal{J}_0|} \sum_{j \in \mathcal{J}_0} Y_{1j}, \\ \hat{\tau}^{\text{Naïve}-all} &= \frac{1}{|\mathcal{S}_1|} \sum_{(t,j) \in \mathcal{S}_1} Y_{tj} - \frac{1}{|\mathcal{S}_0|} \sum_{(t,j) \in \mathcal{S}_0} Y_{tj}.\end{aligned}$$

G.1.2 Inference

We adopt the classic Wald-type confidence interval construction for two independent samples. Denote s_1 as the standard deviation of outcomes with index from \mathcal{T}_1 , \mathcal{J}_1 , or \mathcal{S}_1 , and s_0 as the standard deviation of outcomes with index from \mathcal{T}_0 , \mathcal{J}_0 , or \mathcal{S}_0 for each naïve approach. The confidence intervals for Naïve- t , Naïve- j , and Naïve-all are

$$\begin{aligned}\hat{\tau}^{\text{Naïve}-t} \pm Z_\alpha \sqrt{\frac{(|\mathcal{T}_1| - 1)s_1^2 + (|\mathcal{T}_0| - 1)s_0^2}{|\mathcal{T}_1| + |\mathcal{T}_0| - 2}} \sqrt{\frac{1}{|\mathcal{T}_1|} + \frac{1}{|\mathcal{T}_0|}}, \\ \hat{\tau}^{\text{Naïve}-j} \pm Z_\alpha \sqrt{\frac{(|\mathcal{J}_1| - 1)s_1^2 + (|\mathcal{J}_0| - 1)s_0^2}{|\mathcal{J}_1| + |\mathcal{J}_0| - 2}} \sqrt{\frac{1}{|\mathcal{J}_1|} + \frac{1}{|\mathcal{J}_0|}},\end{aligned}$$

and

$$\hat{\tau}^{\text{Naïve}-all} \pm Z_\alpha \sqrt{\frac{(|\mathcal{S}_1| - 1)s_1^2 + (|\mathcal{S}_0| - 1)s_0^2}{|\mathcal{S}_1| + |\mathcal{S}_0| - 2}} \sqrt{\frac{1}{|\mathcal{S}_1|} + \frac{1}{|\mathcal{S}_0|}},$$

respectively.

G.2 Linear regression estimator

We consider linear regression for the first outcome unit where we regress outcomes across time on time-varying information. Specifically, the linear regression model assumes the outcome Y_t is a linear function of the exposure E_t , the carryover effect R_t , time t , and the summarized covariates $\overline{\mathbf{X}}_{t,S}^{\text{sum}}$:

$$Y_t = \beta_0 + \beta_1 E_t + \beta_2 R_t + \beta_3 t + \beta_4^\top \overline{\mathbf{X}}_{t,S}^{\text{sum}} + \epsilon_t$$

for $t = 1, 2, \dots, T$, where ϵ_t represents independent random errors with $E(\epsilon_t) = 0$ and $\text{Var}(\epsilon_t)$ constant. We use Ordinary Least Squares (OLS) to derive the point estimators $\hat{\beta}_1$ and $\hat{\beta}_2$, alongside their respective standard errors, $\text{se}(\hat{\beta}_1)$ and $\text{se}(\hat{\beta}_2)$. These coefficients serve as the regression estimators for the immediate effect τ^{imm} and the carryover effect τ^{car} , respectively. Finally, the 95% confidence intervals are constructed as $\hat{\beta}_j \pm 1.96 \cdot \text{se}(\hat{\beta}_j)$ for $j \in \{1, 2\}$.

G.3 IPW estimator

Again, we consider an Inverse Probability Weighting (IPW) estimator for the first outcome unit across time. For τ^{imm} , we define the propensity score of E_t as $e(R_t, t, \overline{\mathbf{X}}_{t,S}^{\text{sum.}}) = P(E_t = 1 \mid R_t, t, \overline{\mathbf{X}}_{t,S}^{\text{sum.}})$, and consider the ATT-type estimator

$$\frac{1}{T} \sum_{t=1}^T \left(E_t Y_t - \frac{e(R_t, t, \overline{\mathbf{X}}_{t,S}^{\text{sum.}})}{1 - e(R_t, t, \overline{\mathbf{X}}_{t,S}^{\text{sum.}})} (1 - E_t) Y_t \right).$$

The IPW estimator for the carryover effect is similar, switching the roles of E_t and R_t .

We employ the R package `PSweight` [Zhou et al., 2022] to calculate the estimators for τ^{imm} and τ^{car} . For the immediate effect, the package fits the propensity score using a logistic regression model, yielding the estimate $\hat{e}(R_t, t, \overline{\mathbf{X}}_{t,S}^{\text{sum.}})$. To construct confidence intervals, `PSweight` utilizes the empirical sandwich variance estimator for propensity score weighting.

H Additional Simulations

H.1 Data generation

We consider a setting with $N = 50$ interventional units and $M = 200$ outcome units at randomly generated locations over the $[0, 1] \times [0, 1]$ square, followed over $T = 400$ time periods.

H.1.1 The locations

The locations of the interventional and outcome units, (x, y) , are generated in the following manner. For the interventional units, the x coordinates of units 1 to 10 and 31 to 40 are generated independently from a $\text{Uniform}(0, 0.5)$ distribution, while the x coordinates for the remaining units are generated from a $\text{Uniform}(0.5, 1)$ distribution. The y coordinates for the interventional units are generated independently from a $\text{Uniform}(0, 0.5)$ distribution for units 1 to 10 and 21 to 30, and from $\text{Uniform}(0.5, 1)$ distribution for the remaining units. Similarly, for the outcome units, the x coordinates for units 1 to 68 and 113 to 156 are drawn from a $\text{Uniform}(0, 0.5)$ distribution, while the x coordinates for the remaining outcome units are drawn from a $\text{Uniform}(0.5, 1)$ distribution. The y coordinates are drawn

from a Uniform(0, 0.5) for units 1 to 50 and 101 to 150, and from a Uniform(0.5, 1) for the remaining units.

H.1.2 The covariates

We consider six covariates for the interventional units, six covariates for the outcome units, and one network covariate. We discuss how each variable is generated below.

(a) (Smooth temporal trends) Covariates $f_i^{\text{int}}(t)$ and $f_j^{\text{out}}(t)$ are generated independently from Gaussian processes with the same smooth function of time as the mean, and an exponential decay kernel for the covariance matrix. Therefore, these covariates represent similar but not identical smooth temporal trends. Specifically:

- For the interventional units, we generate a variable that represents a smooth function of time in the following manner. The variable $\mathbf{f}_i^{\text{int}} = (f_i^{\text{int}}(1), f_i^{\text{int}}(2), \dots, f_i^{\text{int}}(T))$ is generated from a Gaussian process with Gaussian correlation kernel and mean representing a smooth temporal trend as $\mathbf{f}_i^{\text{int}} \sim \mathcal{N}(f(t), \Sigma)$, where $\Sigma_{t_1, t_2} = \frac{\exp(-(t_1 - t_2)^2)}{2 \cdot 100^2}$ and $f(t) = \frac{3}{400}t$.
- For the outcome units, the vector $\mathbf{f}_j^{\text{out}}$ is generated by the same distribution as for the interventional units, as $\mathbf{f}_j^{\text{out}} \sim \mathcal{N}(f(t), \Sigma)$, where $\Sigma_{t_1, t_2} = \frac{\exp(-(t_1 - t_2)^2)}{2 \cdot 100^2}$ and $f(t) = \frac{3}{400}t$.

Realizations of the smooth temporal trend $\mathbf{f}_i^{\text{int}}$ for five interventional units and $\mathbf{f}_j^{\text{out}}$ for five outcome units are shown on the top- and bottom-left panels of Figure S.4, respectively. It is evident that the smooth temporal trends are similar but different. Therefore, if $\mathbf{f}_i^{\text{int}}$ is a predictor of the interventional units' treatment across time, and $\mathbf{f}_j^{\text{out}}$ is a predictor of the outcome units' outcome across time, then the common smooth temporal trend in $\mathbf{f}_i^{\text{int}}$ and $\mathbf{f}_j^{\text{out}}$ confounds the exposure-outcome relationship of interest.

(b) (Location-varying covariates) Covariates X_{0i1}^{int} and X_{0j1}^{out} are constant across time, and they are drawn independently from a scaled beta distribution with parameters that depend on the unit's location. Therefore, these covariates have similar structure across space.

- For the interventional units, we consider a time-invariant covariate, X_{0i1}^{int} . For units n_i inside the $[0, 0.5] \times [0, 0.5]$ rectangle, we generate $X_{0i1}^{\text{int}}/8 \sim \text{Beta}(9, 1)$, while for the rest n_i 's, we draw $X_{0i1}^{\text{int}}/8 \sim \text{Beta}(1, 9)$.
- We generate the time-invariant covariate for the outcome units X_{0j1}^{out} in the same manner based on outcome unit m_j 's coordinates.

A visualization of the time-invariant covariate for all interventional and outcome units is shown at the top- and bottom-right panels of Figure S.4, respectively. It is evident that the location-varying covariates of interventional and outcome units share spatial trends. Therefore, if the former is a predictor of the interventional units' treatment, and the latter of the outcome units' outcome, then there exists location-varying confounding of the exposure-outcome relationship.

(c) (Non-smooth time-varying variables) Covariates X_{ti1}^{int} , X_{tj1}^{out} and X_{tij1}^{net} are time-varying covariates that are independent across units but are not smooth over time.

- For the interventional units, we generate $X_{ti1}^{\text{int}} \sim N(0, t/100)$, $i = 1, \dots, N$, $t = 1, \dots, T$. This variable varies across time without a smooth pattern. A realization is drawn on the left of Figure S.5.
- For the outcome units, we generate $X_{tj1}^{\text{out}}/2 \sim \text{Beta}(t/100, 2)$, $j = 1, 2, \dots, M$, $t = 1, 2, \dots, T$. This variable has a *non-smooth* temporal trend.
- The one network covariate has a non-smooth temporal trend. Specifically, the network covariate array $\mathbf{X}_{t..1}^{\text{net}}$ is an $N \times M$ matrix. The entries of the matrix are generated independently as $X_{tij1}^{\text{net}} \sim \text{Beta}(t/50, 10)$, $i = 1, 2, \dots, N$, $j = 1, 2, \dots, M$, $t = 0, 1, \dots, T$.

(d) (Bipartite covariates) We define covariates for one set of units based on the covariates of the other set.

- For interventional units, we define location-varying covariate X_{0i2}^{int} , and the time-varying covariates X_{ti2}^{int} and X_{ti3}^{int} , as averages of covariates X_{0j1}^{out} , X_{tj1}^{out} , and X_{tij1}^{net} , respectively, of neighboring outcome units. Specifically, we define the $N \times M$ matrix \mathbf{R} , with entries $p_{ij} = 1$ if unit i and j are within distance 0.1, and $p_{ij} = 0$ otherwise. We define

$$X_{0i2}^{\text{int}} = \frac{\sum_j p_{ij} X_{0j1}^{\text{out}}}{\sum_j p_{ij}}, \quad X_{ti2}^{\text{int}} = \frac{\sum_j p_{ij} X_{tj1}^{\text{out}}}{\sum_j p_{ij}}, \quad \text{and} \quad X_{ti3}^{\text{int}} = \frac{\sum_j p_{ij} X_{tij1}^{\text{net}}}{\sum_j p_{ij}},$$

for $i = 1, 2, \dots, N$, and $t = 1, 2, \dots, T$.

- Covariates X_{0j2}^{out} , X_{tj2}^{out} and X_{tj3}^{out} for outcome units are similarly defined based on covariates X_{0i1}^{int} , X_{ti1}^{int} , and X_{tij1}^{net} of interventional units, as

$$X_{0j2}^{\text{out}} = \frac{\sum_i p_{ij} X_{0i1}^{\text{int}}}{\sum_i p_{ij}}, \quad X_{tj2}^{\text{out}} = \frac{\sum_i p_{ij} X_{ti1}^{\text{int}}}{\sum_i p_{ij}}, \quad \text{and} \quad X_{tj3}^{\text{out}} = \frac{\sum_i p_{ij} X_{tij1}^{\text{net}}}{\sum_i p_{ij}},$$

for $j = 1, 2, \dots, M$, and $t = 1, 2, \dots, T$. One realization of the location-varying covariate $\mathbf{X}_{0,2}^{\text{out}}$ for all outcome units and one realization of the non-smooth covariate $\mathbf{X}_{t,2}^{\text{out}}$ are presented on the left and right panels of Figure S.6, respectively.

Here, consider the matrix \mathbf{Q} whose columns are the normalized version of the columns of \mathbf{R} , where the (i, j) th entry is equal to $q_{ij} = p_{ij} / \sum_i p_{ij}$. The columns of the matrix \mathbf{Q} correspond to the vectors \mathbf{q} we introduce in Section 4.1 for defining the interventional and network covariate summaries.

- (e) (Common non-smooth time-varying covariate) Covariates $X_{ti4}^{\text{int}}, X_{tj4}^{\text{out}}$ are equal to each other, regardless of i and j , and represent *non-smooth* temporal trends. Specifically, $X_{ti4}^{\text{int}} = X_{tj4}^{\text{out}} = Z_t$, where Z_t is drawn from a $\mathcal{N}(t/200, \log(t)/10)$ distribution, independently across time. A realization of this covariate is shown on the right panel of Figure S.5.

H.1.3 The treatment assignment, bipartite network, and outcome

We consider five scenarios regarding the confounding structure. In what follows, when we write $A_{ti}, G_{tij} \sim (\text{Distribution})$, we implicitly condition on all the variables.

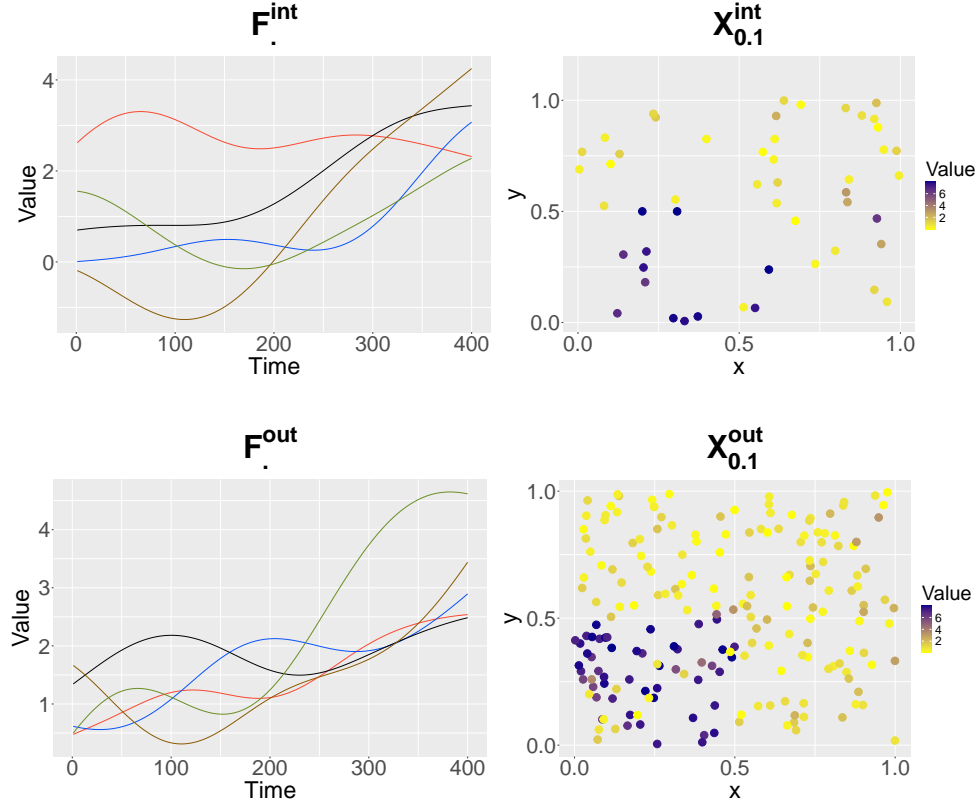
- (a) No confounders:

$$A_{ti} \sim \text{Uniform}(0, 1),$$

Table S.5: Table of five confounding scenarios, in which treatment \mathbf{A} , network graph \mathbf{G} , and observed outcome \mathbf{Y} are associated with corresponding confounding covariates.

Scenario	Component	Smooth time			Location-varying				Time-varying		
		t	$f_i^{\text{int}}(t)$	$f_j^{\text{out}}(t)$	dist	X_{0i1}^{int}	X_{0j1}^{out}	X_{0i2}^{int}	X_{0j2}^{out}	$\mathbf{X}_{ti}^{\text{int}}$	$\mathbf{X}_{tj}^{\text{out}}$
(a) No confounders	\mathbf{A}										
	\mathbf{G}										
	\mathbf{Y}										×
(b) Time-smooth confounders	\mathbf{A}		×								
	\mathbf{G}				×						
	\mathbf{Y}			×							
(c) Location-varying confounders	\mathbf{A}					×		×			
	\mathbf{G}				×						
	\mathbf{Y}						×		×		
(d) Time-varying confounders	\mathbf{A}									×	
	\mathbf{G}	×			×						
	\mathbf{Y}										×
(e) All confounders	\mathbf{A}		×			×		×		×	
	\mathbf{G}	×			×						
	\mathbf{Y}			×			×		×		×

Figure S.4: Visualization of interventional and outcome unit covariates over time and units. The top left panel shows 5 realizations from the Gaussian process for f_j^{int} . The top right figure is the $[0, 1] \times [0, 1]$ location square with one realization for the location of the interventional points and the corresponding location-varying covariate $X_{0.1}^{\text{int}}$. The bottom left figure is 5 realizations from the Gaussian process for f_j^{out} and the bottom right figure is a realization from the locations of the outcome units colored by the values of one realization of $X_{0.1}^{\text{out}}$.



$$G_{tij} \sim \text{Ber}(\rho), \quad \text{where } \rho = 0.17,$$

$$Y_{tj} = E_t + 0.4R_{tj} + X_{0j1}^{\text{out}} + \epsilon_{tj}.$$

(b) Only time-smooth confounders exist:

$$A_{ti} \mid f_i^{\text{int}}(t) \sim \text{Ber}(1/(1 + \exp(f_i^{\text{int}}(t)/1.2)))$$

$$G_{tij} \sim \text{Ber}(\rho_{ij}), \quad \text{where } \rho_{ij} = 1/(2(1 + \exp(\text{dist}(i, j))),$$

$$Y_{tj} = E_t + 0.4R_{tj} + f_j^{\text{out}}(t) + \epsilon_{tj}$$

(c) Only location-varying confounders exist:

$$A_{ti} \sim \text{Ber}(1/(1 + 0.3 \exp(X_{0i1}^{\text{int}} - X_{0i2}^{\text{int}}/40)))$$

Figure S.5: Visualization of non-smooth interventional covariates $\mathbf{X}_{\cdot,1}^{\text{int}}$ and $\mathbf{X}_{\cdot,4}^{\text{int}}$. The left panel shows one realization of $\mathbf{X}_{\cdot,1}^{\text{int}}$, and the right panel shows one realization of $\mathbf{X}_{\cdot,4}^{\text{int}}$.

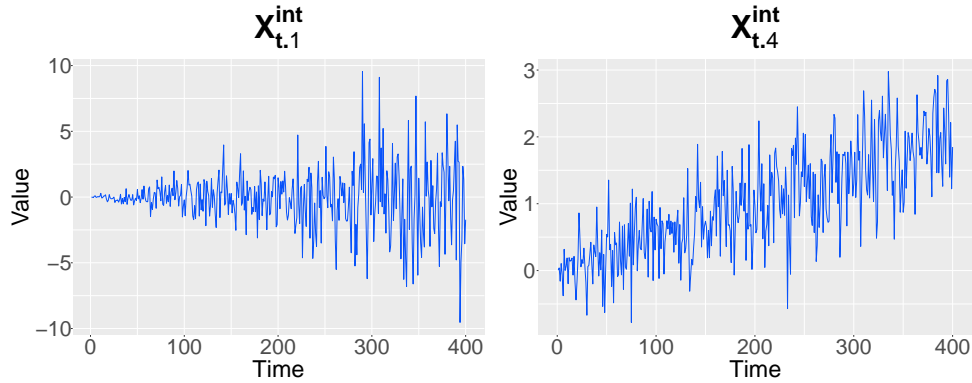
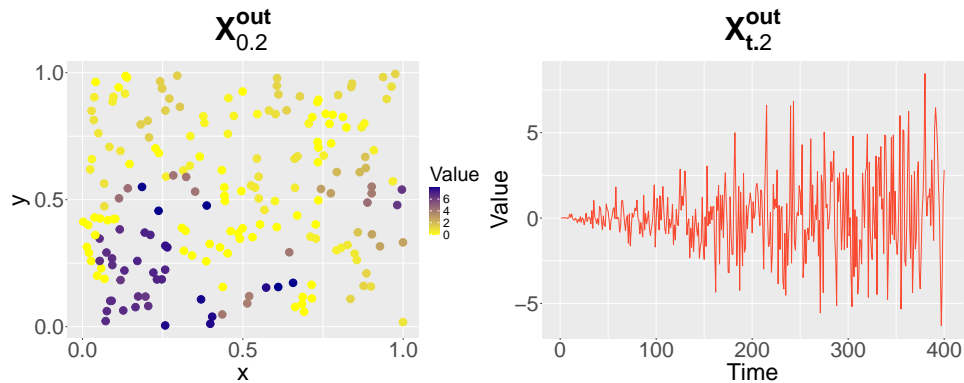


Figure S.6: Visualization of the location-varying outcome covariate $\mathbf{X}_{0,2}^{\text{out}}$ and the non-smooth covariate $\mathbf{X}_{t,2}^{\text{out}}$. The left panel is the $[0, 1] \times [0, 1]$ location square with one realization for the location of the outcome units with colors representing the value of the location-varying covariate $\mathbf{X}_{0,2}^{\text{out}}$. The right panel shows one realization for $\mathbf{X}_{t,2}^{\text{out}}$ for the outcome units which is defined based on the interventional units' covariate $\mathbf{X}_{t,1}^{\text{int}}$ in Figure S.5 and their geographical distance.



$$G_{tij} \sim \text{Ber}(\rho_{ij}), \quad \text{where } \rho_{ij} = 1/(1.7(1 + \exp \text{dist}(i, j)))$$

$$Y_{tj} = E_t + 0.4R_{tj} + 4X_{0j1}^{\text{out}} + 4X_{0j2}^{\text{out}} + \epsilon_{tj}$$

(d) Only time-varying confounders exist:

$$A_{ti} \mid \mathbf{X}_{ti}^{\text{int}} \sim \text{Ber}\left(\frac{1}{1 + \exp(X_{ti1}^{\text{int}}/2 + X_{ti2}^{\text{int}}/2 + X_{ti3}^{\text{int}}/10 + X_{ti4}^{\text{int}})}\right)$$

$$G_{tij} \mid t \sim \text{Ber}(\rho_{tij}), \quad \text{where } \rho_{tij} = 1/(1 + 0.1 \exp(\sin(\pi t/1000) + \exp \text{dist}(i, j)))$$

$$Y_{tj} = E_t + 0.4R_{tj} + X_{tj1}^{\text{out}} + X_{tj2}^{\text{out}} + X_{tj3}^{\text{out}} + X_{tj4}^{\text{out}} + \epsilon_{tj}$$

(e) All confounders exist:

$$A_{ti} \mid \mathbf{f}_i^{\text{int}}, \mathbf{X}_{0i}^{\text{int}}, \mathbf{X}_{ti}^{\text{int}} \sim \text{Ber}(\eta_{ti} + \sum_{j=1}^M R_{tj}/M), \quad \text{where}$$

$$\eta_{ti} = \frac{1}{1 + 0.45 \exp(f_i^{\text{int}}(t)/20 + X_{0i1}^{\text{int}} + X_{0i2}^{\text{int}} + X_{ti1}^{\text{int}}/100 + X_{ti2}^{\text{int}}/20 + X_{ti3}^{\text{int}}/10 + X_{ti4}^{\text{int}}/1.5 + X_{(t-1)i4}^{\text{int}}/3)}$$

$$G_{tij} \mid t \sim \text{Ber}(\rho_{tij}), \quad \text{where } \rho_{tij} = 1/(1 + 0.1 \exp(\sin(\pi t/1000) + \exp \text{dist}(i, j)))$$

$$Y_{tj} = E_t + 0.4R_{tj} + f_j^{\text{out}}(t) + 2 * X_{0j1}^{\text{out}} + 2 * X_{0j2}^{\text{out}} + X_{tj1}^{\text{out}} + 0.1 * X_{tj1}^{\text{out}^2} + X_{tj2}^{\text{out}} +$$

$$1/(1 + \exp(X_{tj2}^{\text{out}})) + \sin(X_{tj3}^{\text{out}}) + 2 * X_{tj4}^{\text{out}} + X_{(t-1)j4}^{\text{out}}/3 + \epsilon_{tj}$$

Table S.5 shows the variables that are used in each data generative model component across the different scenarios. Confounding arises if a predictor of the outcome is correlated with a predictor of the treatment assignment, the bipartite network, or both. For example, in scenario (b), the role of $f_i^{\text{int}}(t)$ and $f_j^{\text{out}}(t)$ induces confounding due to the variables' common smooth temporal trend, and in scenario (d), the covariate X_{ti2}^{int} is defined based on X_{tj1}^{out} which induce confounding in the exposure-outcome relationship. Therefore, these data generative models allow for complex confounding structures.

For each scenario, we consider three sparsity levels for the exposure by tuning d , dense, medium, and sparse, corresponding to about 150-200, 80-120, and 30-60 exposed time periods, respectively. Therefore, in total, we consider 15 simulation scenarios, and generate 500 data sets for each one of them.

H.2 Single-unit estimation and inference across different exposure sparsity levels

Table S.6 shows the estimation and inferential results for estimating the effect for one outcome unit using the three naïve approaches, and the three proposed estimators as also discussed in the simulations of Section 5. For each estimator we report bias, mean squared error and coverage of 95% intervals. For the proposed estimators, we also report the proportion of exposed time periods that were matched.

The performance across different confounding scenarios closely mirrors the results from the simulation study in Section 5. For that reason, we omit a detailed summary here on the relative performance of the methods. We instead focus on comparing the performance of the proposed estimators under the different levels of exposure density.

In terms of MSE, the 1-1 estimator performs best or close to best in the dense scenarios, and the 1-2 estimator performs best or close to best in the sparse scenarios. The 1-1/2 estimator performs as well, or close to as-well as the best estimator across all scenarios considered, while maintaining a

Table S.6: Simulation results of single-unit **immediate** effects. Bias, mean squared error (MSE), coverage of 95% intervals (%), and proportion of exposed time points being matched (%). We show simulation results for the 3 naïve approaches and 3 matching estimators over 5 confounding scenarios, and for 3 exposure levels. ‘N’ stands for ‘naïve’. The scenarios correspond to (a) No confounders, (b) Time-smooth confounders, (c) Location-varying confounders, (d) Time-varying confounders, and (e) All confounders.

Method	Dense				Medium				Sparse				
	Bias	MSE	Cover	Prop	Bias	MSE	Cover	Prop	Bias	MSE	Cover	Prop	
(a)	N-t	-0.00	0.011	95.2	-	-0.01	0.013	95.4	-	-0.01	0.022	95.2	-
	N-j	-0.00	0.216	93.2	-	-0.00	0.214	95.6	-	-0.02	0.248	95	-
	N-all	-0.00	0.000	94.8	-	-0.00	0.001	95.4	-	-0.00	0.001	95.8	-
	Reg	-0.00	0.011	94.4	-	-0.01	0.014	94.6	-	-0.01	0.022	95.2	-
	IPW	-0.00	0.011	94.4	-	-0.01	0.014	95	-	-0.01	0.022	95	-
	1-1	-0.02	0.013	94	97.8	-0.02	0.020	95.6	100	-0.01	0.040	95.8	100
	1-1/2	-0.02	0.012	95.4	97.8	-0.03	0.017	94.6	100	-0.02	0.032	95	100
	1-2	-0.02	0.015	95.6	61.9	-0.03	0.017	93.9	90.6	-0.01	0.029	94.9	98.7
(b)	N-t	-0.77	0.939	14.2	-	-0.85	1.104	14.4	-	-0.92	1.300	17.4	-
	N-j	-0.00	0.048	96.2	-	0.01	0.051	93.2	-	0.00	0.046	94.2	-
	N-all	-0.75	0.567	0	-	-0.82	0.684	0	-	-0.92	0.853	0	-
	Reg	0.01	0.020	92.8	-	0.01	0.032	87.4	-	0.03	0.060	86	-
	IPW	0.01	0.027	94.6	-	0.02	0.027	94.4	-	0.03	0.033	95	-
	1-1	-0.02	0.019	93.8	62.5	-0.02	0.023	95	85	-0.00	0.037	95	97.6
	1-1/2	-0.02	0.020	94.4	62.5	-0.01	0.023	93.8	85	-0.00	0.033	95	97.6
	1-2	-0.02	0.023	93.2	40.8	-0.01	0.025	94.8	59.7	-0.00	0.035	93.6	80
(c)	N-t	-0.00	0.013	94.6	-	0.00	0.023	94.8	-	-0.00	0.048	94.8	-
	N-j	-3.63	22.483	76	-	-3.89	25.117	75	-	-3.91	25.394	78.4	-
	N-all	-3.31	11.404	0	-	-3.54	13.006	0	-	-3.88	15.635	0	-
	Reg	0.00	0.014	94.2	-	0.00	0.023	94.6	-	-0.00	0.050	94.4	-
	IPW	-0.00	0.014	94	-	0.00	0.024	94.2	-	-0.00	0.050	92.6	-
	1-1	-0.01	0.020	94	99.7	0.00	0.040	94.2	100	0.00	0.090	94.6	100
	1-1/2	-0.01	0.018	94.8	99.7	-0.01	0.032	94.2	100	0.00	0.065	94.8	99.9
	1-2	-0.02	0.017	92.7	85.5	-0.00	0.030	94.6	97.3	-0.01	0.068	91.5	99.2
(d)	N-t	-1.08	1.228	0.6	-	-1.15	1.380	0.2	-	-1.35	1.908	4.6	-
	N-j	0.01	0.025	95.6	-	0.01	0.026	94.4	-	0.01	0.023	94.4	-
	N-all	-1.09	1.191	0	-	-1.15	1.326	0	-	-1.34	1.812	0	-
	Reg	0.00	0.014	95.8	-	-0.00	0.016	93.2	-	0.00	0.036	94.4	-
	IPW	-0.01	0.034	95.2	-	0.01	0.027	94.8	-	0.01	0.049	94.6	-
	1-1	-0.05	0.024	98.3	67.5	-0.06	0.026	99.2	84.7	-0.04	0.068	95.2	99.6
	1-1/2	-0.05	0.024	97.9	67.5	-0.06	0.025	99	84.8	-0.05	0.054	96.6	99.6
	1-2	-0.06	0.025	98.5	43.1	-0.06	0.027	97.8	58.9	-0.05	0.055	96.5	86.7
(e)	N-t	-3.13	10.172	0	-	-3.33	11.519	0	-	-3.58	13.284	0	-
	N-j	-1.44	5.533	80.8	-	-1.64	5.827	79.8	-	-1.79	5.847	76.4	-
	N-all	-3.91	15.355	0	-	-4.20	17.698	0	-	-4.59	21.124	0	-
	Reg	0.00	0.018	93.8	-	0.01	0.031	89.2	-	0.00	0.057	83.8	-
	IPW	-0.12	0.133	90.8	-	0.00	0.056	96	-	0.03	0.053	95	-
	1-1	-0.10	0.031	98.8	55.1	-0.09	0.030	98.5	77.1	-0.08	0.042	97.1	94.1
	1-1/2	-0.10	0.029	98.7	55	-0.09	0.030	98.5	77.1	-0.08	0.039	97.1	94
	1-2	-0.09	0.035	99.5	33.6	-0.08	0.031	99.5	51.8	-0.09	0.043	98.4	70.8

high proportion of matched exposed time periods.

As in the simulations of Section 5, the 1-1 and 1-1/2 algorithms yield the same proportion of matched exposed time periods, as the matches generated under the 1-1 algorithm are also possible

Table S.7: Simulation results of single-unit **carryover** effects. Bias, mean squared error (MSE), coverage of 95% intervals (%), and proportion of exposed time points being matched (%). We show simulation results for the 3 naïve approaches and 3 matching estimators over 5 confounding scenarios, and for 3 exposure levels. ‘N’ stands for ‘naïve’. The scenarios correspond to (a) No confounders, (b) Time-smooth confounders, (c) Location-varying confounders, (d) Time-varying confounders, and (e) All confounders.

Method	Dense				Medium				Sparse				
	Bias	MSE	Cover	Prop	Bias	MSE	Cover	Prop	Bias	MSE	Cover	Prop	
(a)	N-t	-8.29	70.166	0	-	-8.06	66.064	0	-	-7.79	61.750	0.8	-
	N-j	-3.30	14.051	65.2	-	-3.88	18.073	49.2	-	-4.44	23.088	33.4	-
	N-all	-9.20	85.015	0	-	-9.30	86.723	0	-	-9.62	92.725	0	-
	Reg	-0.74	0.875	88.2	-	0.20	0.404	65.2	-	0.37	0.680	68.7	-
	IPW	1.50	3.389	14.6	-	0.04	0.347	58.8	-	-0.47	0.356	88.4	-
	1-1	-0.04	0.020	96	86.5	-0.01	0.085	96.1	98.6	-0.05	0.243	86.4	90.7
	1-1/2	-0.04	0.019	96.4	86.5	-0.03	0.074	96.2	98.7	-0.00	0.405	82.2	87.8
	1-2	-0.05	0.035	97.1	37.4	-0.03	0.095	93.7	74.3	-0.06	0.297	92	73.8
(b)	N-t	-0.88	1.474	10.4	-	-0.90	1.531	14.8	-	-0.97	1.719	32.5	-
	N-j	0.01	0.064	94.6	-	-0.00	0.069	93.8	-	0.03	0.054	94	-
	N-all	-0.84	0.706	0	-	-0.87	0.762	0	-	-0.93	0.878	0	-
	Reg	0.01	0.110	68.8	-	0.02	0.184	59	-	0.04	0.261	72.4	-
	IPW	0.25	0.361	64.8	-	0.08	0.109	84.6	-	0.05	0.112	92.3	-
	1-1	-0.04	0.042	95.6	34.7	-0.03	0.053	94.6	63.1	-0.00	0.126	96	87.3
	1-1/2	-0.04	0.043	95.4	34.7	-0.03	0.056	94.4	63.1	-0.01	0.129	95.1	87.8
	1-2	-0.06	0.124	94	10.7	-0.01	0.122	94.2	22.7	-0.00	0.159	93.1	49
(c)	N-t	-0.03	0.059	95.2	-	-0.06	0.205	95	-	-0.06	0.333	94.4	-
	N-j	-6.93	56.281	42.9	-	-7.42	62.293	43.2	-	-	-	-	-
	N-all	-6.62	45.379	0	-	-7.39	56.350	0	-	-8.43	74.005	0.6	-
	Reg	-0.01	0.053	94	-	-0.02	0.304	93.6	-	-0.10	0.442	91.2	-
	IPW	-0.01	0.063	92.4	-	-0.00	0.302	78	-	-0.04	0.448	67	-
	1-1	-0.02	0.074	95.1	96.4	0.00	0.152	95.3	94.8	0.06	0.139	93.8	91.5
	1-1/2	-0.05	0.058	96.4	96.6	-0.02	0.205	94.4	95.3	-0.03	0.261	95.8	91.5
	1-2	-0.03	0.076	95.2	67.4	-0.03	0.231	86.8	76.8	-0.02	0.092	100	75.7
(d)	N-t	-1.05	1.158	0.2	-	-1.13	1.354	0.4	-	-1.34	2.099	55.4	-
	N-j	0.03	0.041	93.4	-	0.02	0.036	93.8	-	0.04	0.031	94	-
	N-all	-1.02	1.035	0	-	-1.11	1.241	0	-	-1.28	1.638	0	-
	Reg	-0.01	0.019	93.4	-	-0.00	0.024	95	-	-0.00	0.186	95.7	-
	IPW	0.23	0.134	80.4	-	0.11	0.068	90.2	-	-0.00	0.231	85.9	-
	1-1	-0.05	0.041	98.2	42	-0.04	0.048	98.4	63.1	-0.04	0.204	93	89.6
	1-1/2	-0.05	0.040	98.2	41.9	-0.04	0.046	98.8	63.2	-0.05	0.226	93.2	91.3
	1-2	-0.05	0.076	98.8	14.8	-0.03	0.103	98.1	23.7	-0.03	0.251	91.4	62.1
(e)	N-t	-3.49	12.943	0	-	-3.70	14.497	0	-	-3.78	15.149	0.6	-
	N-j	-2.70	10.445	65.2	-	-3.28	13.783	49.2	-	-3.84	18.119	33.4	-
	N-all	-4.34	18.866	0	-	-4.84	23.566	0	-	-5.54	30.895	0	-
	Reg	0.01	0.078	74.2	-	0.02	0.166	61.8	-	0.03	0.263	69.9	-
	IPW	1.49	2.935	18	-	0.52	0.503	60.8	-	0.16	0.127	88.2	-
	1-1	-0.02	0.041	99.4	30.7	-0.02	0.049	98.8	53	-0.01	0.095	98.3	83.1
	1-1/2	-0.02	0.039	99.6	30.7	-0.02	0.051	97.6	53.1	-0.01	0.097	97.5	83.3
	1-2	-0.01	0.100	100	9.6	-0.03	0.117	98.3	19	-0.00	0.135	98.6	42.2

under the 1-1/2 algorithm. For all three algorithms, the proportion of matched exposed time periods varies with the sparsity level of the exposure, with higher rates of matched time periods under sparser exposures. As expected, the 1-2 algorithm returns the smallest proportion of matched exposed time

periods. Combined with the fact that it has close to the lowest MSE in sparse scenarios, this illustrates that the 1-2 estimator returns more accurate predictions for the missing potential outcomes compared to the 1-1 and 1-1/2 algorithms. The coverage of 95% intervals for all three estimators is close to or above nominal across all scenarios.

The overcoverage observed in some scenarios for all estimators can likely be explained by the fact that our variance estimator is biased upwards (see Supplement E). In a few settings, we find that coverage of the immediate effect in Table S.6 is below the nominal level. This is more often the case in sparse scenarios. Based on Q-Q plots of our estimates across data sets, we believe that this undercoverage might be explained by violations of the normality approximation, possibly due to the small number of observations used in estimation in the sparse scenarios.

H.3 Testing the global null hypothesis

For the scenarios with temporal confounding (b, d, and e), we consider simulations where all immediate effects are set to zero under a dense frequency for the exposure, and evaluate the properties of the inferential technique of Supplement C.4 for testing the global null hypothesis of no immediate effect in the presence of multiple outcome units at the 0.05 level. We alter the simulations to impose that the global null holds, and impose that $\tau_j^{\text{imm}} = 0$ for all outcome units. We generate 500 data sets for each one of the three scenarios. We acquire point estimates and p-values for the exposure effect on each of the 200 outcome units, and adjust the p-values using the procedure detailed in Supplement C.4.

The optimizer returned a solution for approximately 85% of the outcome units for each matching method. The results are in Table S.8. We report the average estimated effect across outcome units with matches and across data sets, the proportion of the available p-values across the outcome units and data sets that are below 0.05, the proportion of data sets where any of the available p-values is below 0.05, and the proportion of data sets where any of the FDR-adjusted p-values is below 0.05.

Since Naïve- t is biased in the presence of temporal confounding, its inferential performance suffers, and using this estimator would mistakenly reject the global null hypothesis every time, using FDR-corrected p-values or not. For the proposed estimators, up to 6 % of the p-values across outcome units and data sets are below 0.05. Hence, it is not surprising that the minimum (unadjusted) p-value across outcome units is below 0.05 in most data sets, emphasizing the necessity of controlling for multiple comparisons to maintain the level of the test, especially with a large number of outcome units. With FDR-adjusted p-values, the rate of rejection of the null hypothesis is much closer to the target level of the test. Matching methods in cases (d) and (e) are conservative in rejecting the global null hypothesis, consistent with the conservative nature of individual outcome unit hypothesis tests (also discussed in

Table S.8: Simulation results for testing the global null for the immediate effect using the Naïve- t and the estimator based on the three proposed algorithms for scenarios (b), (d) and (e), and under a dense exposure level.

		Average estimator mean	Average rate of p-value ≤ 0.05	Rate of min(p-value) ≤ 0.05	Rate of FDR min (adj.p-value) ≤ 0.05
(b)	Naïve- t	-0.903	0.904	1.000	1.000
	Reg	-0.000	0.063	1.000	0.106
	IPW	0.008	0.059	1.000	0.149
	1-1	-0.005	0.052	1.000	0.078
	1-1/2	-0.005	0.053	1.000	0.074
	1-2	-0.000	0.054	1.000	0.102
	NW1-1	-0.005	0.004	0.524	0.000
	NW1-1/2	-0.005	0.004	0.524	0.004
	NW1-2	-0.000	0.004	0.538	0.010
(d)	Naïve- t	-1.199	0.999	1.000	1.000
	Reg	-0.000	0.049	1.000	0.058
	IPW	-0.038	0.066	1.000	0.204
	1-1	-0.045	0.014	0.900	0.010
	1-1/2	-0.046	0.014	0.922	0.008
	1-2	-0.044	0.013	0.854	0.002
(e)	Naïve- t	-3.321	1.000	1.000	1.000
	Reg	0.001	0.055	1.000	0.068
	IPW	-0.191	0.127	1.000	0.746
	1-1	-0.082	0.000	0.000	0.000
	1-1/2	-0.083	0.000	0.000	0.000
	1-2	-0.075	0.000	0.002	0.000

Supplement E).

In scenario (b), we also considered the Newey-West variance estimator in acquiring the p-values for each outcome unit before applying the FDR correction in testing the global null hypothesis. This is shown in Table S.8 as NW1-1, NW1-1/2, and NW1-2. Using the Newey-West variance estimator yields fewer p-values below 0.05, resulting in substantially lower rates of both minimum unadjusted and adjusted p-values falling below the threshold. We investigate the performance of the Newey-West variance estimator in simulations in more detail in Supplement H.8.

H.4 Algorithms balancing time but not the time-varying covariates

We consider the three algorithms, 1-1, 1-2, and 1-1/2, with balance constraint on the time of matches, but not on the time-varying covariates. We call these algorithms and the corresponding estimators as *unadjusted*. We consider these approaches in order to investigate the impact of ignoring time-varying confounding factors within the proposed framework, and the extent to which the proposed framework can adequately control for smooth temporal trends without explicitly specifying them. We evaluate the performance of the unadjusted estimators in simulations under the generative scenarios described

Table S.9: Bias, mean squared error (MSE), coverage of 95% intervals (%), and proportion of exposed time points being matched (%). We show simulation results for the three estimators of the immediate effect based on the unadjusted algorithms that balance time but not time-varying covariates. ‘U’ stands for ‘unadjusted’. The scenarios correspond to (a) No confounders, (b) Time-smooth confounders, (c) Location-varying confounders, (d) Time-varying confounders, and (e) All confounders.

Method	Dense				Medium				Sparse				
	Bias	MSE	Cover	Prop	Bias	MSE	Cover	Prop	Bias	MSE	Cover	Prop	
(a)	U1-1	-0.04	0.014	93.2	97.8	-0.03	0.021	94.4	100	-0.01	0.039	95.2	100
	U1-1/2	-0.03	0.013	94.4	97.8	-0.03	0.018	94.2	100	-0.02	0.035	95.2	100
	U1-2	-0.07	0.019	90.8	62.3	-0.03	0.017	94.2	90.8	-0.02	0.030	94.4	98.7
(b)	U1-1	-0.03	0.021	94.4	62.5	-0.03	0.026	93.2	85.1	-0.02	0.037	94.8	97.8
	U1-1/2	-0.02	0.021	94.2	62.5	-0.02	0.023	94.4	85.1	-0.02	0.034	94.8	97.8
	U1-2	-0.04	0.026	92.3	40.9	-0.03	0.026	92.8	59.9	-0.03	0.034	95.2	80.6
(c)	U1-1	-0.03	0.021	93.6	99.7	-0.01	0.041	93.8	100	0.00	0.086	94.4	100
	U1-1/2	-0.02	0.019	94.8	99.7	-0.00	0.038	93.6	100	-0.01	0.080	94.6	100
	U1-2	-0.03	0.018	93.5	85.7	-0.01	0.030	92.6	97.4	-0.00	0.064	93.8	99.2
(d)	U1-1	-0.43	0.254	50	69.4	-0.41	0.217	55.8	86.1	-0.37	0.238	78.6	99.8
	U1-1/2	-0.44	0.251	46	69.4	-0.40	0.212	54.8	86.1	-0.37	0.234	74.6	99.8
	U1-2	-0.49	0.321	46.7	46.7	-0.45	0.271	52	63	-0.37	0.223	76	91.7
(e)	U1-1	-0.72	0.601	24	55.6	-0.68	0.530	22	77.8	-0.65	0.508	35.2	95
	U1-1/2	-0.71	0.579	22.8	55.6	-0.66	0.501	23	77.8	-0.62	0.459	34.8	95
	U1-2	-0.72	0.623	34.1	34.9	-0.72	0.601	27.6	54	-0.68	0.549	31.6	74.5

in Supplement H.1. For brevity, we focus here on the performance of the estimator for the immediate effect.

In Table S.9 we show the bias, mean squared error, coverage, and proportion of matched exposed time periods when applying the three unadjusted matching algorithms to estimate the immediate effect. We find that, as expected, the estimators are unbiased in the absence of confounding (scenario (a)), in the presence of smooth temporal trends only (scenario (b)), or in the presence of location-varying confounding only (scenario (c)). We also find that, in these simulations, these estimators which do not adjust for any measured covariates have smaller bias compared to the naïve approaches, likely thanks to the implicit adjustment for the smooth temporal trend.

We also evaluated the performance of the inferential procedure for testing the global null of no immediate effect with unadjusted matching in the presence of multiple outcome units, similarly to the simulations for the proposed estimators in Supplement H.3. The results are shown in Table S.10. The unadjusted methods give reliable inferences for testing the global null in the presence of only time-smooth confounders. In the presence of non-smooth temporal confounding, the unadjusted estimators’ bias will lead to identifying statistically significant causal effects too often.

Table S.10: Simulation results for using the three unadjusted algorithms and estimators to test the global null hypothesis of no immediate causal effect for scenarios (b), (d) and (e), and under a medium exposure level. ‘U’ stands for ‘unadjusted’ and ‘NW’ stands for ‘Newey-West’. The scenarios correspond to (b) Time-smooth confounders, (d) Time-varying confounders, and (e) All confounders.

		Average estimator mean	Average rate of p-value ≤ 0.05	Rate of min(p-value) ≤ 0.05	Rate of FDR min (adj.p-value) ≤ 0.05
(b)	U1-1	-0.004	0.053	1.000	0.078
	U1-1/2	-0.004	0.052	1.000	0.068
	U1-2	-0.001	0.054	1.000	0.098
	NWU1-1	-0.004	0.004	0.512	0.002
	NWU1-1/2	-0.003	0.004	0.526	0.008
	NWU1-2	-0.001	0.004	0.544	0.004
(d)	U1-1	-0.422	0.486	1.000	1.000
	U1-1/2	-0.421	0.504	1.000	1.000
	U1-2	-0.447	0.449	1.000	0.996
(e)	U1-1	-1.073	0.998	1.000	1.000
	U1-1/2	-1.044	0.998	1.000	1.000
	U1-2	-1.098	0.995	1.000	1.000

H.5 Analysis of tuning parameters

Following the simulation study in this section, we consider two additional choices of the algorithmic parameters $(\delta, \delta', \epsilon)$ per simulation. The “strict” choice of algorithmic parameters corresponds to $(\delta, \delta', \epsilon) = (0, 0.05, 2)$ imposing tight constraints on time and covariates, and the “loose” choice of algorithmic parameters $(\delta, \delta', \epsilon) = (2, 0.1, 6)$ corresponds to looser constraints.

The results for the immediate effect are shown in Table S.11, along with the results based on the default setting $(\delta, \delta', \epsilon) = (2, 0.05, 6)$ (the results for which are also shown in Table S.6). Comparing the results under the strict and default values allows us to investigate the impact of (δ, ϵ) that correspond to tuning parameters of time, while comparing the results under the default and loose values allows us to investigate the impact of δ' that is a tuning parameter for the measured covariates. For brevity, we focus on the immediate effect estimates.

Some conclusions from this comparison are discussed in Section 5.4. Here, we also point out that, even though the estimator based on the 1-2 algorithm performed best under sparse scenarios in Table S.6, when (δ, ϵ) are small under strict tuning parameters, this approach no longer performs best. That is because of the large variability for the corresponding 1-2 estimator since the number of available unexposed time periods to form matches is smaller and the proportion of matched exposed time points is almost half of that based on the 1-1 or 1-1/2 algorithms.

Table S.11: Simulation results for estimating the immediate effect under different values of the tuning parameters. The tuning parameters in this table correspond to (1) strict: $(\delta, \delta', \epsilon) = (0, 0.05, 2)$, (2) medium: $(\delta, \delta', \epsilon) = (2, 0.05, 6)$ (the results in Table S.6 correspond to this choice of tuning parameters), (3) loose: $(\delta, \delta', \epsilon) = (2, 0.1, 6)$.

Method	Dense				Medium				Sparse				
	Bias	MSE	Cover	Prop	Bias	MSE	Cover	Prop	Bias	MSE	Cover	Prop	
(a) No confounders													
1-1	(1)	-0.02	0.013	96.0	83.5	-0.02	0.021	94.2	97.3	-0.02	0.039	94.3	99.8
	(2)	-0.02	0.013	94.0	97.8	-0.02	0.020	95.6	100.0	-0.01	0.040	95.8	100
	(3)	-0.03	0.013	94.2	97.8	-0.03	0.021	95.6	100.0	-0.02	0.037	95.8	100
1-1/2	(1)	-0.02	0.014	94.3	83.5	-0.03	0.020	94.4	97.3	-0.02	0.037	94.3	99.8
	(2)	-0.02	0.012	95.4	97.8	-0.03	0.017	94.6	100.0	-0.02	0.032	95	100
	(3)	-0.03	0.013	94.0	97.8	-0.03	0.019	94	100.0	-0.02	0.032	93.7	100
1-2	(1)	-0.03	0.023	94.6	39.7	-0.02	0.023	94.6	63.8	-0.01	0.037	93.7	81.9
	(2)	-0.02	0.015	95.6	61.9	-0.03	0.017	93.9	90.6	-0.01	0.029	94.9	98.7
	(3)	-0.04	0.017	92.6	62.3	-0.03	0.018	95.2	90.8	-0.02	0.028	94.9	98.7
(b) Time-smooth confounders													
1-1	(1)	-0.01	0.021	95.0	57.1	-0.01	0.028	94.6	76.9	-0.00	0.039	95.7	91.1
	(2)	-0.02	0.019	93.8	62.5	-0.02	0.023	95	85.0	-0.00	0.037	95	97.6
	(3)	-0.03	0.021	94.4	62.5	-0.02	0.025	94.2	85.1	-0.02	0.039	94.0	97.8
1-1/2	(1)	-0.01	0.021	95.0	57.1	-0.01	0.026	95	76.9	0.00	0.037	94.3	91.1
	(2)	-0.02	0.020	94.4	62.5	-0.01	0.023	93.8	85.0	-0.00	0.033	95	97.6
	(3)	-0.02	0.019	94.2	62.5	-0.03	0.024	93.4	85.1	-0.01	0.035	95.7	97.7
1-2	(1)	-0.00	0.034	94.2	27.9	-0.01	0.038	94.4	42.3	0.01	0.048	95.1	58.5
	(2)	-0.02	0.023	93.2	40.8	-0.01	0.025	94.8	59.7	-0.00	0.035	93.6	80.0
	(3)	-0.03	0.023	94.6	40.9	-0.03	0.026	94	59.9	-0.02	0.034	93.7	80.4
(c) Location-varying confounders													
1-1	(1)	-0.02	0.023	94.8	95	-0.01	0.041	94.8	99.4	0.01	0.075	95.3	99.4
	(2)	-0.01	0.020	94	99.7	0.00	0.040	94.2	100	0.00	0.090	94.6	100
	(3)	-0.02	0.020	95.2	99.7	0.00	0.037	95.6	100	-0.01	0.079	93.7	100
1-1/2	(1)	-0.02	0.021	93.5	95	0.00	0.036	94.6	99.4	-0.01	0.085	94.9	99.5
	(2)	-0.01	0.018	94.8	99.7	-0.01	0.032	94.2	100	0.00	0.065	94.8	99.9
	(3)	-0.01	0.020	94.4	99.7	-0.00	0.032	94.6	100	-0.01	0.070	94.3	99.9
1-2	(1)	-0.01	0.026	93.5	59.3	0.00	0.037	94.4	78.9	-0.00	0.074	94.2	87.6
	(2)	-0.02	0.017	92.7	85.5	-0.00	0.030	94.6	97.3	-0.01	0.068	91.5	99.2
	(3)	-0.03	0.017	92.7	85.6	-0.01	0.030	93.6	97.4	-0.01	0.071	93.1	99.1
(d) Time-varying confounders													
1-1	(1)	-0.06	0.026	98.8	57.7	-0.06	0.030	98.4	72.9	-0.05	0.071	96.3	90.7
	(2)	-0.05	0.024	98.3	67.5	-0.06	0.026	99.2	84.7	-0.04	0.068	95.2	99.6
	(3)	-0.11	0.042	96.2	68.4	-0.10	0.040	94.8	85.6	-0.06	0.069	94.2	99.7
1-1/2	(1)	-0.06	0.025	98.8	57.7	-0.06	0.030	99	73	-0.04	0.068	97	90.9
	(2)	-0.05	0.024	97.9	67.5	-0.06	0.025	99	84.8	-0.05	0.054	96.6	99.6
	(3)	-0.11	0.045	95.6	68.5	-0.11	0.042	95.8	85.6	-0.07	0.062	95.1	99.8
1-2	(1)	-0.05	0.037	98.2	26.5	-0.06	0.042	98.8	37.2	-0.03	0.074	97.5	55.6
	(2)	-0.06	0.025	98.5	43.1	-0.06	0.027	97.8	58.9	-0.05	0.055	96.5	86.7
	(3)	-0.12	0.047	96.8	44.6	-0.11	0.045	96.9	60.7	-0.09	0.065	94.4	89
(e) All confounders													
1-1	(1)	-0.11	0.035	99.2	48.3	-0.09	0.033	98.6	67.3	-0.09	0.047	98.2	83.1
	(2)	-0.10	0.031	98.8	55.1	-0.09	0.030	98.5	77.1	-0.08	0.042	97.1	94.1
	(3)	-0.20	0.067	94	55.4	-0.18	0.061	93.2	77.6	-0.16	0.062	95.2	94.7
1-1/2	(1)	-0.10	0.035	99.4	48.3	-0.09	0.035	99.2	67.4	-0.09	0.049	98	83.3
	(2)	-0.10	0.029	98.7	55	-0.09	0.030	98.5	77.1	-0.08	0.039	97.1	94
	(3)	-0.19	0.068	91.7	55.4	-0.18	0.062	92.2	77.5	-0.16	0.063	93.2	94.7
1-2	(1)	-0.08	0.044	99.4	20.9	-0.09	0.048	99.6	33.3	-0.07	0.053	99	45.8
	(2)	-0.09	0.035	99.5	33.6	-0.08	0.031	99.5	51.8	-0.09	0.043	98.4	70.8
	(3)	-0.20	0.073	96.4	34.4	-0.18	0.066	94.8	53.2	-0.18	0.074	95.1	72.7

H.6 Modification of the algorithms to impose constraints within each match

Here, we investigate the performance of our inferential procedure when applied on the estimator derived from an alternative matching algorithm that imposes constraints on time-varying covariates within each match, instead of overall balance constraints. We consider this approach in accordance to the observations made in Supplement E, and particularly Supplement E.2. Specifically, here, we illustrate that this issue of over-coverage that is sometimes observed based on our inferential procedure and for our algorithm and estimator is alleviated when covariate balance is imposed for *every* match.

To do so, we consider the following extension to our algorithms in Section 4 and Supplement C.1 to include additional constraints. Given a small value δ'' when matching on all covariates, the 1-1 algorithm in Section 4 is extended to impose

$$|a_{t_e t_u}(\bar{\mathbf{X}}_{t_e, S} - \bar{\mathbf{X}}_{t_u, S})| \leq \mathbf{1}_{Np^{\text{int}} + Np^{\text{net}} + p^{\text{out}}} \cdot \delta'',$$

and similarly for the 1-2 algorithm in Supplement C.1.1

$$\left| a_{t_e t_{u_1} t_{u_2}} \left(\bar{\mathbf{X}}_{t_e, S} - \frac{\bar{\mathbf{X}}_{t_{u_1}, S} + \bar{\mathbf{X}}_{t_{u_2}, S}}{2} \right) \right| \leq \mathbf{1}_{Np^{\text{int}} + Np^{\text{net}} + p^{\text{out}}} \cdot \delta''.$$

For the 1-1/2 algorithm in Supplement C.1.2 we impose both constraints. If constraints are imposed on summarized covariates only, we replace $\bar{\mathbf{X}}_{t, S}$ with $\bar{\mathbf{X}}_{t, S}^{\text{sum.}}$ for all constraints above. We refer to these algorithms and the corresponding estimators as *extended* algorithms and estimators.

We evaluated the performance of these extended algorithms and estimators against the standard algorithms and estimators introduced in Section 4 (which impose only constraints on the overall matched populations, and not within each match). We consider the confounding scenario (d) with time-varying confounder and medium sparsity level. We set $\delta'' = 0.25$, assuming the covariates have been standardized as discussed in Section 5.2. We set the remaining tuning parameters equal to the values $(\delta, \delta', \epsilon) = (2, 0.05, 6)$.

In Figure S.7, we see that the three extended matching estimators are close to unbiased for the true causal effect (which is equal to 1). The bias of the three estimators based on the extended algorithms is 0 for the 1-1 algorithm, -0.04 for the 1-1/2 algorithm, and -0.05 for the 1-2 algorithm. Any residual bias is most likely due to residual covariate imbalance. Since bias can affect coverage rates, we compare coverage of 95% intervals of the extended matching estimators, with the results of the standard estimators under tuning parameters $(\delta, \delta', \epsilon) = (2, 0.05, 6)$ which show similar bias (see Table S.11, bias equal to -0.06 for all three estimators). The coverage rate for the extended 1-1, 1-1/2, and 1-2

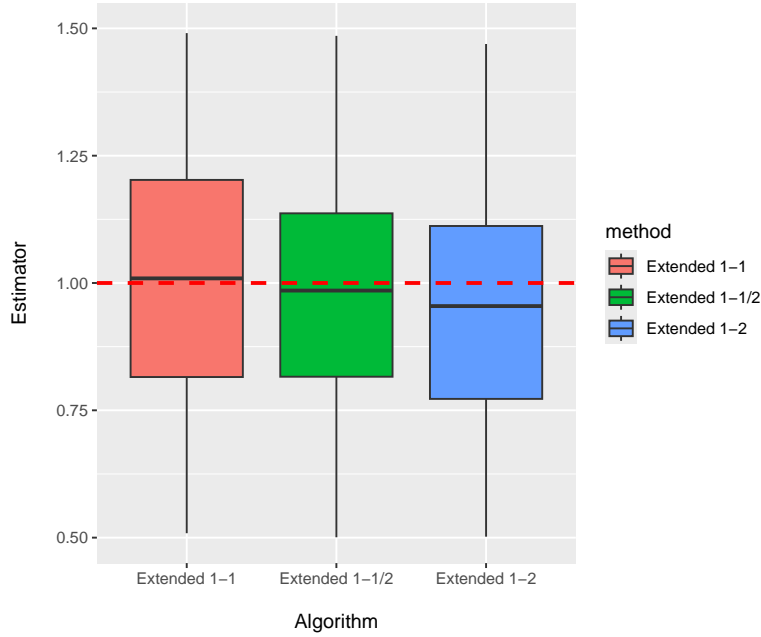


Figure S.7: Boxplots of estimated causal effects over 500 data sets based on the extended estimators. The horizontal line in the boxplot corresponds to the median estimate.

estimators is equal to 97.2%, 95.4%, and 95.0%, respectively, closer to the nominal level compared to the corresponding coverage rates of the standard 1-1, 1-1/2, and 1-2 estimators (included in Table S.11) which are equal to 99.2%, 99% and 97.8%, respectively.

However, even though inference might be closer to the nominal level (rather than being conservative) when the extended estimators are employed, they might suffer due to small number of matches depending on the value of δ'' . Even with $\delta'' = 0.25$, the proportion of matched exposed time periods decreases significantly (compared to the algorithms that do not impose constraints within each match) to 10.8%, 21.3%, and 12.6% for the Extended 1-1, Extended 1-1/2, and Extended 1-2 algorithm, respectively (compared to 63.1%, 63.2% and 23.7% for the standard 1-1, 1-1/2, and 1-2 algorithm, respectively).

We conclude that incorporating the within-match adjustment has the benefit of coverage that is closer to the nominal level, but suffers from a lower proportion of matched exposed time periods, which might lead to higher overall uncertainty and lower estimation efficiency.

H.7 Simulations under heterogeneous treatment effects

We performed a simulation where exposure effects are no longer homogeneous over time for an individual outcome unit. We define three new quantities, denoted as $\tilde{\gamma}^{\text{imm},1-1}(1,0)$, $\tilde{\gamma}^{\text{imm},1-1/2}(1,0)$ and $\tilde{\gamma}^{\text{imm},1-2}(1,0)$, as the average difference in the potential outcomes under exposures 0 and 1 over the

exposed time periods *that are matched* according to the 1-1, 1-1/2, and 1-2 algorithm, respectively. For example, $\tilde{\tau}^{\text{imm},1-1}(1,0)$ is defined as

$$\tilde{\tau}^{\text{imm},1-1}(1,0) = \frac{1}{\sum_{t: \text{ matched in 1-1}} I(E_t = 1)} \sum_{t: \text{ matched in 1-1}} (Y_t(1, R_t) - Y_t(0, R_t)) I(E_t = 1).$$

These quantities resemble the estimand $\tau^{\text{imm}}(1,0)$ defined in Section 3, but they average over the *matched* exposed time periods only. For ease of notation, we denote them as $\tilde{\tau}^{\text{imm},1-1}$, $\tilde{\tau}^{\text{imm},1-1/2}$ and $\tilde{\tau}^{\text{imm},1-2}$.

The data generating models follow the scenarios (b) and (d) with medium exposure, where we alter the outcome model to specify heterogeneous treatment effects. Specifically, we generate outcomes according to

$$Y_{tj} = (1 + \epsilon'_{tj})E_t + 0.005(400 - t)E_t + (0.4 + \epsilon''_{tj})R_t - 0.0005tR_t + X_{tj3}^{\text{out}} + X_{tj5}^{\text{out}} + \sum_i q_{ij} X_{tij}^{\text{net}} + X_{tj6}^{\text{out}} + \epsilon_{tj},$$

where ϵ'_{tj} and ϵ''_{tj} are generated independently from $N(0,1)$. We simulate 500 data sets and consider the estimation of effects for the first outcome unit.

We compare the matching approaches to Naïve- t . We exclude Naïve- j and Naïve-all from simulations under heterogeneity since the estimands they target average across units, whereas Naïve- t and the matching estimators target unit-specific effects that average across time.

The bias, MSE, Coverage and proportion of exposed units that are matched are shown in Table S.12. We evaluate the performance of the three proposed estimators and Naïve- t for estimating the average effect over all exposed time points τ^{imm} . The proposed estimators perform relatively well for estimating τ^{imm} , and substantially better than the Naïve- t approach that suffers from confounding bias. Particularly, the estimators based on the 1-1 and 1-1/2 algorithms which find matches for 85% of the exposed time points are close to unbiased with appropriate coverage of confidence intervals.

We also evaluate the performance of each estimator against the causal effect over the set of exposed time periods that are in fact matched, in that we evaluate the estimator based on the 1-1 algorithm for estimating $\tilde{\tau}^{\text{imm},1-1}$, the estimator based on the 1-1/2 algorithm for estimating $\tilde{\tau}^{\text{imm},1-1/2}$ and the estimator based on the 1-2 algorithm for estimating $\tilde{\tau}^{\text{imm},1-2}$. When compared against the effect over the matched exposed population, the estimators are unbiased with appropriate coverage. This suggests that even though the effect of exposure is not constant at each time point, matching approaches can

Table S.12: Simulation results under heterogeneous immediate effect over time. Bias, mean squared error (MSE), coverage of 95% intervals (%) of the Naïve- t and the proposed estimator for the causal effect over the exposed time periods and over the matched exposed time periods. The proportion of exposed time periods that are matched on average when employing each matching method is reported once.

Estimand	Method	Bias	MSE	Coverage	Proportion
(b) Time-smooth confounders					
τ^{imm}	Naïve- t	-1.14	1.35	0.00	-
	1-1	-0.13	0.05	98.09	84.82
	1-1/2	-0.13	0.05	97.51	84.82
	1-2	-0.26	0.11	91.78	58.84
$\tilde{\tau}_{1-1}^{\text{imm}}$	Naïve- t	-1.05	1.17	0.76	
	1-1	-0.05	0.03	99.81	
$\tilde{\tau}_{1-2}^{\text{imm}}$	Naïve- t	-1.05	1.17	0.96	
	1-2	-0.05	0.03	99.43	
$\tilde{\tau}_{1-1/2}^{\text{imm}}$	Naïve- t	-0.93	0.94	2.29	
	1-1/2	-0.05	0.03	99.43	
(d) Time-varying confounders					
τ^{imm}	Naïve- t	-0.99	1.04	2.36	-
	1-1	-0.08	0.04	97.98	84.96
	1-1/2	-0.08	0.04	97.47	84.96
	1-2	-0.19	0.08	94.95	59.59
$\tilde{\tau}_{1-1}^{\text{imm}}$	Naïve- t	-0.92	0.91	3.20	
	1-1	0.00	0.03	99.49	
$\tilde{\tau}_{1-2}^{\text{imm}}$	Naïve- t	-0.92	0.92	3.54	
	1-2	-0.01	0.03	99.16	
$\tilde{\tau}_{1-1/2}^{\text{imm}}$	Naïve- t	-0.82	0.74	8.75	
	1-1/2	-0.02	0.03	99.83	

still serve as a useful tool for inferring the average effect of the exposure over the population that was in fact matched.

H.8 The impact of outcome temporal correlation on inference

When outcomes exhibit temporal autocorrelation, conventional Wald-type intervals in a regression analysis generally underestimate the true variance of the coefficients' OLS estimator. In these situations, the Newey-West variance estimator provides robust inference for regression coefficients.

Here, we perform simulations to investigate the impact of outcome autocorrelation on inference. First, we investigate the extent to which this is an issue within our framework. Second, we consider an alternative inference strategy that uses the Newey-West variance estimator.

Table S.13: Simulation results for the immediate effect in the presence of outcome temporal correlation. Coverage of 95% intervals (%) of the proposed estimators based on Wald-type and Newey-West intervals for estimating the immediate effect. We consider autocorrelation values $\rho = 0.2, 0.4, 0.6$ and 0.8 in the random error term for the outcome variable.

ρ	Standard Method			Newey-West Method		
	1-1	1-1/2	1-2	1-1	1-1/2	1-2
0.2	96.34	96.99	95.91	97.85	98.06	95.91
0.4	95.70	95.48	95.70	98.92	98.28	98.49
0.6	95.73	94.87	95.09	99.79	100.00	99.57
0.8	93.36	94.22	93.58	100.00	100.00	100.00

We describe first the alternative inference strategy. In Supplement E.5 we showed that our point estimator is equal to the OLS estimator of an outcome on exposure regression on the matched sample. Then, standard errors are acquired by replacing the standard regression covariance matrix with the Newey-West matrix. This approach incorporates squared residuals and distance-weighted autocovariances to robustly correct for both heteroskedasticity and serial correlation [Newey and West, 1986]. We compute the Newey-West variance-covariance matrix using the `NeweyWest()` function from the `sandwich` R package. We then performed revised statistical tests using the `coefTest()` function from the `lmtest` package to ensure the significance levels accounted for the adjusted standard errors.

Our simulation setup is as follows. We adopt scenario (a) without any confounders to eliminate any impact of confounding on simulation results. We consider the scenario under dense exposure. Importantly, we alter how the outcome error terms ϵ_t are generated across time to impose temporal autocorrelation. Specifically, we set $\epsilon_t = \rho\epsilon_{t-1} + \sqrt{1 - \rho^2}e_t$, where $e_t \sim N(0, 1)$, and ρ is a tuning parameter adjusting the amount of autocorrelation of the error terms. We simulate 500 data sets under different levels of autocorrelation, $\rho = 0.2, 0.4, 0.6$ and 0.8 , and record whether the true value of the causal effect is included in the 95% confidence intervals created based on each of the three estimators, and based on the Wald-type intervals in Section 4.3 and the intervals employing the Newey-West estimated variance.

The results for the immediate effect are shown in Table S.13. Temporal correlation in the outcome variable has a minimal impact in confidence interval coverage for the approach described in Section 4.3. Even in the presence of high outcome variable autocorrelation ($\rho = 0.8$) coverage is above 93%. Implementing the Newey-West estimator yields more conservative inference across all degrees of temporal correlation, illustrating that it might be more robust, albeit too conservative when autoregression is suspected.

I Additional study information

I.1 Additional information on the study data set

I.1.1 Additional information on the wildfire data

Satellite instruments scanning the Earth’s surface provide the primary evidence for wildfire activity. The National Oceanic and Atmospheric Administration’s Hazard Mapping System (HMS) integrates automated detection with human verification to delineate fire perimeters, producing a spatio-temporal dataset that includes Fire Radiative Power (FRP). These FRP values identify the most intense segments of a fire, characterized by high rates of energy release. The wildfire occurrence and intensity data in Figure 1a are acquired from <https://www.ospo.noaa.gov/Products/land/hms.html> and plotted for August 31, 2021.

I.1.2 Additional information on regions’ exposure

Hazardous smoke produced by wildfires can travel long distances, and affect population exposure and behavior across different areas. HMS combines data from polar and geostationary satellites in real time, enabling experts to accurately identify and track the dispersion of smoke. The HMS smoke data are acquired from <https://www.ospo.noaa.gov/Products/land/hms.html>. Smoke plumes are labeled qualitatively as light, medium, or heavy based on their apparent opacity in satellite imagery. Each smoke polygon includes metadata such as the time window of observation and the satellite used.

I.1.3 Additional information on the outcome

The outcome represents the daily total number of bikeshare hours in the San Francisco, East Bay, and San Jose areas in California, US, as measured through the publicly-available Bay Wheels data provided by Lyft at <https://www.lyft.com/bikes/bay-wheels/system-data>.

We find that over 97% of rides last less than one hour, indicating that long-lasting rentals are rare. Additionally, we find that only 206 out of approximately 6 million rentals started in one area and ended in a different one. This suggests that our data include very minimal commuting by bicycle that crosses area boundaries, which supports the assumption of minimal spillover effects across outcome units, and allows us to analyze the three areas separately. We exclude these rare cross-region trips from our analysis.

I.1.4 Additional information on the collected covariates

The time-varying covariates are regional temperature, precipitation, humidity, wind speed and wind direction among three bike locations, which are retrieved from <https://www.ncei.noaa.gov/>

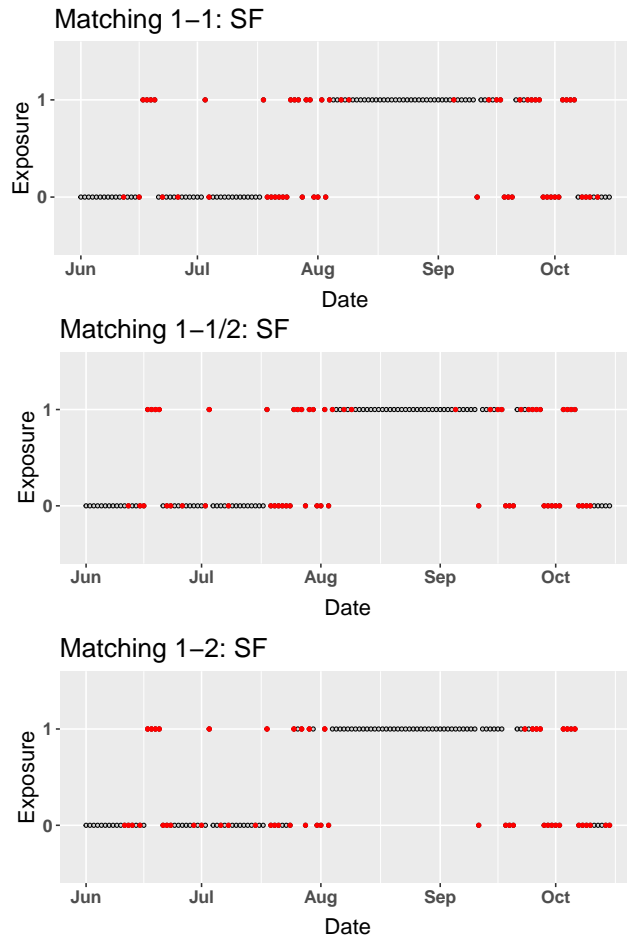


Figure S.8: Exposure and matching information for the 1-1, 1-1/2, and 1-2 algorithms detailed in Section 4 and Supplement C.1 for San Francisco during the period from June 1, 2021, to October 15, 2021. The red and hollow points correspond to time periods that are or are not part of the resulting data set of matched time periods, respectively.

`cdo-web/datasets`. Due to high temperatures and the dry season, there are more wildfires and gusty winds in late summer than in the other seasons. As a result, the exposed time periods concentrate around the summer and fall months (see Supplement I.2).

I.2 Illustrations of resulting data for San Francisco based on the proposed algorithms

Our data set includes information from January 2021 until September 2023. Most exposed time periods, and as a result most matches for the immediate and the carryover effect, occur during the summer and fall months. As an illustration, the exposed and unexposed time periods for a *subset* of our time window and for San Francisco are shown in Figure S.8, with the red color denoting whether the time period was used in a match according to the 1-1, 1-1/2, or 1-2 algorithms for the immediate effect.

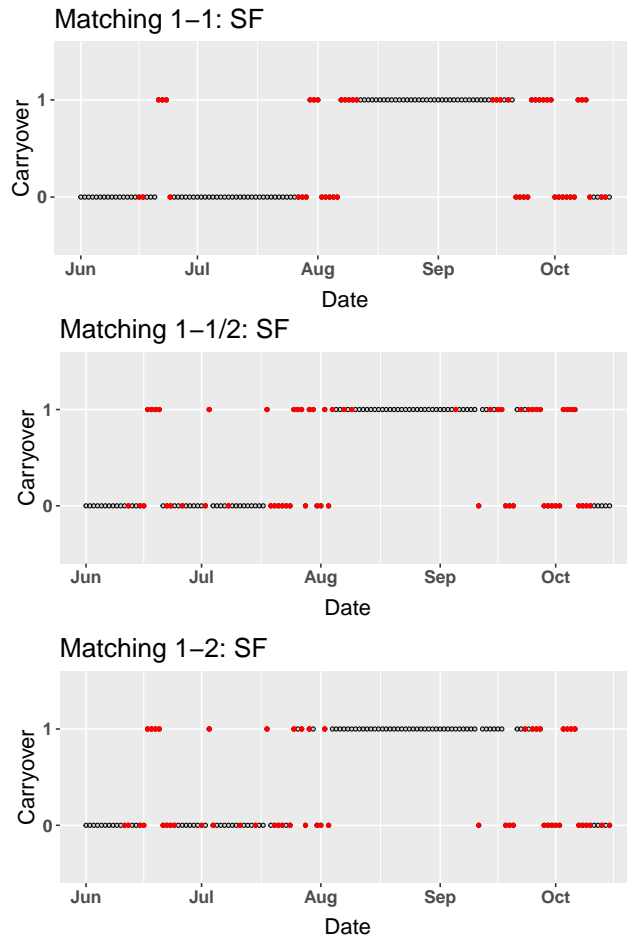


Figure S.9: Carryover exposure and matching information for the 1-1, 1-1/2, and 1-2 algorithms in Supplement C.2 for San Francisco during the period from June 1, 2021, to October 15, 2021. The red and hollow points correspond to time periods that are or are not part of the resulting data set of matched time periods, respectively.

Under $\epsilon = 6$, the 1-1 and 1-1/2 algorithms return similar but not identical matching patterns, while the 1-2 algorithm matches fewer exposed time periods.

Figure S.9 is similar figure for the algorithms for the carryover effect. Here, we see a strong temporal trend in the carryover exposure with almost almost all of the time periods in the late summer and early fall, and almost in the rest of the time window have carryover exposure. This explains why the algorithm matching one time period with carryover exposure to two time periods without carryover exposure manages to find such few number of matches (Table 3).

I.3 Results under alternative definition of exposure

As discussed in Supplement I.1, the HMS categorizes smoke exposure as no exposure, light, medium, or high exposure. In our analysis of Section 6, we considered an area at a given time period as exposed

if the HMS classification was light or higher, and unexposed otherwise. Here, we evaluate the sensitivity of our conclusions when an area is considered exposed under medium or high smoke exposure, and unexposed under no smoke exposure or light smoke. Under this definition, out of the 1003 total number of days, San Francisco was exposed during 39 days, the East Bay during 40 days, and San Jose during 37 days. The number of days with carryover exposure is 16 in all three areas.

Table S.14: The immediate and carryover effect estimates of wildfire smoke on bikeshare hours in San Francisco, East Bay, and San Jose for Naïve- t and the matching estimators. For each region, the three columns correspond to the estimate, p-value, and number of matches. In this analysis, an area is considered exposed at a given time period if it is classified to have medium or high smoke exposure according to HMS, and unexposed if it is classified to have no smoke or light smoke exposure.

	San Francisco			East Bay			San Jose		
	Est	p-value	#Exp	Est	p-value	#Exp	Est	p-value	#Exp
	<u>Immediate effect</u>								
Naïve- t	159.337	(0.983)	39	25.773	(1.000)	40	37.640	(1.000)	37
1-1	-26.349	(0.354)	34	-2.757	(0.319)	35	-4.633	(0.233)	32
1-1/2	-35.746	(0.289)	34	-1.698	(0.382)	35	2.190	(0.783)	32
1-2	-60.263	(0.169)	25	-5.908	(0.086)	26	-5.302	(0.129)	23
	<u>Carryover effect</u>								
Naïve- t	-6.389	(0.478)	16	31.904	(1.000)	16	47.135	(1.000)	16
1-1	-132.589	(0.139)	15	-12.256	(0.110)	10	-1.993	(0.586)	12
1-1/2	-102.387	(0.163)	15	-7.918	(0.208)	10	-2.818	(0.588)	12
1-2	-179.933	(0.223)	4	-	-	0	-12.256	(0.003)	3

Table S.14 shows the causal effect estimates under this alternative specification of exposure. We focus on the immediate effect first. We find that estimates are either negative or very close to zero, indicating that, if smoke exposure has an effect, it leads to a reduction in bikeshare hours. The effect estimates here, where a time period is defined as exposed under medium or high smoke and unexposed otherwise, are similar or larger in magnitude compared to the effect estimates reported in Table 3, where a time period is defined as exposed under light, medium or high smoke and unexposed otherwise. Since, here, a time period is classified as exposed under heavier smoke conditions, we believe that this comparison might be because heavier smoke has a larger impact on bikeshare hours compared to lighter smoke exposure. However, the effect estimates in Table S.14 are not statistically significant. We believe that this is largely because of the small number of matches (ranging from 23 to 35), that is partially explained by the small number of days with medium or high smoke exposure.

For the analysis of the carryover there are at most 15 matched time periods with carryover exposure. As a result, there is insufficient statistical support to draw meaningful conclusions when categorizing medium and heavy smoke as exposed.

A similar analysis that considers time periods to be exposed under heavy smoke exposure only would not be feasible in our data set. That is because the number of days with heavy smoke thickness was small across our time window. Specifically, in the three areas there are approximately 17 days of heavy exposure, 22 days of medium exposure, 70 days of light exposure, and more than 800 days of no exposure. Therefore, analyzing this exposure as categorical would be largely infeasible.